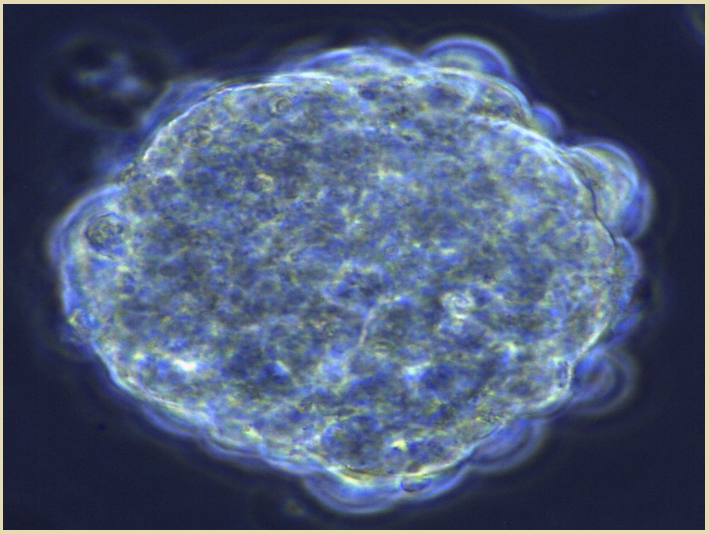
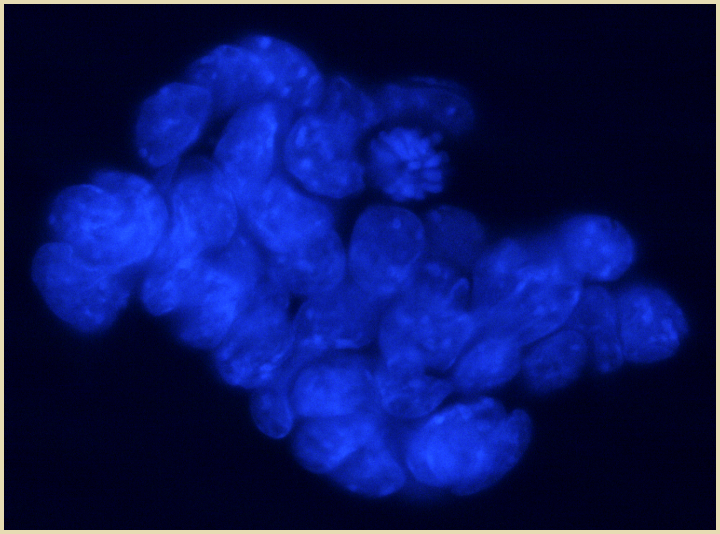

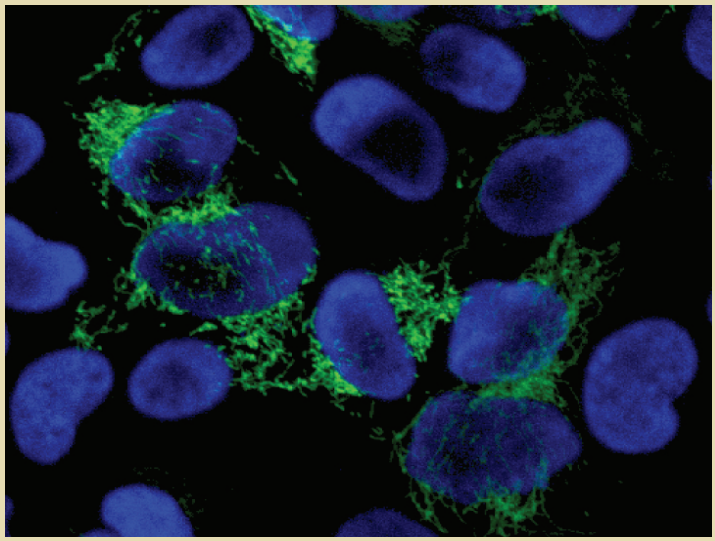

Ana Sofia de Jesus Rodrigues

The role of metabolism and mitochondrial function in embryonic stem cells

Tese de Doutoramento na área científica de Biologia Celular, orientada pelo Professor Doutor João Ramalho-Santos do Departamento de Ciências da Vida da Faculdade de Ciências e Tecnolologia da Universidade de Coimbra, e apresentada ao Departamento de Ciências da Vida da Faculdade de Ciências e Tecnolologia da Universidade de Coimbra

Setembro de 2013

· U C ·

UNIVERSIDADE DE COIMBRA

UNIVERSIDADE DE COIMBRA

The role of metabolism and mitochondrial function in embryonic stem cells

Tese apresentada à Faculdade de Ciências e Tecnologia da Universidade de Coimbra, para cumprimento dos requisitos necessários à obtenção do grau de Doutor na Especialidade Biologia Celular, realizada sob a orientação científica do Professor Doutor João Ramalho-Santos (Universidade de Coimbra e Centro de Neurociências e Biologia Celular da Universidade de Coimbra). Este trabalho foi desenvolvido no Centro de Neurociências e Biologia Celular da Universidade de Coimbra, departamento de Ciências da Vida, Universidade de Coimbra, Portugal e no Pittsburgh Development Center, Magee Womens Research Institute, Pittsburgh, Pennsylvania, Estados Unidos da America.

Thesis presented to the Faculty of Sciences and Technology of the University of Coimbra in partial fulfillment of the requirements for the PhD degree in Cell Biology, under supervision of Professor João Ramalho-Santos (University of Coimbra, and Center for Neurosciences and Cell Biology of University of Coimbra). This work was conducted at the Center for Neurosciences and Cell Biology, Department of Life Sciences, University of Coimbra, Coimbra, Portugal and at Pittsburgh Development Center, Magee Womens Research Institute, Pittsburgh, Pennsylvania, United States of America.

O trabalho incluido nesta tese foi financiado pela Fundação para Ciência e a Tecnologia com uma bolsa individual de doutoramento (SFRH/BD/33463/2008) e projectos de investigacao (PTDC/QUI/64358/2006 and PTDC/EBB-EBI/101114/2008 PEst-Fundação para Ciência e a Tecnologia co-C/SAU/LA0001/2011).

“Quis saber quem sou
O que faço aqui
Quem me abandonou
De quem me esqueci
Perguntei por mim
Quis saber de nós
Mas o mar
Não me traz
Tua voz.”

“E depois do adeus” de José Niza

Dedico esta tese à minha maior lição de vida: **o meu pai**.

Às saudades intermináveis, aos sorrisos improváveis e à coragem inabalável. Estarás sempre presente.

“Nothing is impossible, the word itself says 'I'm possible'!”

By Audrey Hepburn

“Foi o tempo que tu perdeste com a tua rosa que tornou a tua rosa tão importante.”

“O Principezinho” de Antoine de Saint-Exupery

“So be sure when you step,
Step with care and great tact.
And remember that life's
A Great Balancing Act.
And will you succeed?
Yes! You will, indeed!
(98 and ¾ percent guaranteed)
Kid, you'll move mountains.”

By Dr. Seuss

Partilho a concretização desta tese com as três gerações de mulheres mais importantes na minha vida: **a minha avó, a minha mãe e a minha mana**. Obrigada pelo constante exemplo de coragem e dedicação, obrigada por serem a minha base e o meu porto seguro. Obrigada…

Agradecimentos / Acknowledgements:

O meu primeiro agradecimento é dirigido ao meu orientador, ao Professor Doutor João Ramalho-Santos. O meu sincero e sentido obrigada pela orientação, disponibilidade e paciência constantes. Há 8 anos atrás, contactei-o para fazer um estágio de licenciatura e desde então tenho a sorte e o privilégio de fazer efectivamente o que gosto. Devo ao professor, uma aprendizagem constante e curiosidade permanente, que permitiram o meu percurso ate aqui. Obrigada por exigir sempre o melhor de nós e fomentar o espírito critico. Obrigada por acreditar em mim.

To PhD Gerald Schatten, my special acknowledgment for receving me in his lab and for assuring that I had everything I need to work in the best conditions ever. I will always remember my days in Pittsburgh as happy ones, thanks to you and all the members in your lab.

Para a Sandra Varum, um agradecimento muito especial por ter partilhado o seu conhecimento comigo, pela paciência a ensinar e por me ter recebido de braços abertos. Esta tese não seria possível sem ela que me segurou nos primeiros passos nesta área.

Quero também agradecer ao meu grupo "Biologia da reprodução e células estaminais". O percurso foi longo e esta tese não seria possível sem o vosso contributo cientifico e pessoal. Obrigada pela paciência e inputs científicos neste trabalho, mas acima de tudo obrigada por terem feito do laboratório, um local onde é bom trabalhar e com excelente ambiente. São efectivamente extraordinárias/os e foi um privilegio partilhar espaço, momentos e ciência com vocês.

Por ultimo, gostaria de agradecer ao PhD programme in Experimental Biology and Biomedicine por me ter dado uma oportunidade única de ter acesso a uma formação de excelência e à Fundação

para Ciência e Tecnologia pela bolsa individual que me foi atribuída. Um muito humilde obrigada a ambos.

Table of Contents:

List of Abbreviations:

3-Bromopyruvate	3BRP
Acetyl-Coenzyme A	Acetyl-CoA
Adenine Diphosphate	ADP
Adenine Monophosphate	AMP
Adenine Nucleotide Translocator	ANT
Adenine Triphosphate	ATP
Adenine Triphosphate	ATP
adult stem cells	ASC
Alkaline Phosphatase	AP
Antimycin A	AA
ATP-Citrate Lyase	ACL
Basic Fibroblast Growth Factor	bfgf or FGF2
Basic–Helix-Loop-Helix	Bhlh
Bicinchoninic Acid	BCA
Bone Morphogenic Protein 4	BMP4
Bovine Serum Albumin	BSA
Carbonyl Cyanide M-Chlorophenylhydrazone	CCCP
Chromatin Immunoprecipitation	Chip
Cristae Membrane	CM
Dichroloacetic Acid or Dichroloacetate	DCA
DNA Polymerase γ	Pol γ
Dulbecco's Phosphate Buffered Saline	D-PBS
Electron Transport Chain	ETC
Embryonal Carcinoma Cells	ECC
Embryonic Day	E
Embryonic Germ Cells	EGC
Embryonic Stem Cells	ESC
Enzyme-Linked Immunosorbent Assay	ELISA
Epiblast Stem Cells	EpiSC
Fatty Acid Oxidation	FAO

Fibroblast Growth Factor 5	FGF5
Flavin Adenine Dinucleotide	FAD
Glucose-6-Phosphate	G-6-P
Glutamate Dehydrogenase	GDH
Glutamine	Gln
Glutathione Oxidized Form	GSSH
Glutathione Peroxidase	GP
Glutathione Reduced Form	GSH
Glyceraldehyde-3-Phosphate Dehydrogenase	GAPDH
Glycogen Synthase Kinase 3	GSK3
High Mobility Group	HMG
High Performance Liquid Chromatography	HPLC
Horseradish Peroxidase	HRP
Human Embryonic Stem Cell	hESC
Hydrogen Peroxide	H_2O_2
Hypoxia-Inducible Transcription Factor 1 Alpha	HIF-1α
Immunocytochemistry	ICC
Induced Pluripotent Stem Cells	iPSC
Inhibitors Of Differentiation Genes	Id
Inner Cell Mass	ICM
Inner Mitochondrial Membrane	IMM
Interleukine 6	IL6
Knockout Serum Replacement	KSR
Lactate Dehydrogenase A	LDHA
Leukemia Inhibitor Factor	LIF
Manganese Superoxide Dismutase	MnSOD
Mitochondrial DNA	mtDNA
Mitochondrial Membrane Potential	MMP
Mitochondrial Membrane Potential – electric component	Δψm
Mouse Embryonic Stem Cell	mESC
Nicotinamide Adenine Dinucleotide Oxidized Form	NAD^+
Nicotinamide Adenine Dinucleotide Phosphate	NADPH
O_2 Consumption Rate	OCR

Octamer 4	Oct4
Outer Mitochondrial Membrane	OMM
Oxidative Phosphorilative Chain	OXPHOS
Paraformaldehyde	PFA
Pentose Phosphate Pathway	PPP
Peroxiredoxin	Prx
Phenylmethylsulphonyl Fluoride	PMSF
Phosphate-Activated Glutaminase	PAG
Phosphoenolpyruvate	PEP
Phosphoinositide 3 – Kinase	PI3K
Pluripotent Stem Cells	PSC
Primordial Germ Cell	PGC
Primordial Germ Cells	PGC
Proliferating Cell Nuclear Antigen	PCNA
Propidium Iodide	PI
Protomotive Force	Δp
Pyruvate Dehydrogenase Complex	PDH
Pyruvate Dehydrogenase Kinase	PDHK
Pyruvate Kinase	PKM
Reactive Oxygen Species	ROS
Reduced Nicotinamide Adenine Dinucleotide	$FADH_2$
Room Temperature	RT
Semiubiquinone	$UQ^{\cdot-}$
Sex Determining Region Y Box 2	Sox2
Signal Transducer And Activator Of Transcription-3	STAT3
Similar To Mothers Against Decapentaplegic Homologue 1/5 And 8	SMAD
Spermatogonial Stem Cells	SSC
Stage Specific Embryonic Antigen	SSEA
Sulforhodamine b	SRB
Superoxide Anion	$O_2^{\bullet-}$
Superoxide Dismutase	SOD
Tetramethylbenzidine	TMB
Tetramethylrhodamine Methyl	TMRM

Thiazolyl Blue Tetrazolium Bromide	MTT
Transcription Factors	TF
Transforming Growth Factor Beta	Tgfβ
Tricarboxilic Acid Cycle	TCA
Tris-Buffered Saline with Tween	TBST
Trophectoderm	TE
Ubiquinol	UQH_2
Ubiquinone	UQ
Uncoupling Protein	UCP
Uncoupling Protein 2	UCP2
Vascular Endothelial Growth Factor A	VEGF-A
Voltage-Dependent Anion Channel	VDAC

Abstract:

Human pluripotent stem cells have the ability to generate all cell types present in the adult organism, therefore harboring great potential for the *in vitro* study of differentiation and for the development of cell-based therapies. Nonetheless their use may prove challenging as incomplete differentiation of these cells might lead to tumoregenicity. Therefore it is of outmost importance to unveil the physiological characteristics of these cells, including mitochondrial function and metabolic status. Interestingly, many types of cancer have been reported to display metabolic modifications with features that might be similar to stem cells. The goal of this thesis was to test the hypothesis that both metabolism and mitochondrial function could have a role in the pluripotency of both embryonic (ESC) and induced pluripotent stem cells (iPSC). For that purpose, the experimental work was divided into three goals and results for each one are presented in chapters three, four and five. Given that at the time the information concerning mitochondria in embryonic stem cells was sparse and the metabolic status of these cells was unknown, the first goal consisted in comparing the energy metabolism of human ESC iPSC, and their somatic counterparts. Mitochondria localization, morphology and function were evaluated. Gene expression analysis of several pathways related to glucose metabolism, including glycolysis, the pentose phosphate pathway and the tricarboxylic acid (TCA) cycle were assessed. Finally in order to understand how metabolism was being regulated we explored the expression of key proteins involved in the regulation of glucose metabolism, focusing on strategies that could be similar to the ones present in some types of cancer cells. Our results demonstrate that, although the metabolic signature of iPSC is not identical to that of ESC, they cluster with ESC rather than with their somatic counterparts. ATP levels lactate production and Oxygen consumption rates (OCR) revealed that human pluripotent cells rely mostly on glycolysis to meet their energy demands. Furthermore, the results pointed to some possible strategies that pluripotent stem cells may use to maintain high glycolytic rates, such as high levels of Hexokinase II and inactive pyruvate dehydrogenase (PDH), suggesting these two enzymes as possible targets for metabolic modulation. Therefore, the second and third goal consisted in the pharmacological inhibition of these two possible targets, assessing possible alterations in pluripotency on mouse ESC. In order to block the first step of glycolysis, Hexokinase II was inhibited using 3-Bromopyruvate, a chemical used in clinical trials for cancer treatment. The pluripotent state was evaluated, as was mitochondrial function. Overall, pluripotency was affected although there wasn't a clear metabolic switch. A negative effect on p53 and c-Myc were also observed. Also, as a positive control for differentiation, we grew cells without LIF, which is essential for mouse pluripotency. Under

normoxic conditions glucose will be converted to pyruvate that can be further metabolized in the mitochondria via the activity of pyruvate dehydrogenase (PDH), converting it to acetyl-CoA. PDH E1-α subunit, functions as an on/off switch regulated by phosphorylation/dephosphorylation. One of the four-pyruvate dehydrogenase kinase isoforms (PDHK1-4) will phosphorylate this subunit causing inactivation of PDH. Given that an inactive PDH would be beneficial for ESC, we wondered if metabolic modulation, via PDHK inhibition, could impact metabolism and pluripotency. PDHK activity was inhibited using the therapeutic compound dichloroacetate (DCA). We observed that in the presence of DCA ESC start to differentiate with alterations in mitochondrial function and proliferation potential. The PDH cycle was also assessed by monitoring protein levels for PDH (both phosphorylated and non-phosphorylated) and PDHK1. Interestingly, we were also able to describe a possible pathway that involves Hif-1alpha, c-Myc and p53 during the loss of pluripotency due to DCA action. It is important to mention that the results with DCA were comparable to ones obtained for cells grown without LIF. This way, we demonstrate a possible role for PDHK as a gatekeeper for metabolism in ESC, and therefore a good target to modulate metabolism and differentiation by controlling PDH status. As a general conclusion, our research points to the fact that indeed an inactive PDH favors pluripotency and that ESC have similar strategies as cancer cells to maintain the glycolytic profile by making use of some of the signaling pathways found in the latter. Overall, the results presented in this thesis helped to improve the current knowledge about which possible metabolic players could be involved in differentiation and more importantly it was demonstrated that a normal function of Hexokinase II and PDHK are important for pluripotency.

Resumo:

As células estaminais pluripotentes são capazes de se diferenciar em todos os tipos celulares presentes num organismo adulto. Por esta mesma razão, estas células, representam um potencial tremendo quer para estudos de diferenciação, quer para um possível futuro na terapia celular. Contudo, o risco de indução de tumores devido a diferenciações incompletas compromete este objectivo. Desta forma torna-se imperativo o desenvolvimento de estudos extensivos que permitam compreender a fisiologia da célula estaminal pluripotente. Conhecendo as suas propriedades metabólicas e mitocondriais, será possível garantir diferenciações mais bem sucedidas, eliminando o risco mencionado. O facto de alguns tipos de tumores apresentarem características comuns com células estaminais pluripotentes levanta a questão se em termos metabólicos essa semelhança se mantêm. Assim sendo, o principal objectivo desta tese consiste em testar a hipótese que tanto o metabolismo como a função mitocondrial são fulcrais para a pluripotencia de células estaminais pluripotentes. Os resultados de investigação cientifica aqui apresentados foram obtidos utilizando dois tipos de células pluripotentes: células estaminais embrionárias e células estaminais pluripotentes induzidas. O trabalho experimental encontra-se dividido em três objectivos distintos e os resultados estão descritos ao longo dos capítulos, três, quatro e cinco. ‘E importante ter em conta, que aquando do inicio deste trabalho pouco se sabia sobre a função mitocondrial de células estaminais embrionárias, e relativamente ao estado metabólico destas células a literatura disponível era ainda mais escassa. Tendo estes factores em mente, o primeiro objectivo prendeu-se com a caracterização da função mitocondrial e estado metabólico nestas células, bem como o de células diferenciadas a partir delas. Relativamente a mitocondria, foram avaliadas a localização, morfologia e a actividade deste organelo foram avaliadas. Estudos de expressão genética foram realizados de modo a inferir sobre o estado geral de vias metabólicas como sendo a glicolise, via das pentoses fosfato e o ciclo do acido tricarboxilico. Por ultimo, baseando-nos na possível similaridade com células tumorais, avaliamos os níveis de proteína para alguns elementos chave envolvidos na regulação metabólica. Os resultados obtidos permitem concluir que a assinatura metabólica das células estaminais pluripotentes induzidas não ‘e igual a de células estaminais embrionárias. Contudo estes dois tipos de células estaminais agrupam-se aquando da analise da expressão genética. A analise da actividade mitocondrial permitiu obter valores de ATP, lactato e consumo de oxigénio compatíveis com um perfil metabólico glicolitico. Curiosamente, no seu conjunto, os resultados realçam algumas possíveis estratégias para manter níveis elevados de glicolise, como

sendo níveis proteicos elevados de Hexokinase II e uma piruvato desidrogenase inactiva. Artigos científicos recentes provaram que para haver reprogramação de uma célula somática a célula pluripotente, primeiro o metabolismo dessa célula terá de se tornar glicolitico e só apos esta alteração ‘e que os genes responsáveis pelo estado de pluripotencia são activados. Para alem disso, outros estudos demonstraram que a manipulação da via das pentoses fosfato permite um controlo na diferenciação celular. No seu conjunto, estes estudo reenfocaram a nossa hipótese central e por isso mesmo, os nossos objectivos seguintes centraram-se na inibição farmacológica dos dois alvos identificados no primeiro objectivo. Com o intuito de bloquear o primeiro passo da glicolise, a Hexokinase II foi inibida recorrendo ao fármaco 3-Bromopiruvato que actualmente ‘e usado em ensaios clínicos na luta contra o cancro. A pluripotencia foi avaliada, bem como a função mitocondrial. No geral, foi possível concluir que a pluripotencia foi afectada sem uma alteração metabólica obvia. No entanto, foi possível observar um efeito negativos a nível proteico para p53 e c-Myc. Como controlo para as nossas experiencias, crescemos células sem LIF que ‘e essencial para a pluripotencia. Em normoxia a glicose ‘e convertida a piruvato que, por sua vez, pode ser metabolizado na mitocondria pela piruvato desidrogenase (PDH) originando acetil- coenzimA. Esta enzima possui uma subunidade (E1-α) que funciona como um interruptor regulado por processos de fosforilacao/desfosforilacao. A enzima responsável pela fosforilacao e consequente inibição, da PDH ‘e a piruvato desidrogenase cinase que possui quatro isoformas (PDHK1-4). Uma vez que os resultados no primeiro objectivo demonstram que uma forma inactiva da PDH poderá ser benéfica para as células estaminais pluripotentes, o ultimo objectivo consistiu em clarificar se a inibição da PDHK poderia comprometer a pluripotencia nestas células. A actividade da PDHK foi inibida recorrendo ao fármaco acido dicloroacetico (DCA), que também se encontra em ensaios clínicos oncológicos. Os resultados obtidos permitem concluir que na presença de DCA as células estaminais embrionárias começam a diferenciar demonstrando alterações na função mitocondrial bem como na sua capacidade de proliferação. Para alem de um efeito negativo na pluripotencia os resultados presentes neste capitulo permitem inferir sobre possíveis vias activas na regulação metabólica nestas células, demonstrando mais uma vez, a semelhança com as células tumorais e que ao regular o estado da PDH, PDHK poderá funcionar como um elemento chave na regulação metabólica constituindo um possível alvo para modulação do mesmo. Como conclusão geral, podemos inferir que efectivamente, as células estaminais embrionárias beneficiam de um metabolismo mais glicolitico com uma PDH inactiva e que uma perturbação nestes factores leva ‘a perda de pluripotencia. Curiosamente, as vias de sinalização possivelmente envolvidas nesta regulação são efectivamente semelhantes as presentes em células tumorais. De um modo geral, os resultados presentes nesta dissertação permitem um esclarecimento sobre o status/regulação metabólica nestas

células e demonstra que uma actividade normal de enzimas como a Hexokinase II e PDHK são importantes para a pluripotencia celular.

General Introduction

Chapter 1

Partially based on:

João Ramalho-Santos, Ana Sofia Rodrigues. Justin C. St. John Stem Cell Biology and Regenerative Medicine Mitochondrial DNA, Mitochondria, Disease and Stem Cells 2013 10.1007/978-4. From Oocytes and Pluripotent Stem Cells to Fully Differentiated Fates:(Also) a Mitochondrial Odyssey.

1.1 A little bit of history about pluripotent stem cells:

When Evans, Kaufman and Martin derived the first embryonic stem cells (ESC) a new exciting era in science began [2,3]. The capacity to unlimited self-renew coupled to their ability to differentiate into cells from all the three germ layers [4] have put ESC in the spotlight for their potential in clinical applications, such as cell therapy replacement and turn them into a very powerful tool in developmental research. However, research focusing on pluripotent stem cells had truly begun in the 1950's with the study of teratocarcinomas, which presented cells - embryonal carcinoma cells (ECC) - capable of unlimited self-renewal and differentiation into cells from different lineages establishing, for the first time, the concept of a pluripotent stem cell [5]. Research continued focusing on these cells, defining culture conditions and specific cell surface markers [6,7].

ESCs were first derived by explanting blastocysts. Basically, by allowing the inner cell mass (ICM) cells to migrate from the blatocyst they will attach to a "feeder" layer of cells (mitotically inactivated fibroblasts) in a medium similar to the one used for the ECC [2,3]. Pluripotency was assessed by injection of these cells into the ICM of another blastocyst, which yielded chimeric mice with extensive contribution from the injected ESC progeny to all tissues, including functional colonization of the germline [4]. In 1998, Thomson's group established the first ESC line derived from a human embryo [8] and 8 years later another major breakthrough was accomplished with induced pluripotency, when Yamanaka's group turned mouse fibroblasts into induced pluripotent stem cells (iPSC) by transfecting the fibroblasts with four factors (Yamanaka's factors) Oct4, Sox2, c-Myc and Klf4 [9].

Since 1981 huge advances have been accomplished in the stem cell field, regarding differentiation into different cell types, how the pluripotency circuit works in these cells or the role of epigenetics.

More recently mitochondria and metabolism have become a major topic of interest, and will be discussed ahead.

1.2 Stem cells throughout development:

Given the promise that stem cells hold it is important to start by introducing some basic concepts. A stem cell is characterized by its ability to constantly and perpetually self-renew and by its differentiation potential [2,3,8].

If it is easy to define self-renewal as a specific cellular action that involves cell division in which at least one of the progeny must be an undifferentiated cell, talking about differentiation potential is not as simple [10,11]. In order to address this last topic we must take into consideration that embryogenesis is a process in which the totipotent zygote progressively loses its developmental capacity, meaning that the differentiation potential becomes limited with development [12,13]. While the zygote has the ability to develop into all embryonic and extraembryonic tissues, with cell divisions and development commitment when the embryo reaches the blastocyst stage two types of cells will be present. The trophectoderm (TE) cells – oligopotent cells - that have the ability to only generate extraembryonic tissues and the Inner Cell Mass (ICM) cells – pluripotent cells – that will give rise to all the different cell types in the embryo and other extra embryonic tissues [4,14].

As development continues the embryo reaches the late blastocyst stage, and after cavitation the ICM becomes partitioned into two layers with different differentiation potential. While the hypoblast can only give rise to primitive endoderm, the epiblast is pluripotent and will originate the three primordial germ layers (ectoderm, mesoderm and endoderm). Cells constituting each germ layer are

multipotent given that, at this point in development, they can only originate cells from the same lineage. When the embryo cells are fully committed they are designated as unipotent because they will only sustain one cell type such as some adult stem cells (ASC) [12]. Taking into account that the object of this study was embryonic stem cells, this introduction will not focus on ACS. However it is important to mention that ASC are postnatal derivates of ESC that have been described in different organs. Their ultimate purpose is to regenerate tissues, which justifies their wide distribution throughout the adult body. Some types of ASC include hematopoietic, adult spermatogonial, neural, intestinal and muscle stem cells among others, for review see [12,15].

In conclusion we can state that a stem cell represents a cell capable of indefinitely self-renewal with a capacity to differentiate into a wide range of cell types according to its differential potential. These characteristics are extremely interesting and promising in research [16].

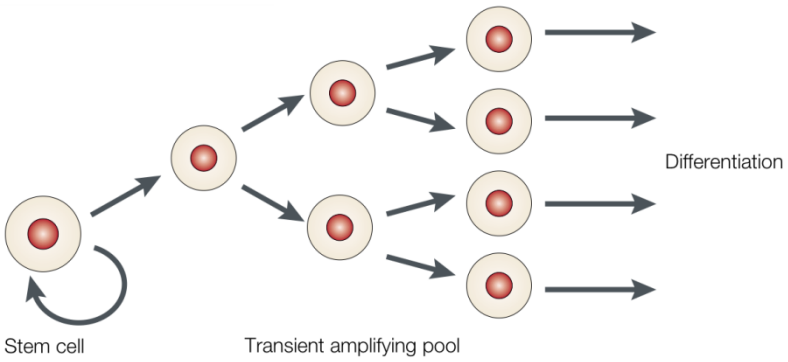

Figure 1.1. Schematic representation of a stem cell: A cell with the ability to enter the cell cycle in order to promote proliferation producing a transient pool of cells that have the ability either to maintain an undifferentiated state or under specific cues will differentiate according to their differentiation potential. Adapted from Knoblich JA, Nature reviews (2001).

1.3 Characteristics of Pluripotent Stem cells (PSC):

Stem cell biology is currently one of the areas of major interest for the scientific community due to their tremendous potential as a model to study development and perform research with distinct goals, ranging from drug screening to the cell therapy [17]. Before introducing different types of pluripotent stem cells (PSC), in the next sub-sections, some considerations should be made regarding different characteristics that define these cells, summarized in table 1.1.

1.3.1 Morphology, chromosome stability and telomere length:

In order to characterize PSC some features should be taken into consideration such as morphology, karyotype and telomerase activity. Such analysis are important given that usually PSC populations can be highly heterogeneous and understanding this heterogeneity might be necessary to assess the pluripotent state of the cells [18]. Moreover, it's important to note that different types of PSC will differ with respect to some of the pluripotency markers and growth factors required for the maintenance of self-renewal, especially when we take into consideration species-specific characteristics.

In general, PSC will grow in colonies, with very well defined borders, and tightly packed cells characterized by high nuclear/cytoplasmatic ratios with some species-specific differences. For instance, mouse embryonic stem cells (mESC) grow as three-dimensional colonies whereas human embryonic stem cells [1], iPSC and epiblast stem cells (Epics) grow in thin and larger colonies. The maintenance of a stable diploid karyotype (46, XX or XY and 40, XX or XY in the human and mouse, respectively) over extended periods of culture is extremely important to avoid genomic instability involves high frequency

of mutations that include changes in nucleic acid sequences, chromosomal rearrangements or aneuploidy, which could result in diseases such as cancer. Therefore, cytogenetic analysis monitoring their stability should be performed regularly. Eukaryotic chromosomes are capped by structures called telomeres, which function to maintain chromosome integrity. The synthesis of the telomeric repeats is carried out by Telomerase reverse transcriptase (TERT). As observed for most of the immortalized cells, PSC also presents high TERT activity in order to maintain their telomere length for unlimited proliferative capacity [8,19,20].

1.3.2 Differentiation potential:

A PSC should be able to originate all cells of the organism and there are some research tools available to assess this pluripotency potential. In the case for mESC we can inject this cells in blastocysts and produce a chimeric mouse that is germ line competent, or produce a whole mouse by tetraploid complementation. In the tetraploid complementation method mESC are injected in a 4n blastocyst and only these injected cells will be able to originate all the cells of the organism, whereas, the 4n cells of the original blastocyst will give rise to the placenta [21]. The stringent method for evaluating PSC derived from humans is the *in vivo* assay of Teratoma formation. Teratomas are produced by introduction of PSC into immunodeficient mice via subdermal, intratesticular, intramuscular, or kidney- capsule injection. Once introduced to the host, pluripotent cells will develop into teratocarcinomas-like structures that contain cells from all three lineages. In addition, the differentiation potential of PSC can be assessed *in vitro* through embryoid body (EB) formation. By culturing these cells in suspension spontaneous

differentiation will occur and form clusters of differentiated cells that are called EBs. EBs gene expression reveals the presence of specific markers for all germ layers [22].

1.3.3 Surface markers:

Specific surface markers including glycolipids and glycoproteins can identify PSCs. The surface markers that characterize human and mouse PSCs differ, similarly to what has been reported for mouse and human ECCs. While human PSCs are positive for the globo-series glycolipid antigens, stage specific embryonic antigen-3 (SSEA-3) and -4 (SSEA-4), and the keratin sulfate antigens TRA-1-60, TRA-1-81 and GCTM-2, mouse PSC lack these markers and express SSEA-1[23].

1.3.4 The three main transcription factors in pluripotency:

Although there are differences between human and mouse PSCs regarding surface markers and even growth factor dependence (which will be addressed ahead) all PSCs have in common three specifically active transcription factors (TF) responsible for self-renew and pluripotency, namely Nanog, Oct-4 and Sox2 [24,25,26]. Each factor will be briefly introduced and the intricate pluripotency network involved will be dicussed latter on.

The transcription factor **POU5F1 (known as Oct4)** belongs to the POU family of genes that regulate gene transcription. There are two variants resulting from alternative splicing, Oct4A that is present in the cell nucleus and has a role in maintaining pluripotency and Oct4B that localizes in the cytoplasm and it is not involved in pluripotency mechanisms. The interesting feature about this TF relies on its ability to function as a gatekeeper, meaning that transcription levels must be maintained under a certain range given that overexpression of Oct4 will result in differentiation to endoderm or mesoderm, whereas a decrease will lead to differentiation towards trophectoderm. This way, it can either contribute to pluripotency or to lineage specification [27,28]. This central role of Oct4 in pluripotency is particularly clear when we consider reprogramming experiments for iPSC, where Oct4 is one of the reprogramming factors, that usually also include Sox2, Klf4, and c-Myc [12] but while the last three can be replaced without Oct4 reprogramming doesn't occur. Oct4 often acts cooperatively with the SRY-box- containing transcription factor Sox2 [29] and with key transcription factor Nanog [30], so these two TF should also be taken into consideration [4].

The transcription factor **SRY-type high mobility group box 2 (Sox2)** belongs to a large family of proteins that present a high mobility group (HMG) DNA binding motif. During mouse development Sox2 mRNA is detected in the oocyte, blastomeres, ICM, epiblast and germ cells, and its expression persists in the extraembryonic endoderm and in precursor cells of the central nervous system. In order to have a role in pluripotency maintenance, and similarly to Oct4, Sox2 expression levels must be kept within a certain range. Downregulation of Sox 2 results in differentiation of both mESC and hESC towards the trophectoderm lineage, while moderate Sox2 overexpression seems to direct differentiations to other cell fates [31]. The resemblance in phenotypes for loss of both TF and their expression patterns is

attributed to the cooperative action of Oct4/ Sox2 in controlling several ESC-specific genes, including themselves [32,33].

Nanog has a critical role in embryo development given that its expression is maximal throughout the morula, late blastocyst and then becomes restricted to the epiblast disappearing upon implantation being only present latter on in primordial germ cells (PGCs) [24] . *In vitro*, Nanog is present in pluripotent cell lines whereas in the adult tissues it is absent. Mouse embryos lacking Nanog fail to develop beyond the blastocyst stage due to the absence of the epiblast. It is possible to derive mESC from Nanog null blastocysts; however, these cells tend to differentiate towards the extraembryonic endoderm lineage [34,35]. Nanog has a single homeodomain DNA-binding region and it's the only TF whose overexpression allows proliferation of mESC in the absence of LIF (growth factor for mESC), prevents neuroectoderm differentiation and circumventing the need for both TGFβ and FGF signaling in the maintenance of hESC self-renewal. In contrast low or undetectable levels of Nanog lead to differentiation of mESC towards primitive endoderm and hESC into extraembryonic cell lineages [24,36]. However, in vitro, some of these cells can reexpress Nanog and generate undifferentiated ESC colonies, so we can conclude they are not yet fully committed [26,34].

Table 1.1 - Differences and similarities between mouse and human PSC. Summary for some of the major characteristics of EpiSC, iPSC and ESC, the species-specific differences were also distinguished by separating human and mouse PSC.

Properties	hEpiSCs	hiPSCs	hESCs	mESCs
Morphology				
Colonies	+	+	+	+
Tightly packed cells	+	+	+	+
Chromosomal Stability	+	+	+	+
High Telomerase activity	+	+	+	+
Cell surface marker				
SSEA-1	-	-	-	+
SSEA-3	+	+	+	-
SSEA-4	+	+	+	-
TRA-1-60	+	+	+	-
TRA-1-81	+	+	+	-
GCTM-2	+	+	+	-
Alkaline Phosphatase	+	+	+	+
Core of Transcription Factors				
Nanog	+	+	+	+
Oct-4	+	+	+	+
Sox 2	+	+	+	+
Other Transcription Factors				
Rex 1	-	+	+	+
FGF5	+	+	+	+
Alkaline Phosphatase	-	+	+	+
Differentiation Potential				
Embryo Bodies	+	+	+	+
Teratoma Formation	+	+	+	+
Chimeras	not tested	not tested	not tested	+

Signaling required for pluripotency				
LIF	-	-	-	+
bFGF	+	+	+	-
BMP	-	-	-	+
Activin/Nodal	+	+	+	-

1.4 Different types of Pluripotent Stem cells:

It is reasonable to consider that if we isolate cells from different states of embryo development, we should have different type of PSC. Accordingly, we can derive pluripotent cells lines for long-term culture from distinct cell populations such as: embryonal carcinoma cells (ECC); epiblast stem cells (EpiSC) derived from an embryonic day (E) 5.5-E6.5 of a mouse epiblast; embryonic germ cells (EGC); primordial germ cells (PGC) from E8.5-E13.5 mouse; spermatogonial stem cells (SSC) and, embryonic stem cells (ESC) from the inner cell mass of a mouse blastocyst E3.5. All the above PSC are going to be introduced, however special focus will be given to ESC and iPSC, the main PSC used for the research presented in this thesis.

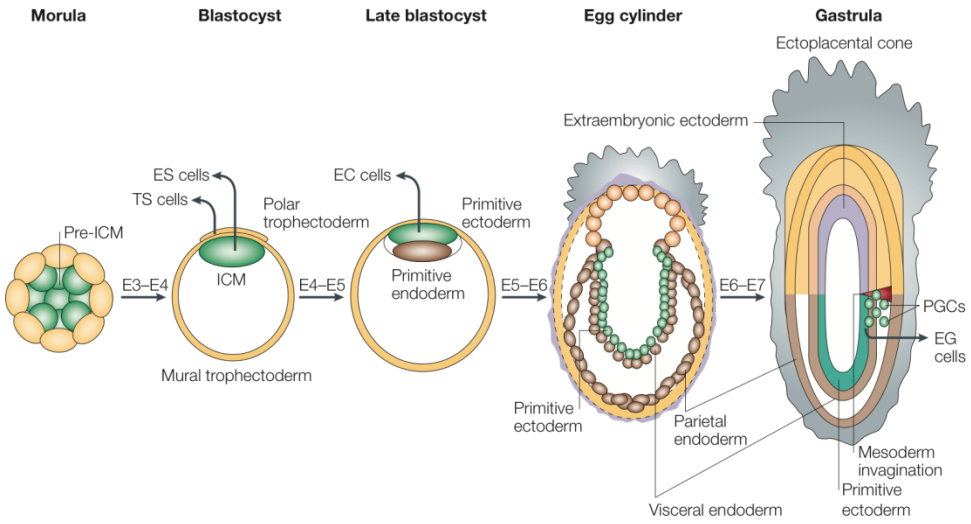

Figure 1.2. Schematic representation of the sites of pluripotency in the developing mouse embryo. The first pluripotent cells in the embryo appear as the ICM of the blastocyst by E3.5. This is followed by ICM segregation into the primitive endoderm and epiblast in the late blastocyst. EpiSCs are derived from the postimplantation epiblast at E5.5. After implantation, the pluripotent cells become restricted to the germ line when they develop into PGC E6.5. Adapted from [37].

1.4.1 Embrynomal carcinoma cells (ECC):

As introduced in the first topic of this introduction, ECC were the first type of PSC to be derived from teratocarcinomas and were extremely useful to establish the concept of stem cell and *in vitro* culture conditions for stem cells [5]. ECC created the framework to the study of pluripotency and differentiation potential. However due to their limitations, regarding the latest, and by having no contribution to germline transmission in chimeras, ECC were put aside in research, especially with the appearance of other types of PSC that have a real potential in clinical applications [38].

1.4.2 Epiblast stem cells (EpiSCs):

As introduced in topic 1.2, with cavitation, ICM becomes partitioned into two distinct layers, the primitive endoderm (hypoblast) and the epiblast cells [39]. The formation of this last layer is dependent on Nanog expression. The hypoblast layer is thought to be form due to the secretion of paracrine factors from the epiblast [40,41,42]. EpiESCs from pre-implantation epiblast and rodent ESC have been denominated as "naïve" stem cells given the two activated X chromosomes in females and expression of pluripotent associated transcription factors Oct4, Sox2 and Nanog. In opposition, when one X chromosome is inactivated but the expression of the pluripotent factors remains the cells are called primed [43,44].

A large nuclear/cytoplasm ratio and prominent nucleoli is also present, but in terms of morphology they grow in two-dimensional and epithelial colonies, they do not survive efficiently as isolated single cells and are dependent on bFGF/activin combination. Because of these similarities with hESCs it is believed that both types of PSCs represent the same developmental state [45], however the epiblast is not a fixed state, which could justify why there is not a defined set of markers to identify EpiSCs. Although they express Oct4, other transcription factors can either be absent or present in reduced levels. Instead, they present higher expression of factors existing in the post-implantation epiblast, such as Fibroblast growth factor 5 (FGF5) and Brachyury [4,40,42,43,45].

1.4.3 Embryonic germ cells (EGCs), Primordial germ cells (PGCs) and Spermatogonial stem cells (SSCs):

During fetal development embryonic germ cells (EGCs) as well as germ line stem cells from neonatal mouse testis are pluripotent and have a differentiation potential similar to ESCs. Just prior/during gastrulation, mouse germ cells are identified as a cluster of cells that are called primordial germ cells (PGCs). Following establishment of the initial germ cell population, the PGCs expand in number and eventually migrate from the extra-embryonic spaces into the nascent embryonic gonads. All of the immature germ cells migrate to the basement membrane of the seminiferous tubules where they differentiate into spermatogonial stem cells (SSCs), which will provide cells for sperm differentiation throughout male adult life [46,47,48]. Their pluripotency potential has been explored in research as alternatives for the use of ESC in tissue replacement therapy, for review see [49].

1.4.4 Embryonic Stem Cells (ESCs):

Due to their self-renewal and differentiation abilities into cells from three germ layers ESC can be considered as “blank sheets” capable of responding to endogenous and external signals that will determine their fate. Both mouse and human ESCs will be addressed.

An important feature of ESCs is the ability to maintain these cells in culture for unlimited time, conferring almost a immortal state, which is accomplished due to the characteristics already described and summarized in table 1.1 [8,50]. The self-renewal ability it’s intrinsically linked with the cell cycle. ESCs present a shortened cell cycle with a very high percentage of cells in S phase, when compared with

differentiated cells, with an almost non-existent G1 phase [51,52]. mESC for instance, have a doubling time of about 8-10h, which is a consequence of the cell cycle profile just described. If cell-cycle regulation is very well described for these cells, the same does not happen for hESC which grow much slower with a doubling time of about 30-36h, which is probably a species-specific feature [53,54]. Interestingly, more recent reports have shown that cell cycle genes such as p27KIP, Cyclin D1, and p53 play an important role in pluripotency of hESCs and iPSCs cells respectively, demonstrating the importance of such a cell cycle profile in pluripotency. [55,56,57,58].

As already mentioned, there are some common morphological features of ESC for both species (table 1.1). Most chromatin in these cells is euchromatin, meaning that chromatin is in an open state allowing transcription to occur if necessary [59,60]. Also, regarding colony morphology, mESCs differ from hESCs, given that the former tend to form colonies shaped as a doom, in a three-dimensional arrangement, and the latter form flatter and bigger colonies. Another interesting different feature between the two species involves the X chromosome, while female mESC lines have both X chromosomes activated female hESC lines, in their vast majority, present complete or partial inactivation of one of the chromosomes [61].

Culture conditions are also different for both types of ESCs, which is manly due to the fact that they respond to different extrinsic growth factors in order to maintain pluripotency. mESCs will respond to the leukemia inhibitor factor (LIF), a cytokine member of the family of interleukine 6 (IL6) and bone morphogenic protein 4 (BMP4) [4,62]. hESCs will maintain pluripotency in the presence of basic fibroblast growth factor (bFGF or FGF2) and a combination of Activin/Nodal signaling pathways (table 1.1). More interesting is the fact that hESCs in the presence of BMP4 will differentiate into trophectoderm and LIF is incapable of sustaining a pluripotent state, demonstrating that the

pluripotency signaling occurs through different pathways, although with the same ultimate goal: to activate transcription of the core pluripotency genes [63,64].

1.4.5 Induced pluripotent stem cells (iPSCs):

For some time nuclear plasticity has been a hot topic of research, namely in trying to revert the loss of development potential that occurs with differentiation. ESCs have helped to better comprehend the plasticity of the cell, as have experiments such as nuclear reprogramming (term used to describe either functional or molecular modifications of cells undergoing cell fate changes) and formation of pluripotent tetraploid hybrid cells which basically demonstrated that somatic cells are able to generate viable cloned animals, in the first case, and that a fully differentiated cells will be reprogrammed if fused with ESCs in the second. Somatic cell nuclear transfer (SCNT) is also another used methodology and consists basically in substituting the nucleus of an oocyte with a donor nucleus of another cell. This process is also known as cloning [3,59,65,66,67].

One big achievement in this area was accomplished when Yamanaka's group was able to identify four factors, Oct-4, Sox 2, Klf4 (Kruppel-like factor 4) and c-Myc that when retrovirally expressed were sufficient to reprogram adult mouse fibroblasts into mESCs like cells (so called induced pluripotent cells – iPSCs), [9,68,69] forcing differentiated cells to express pluripotency factors that otherwise would be silenced. This resulted in morphological alterations and the bypass of the epigenetic barrier that differentiation imposes, with the cells obtaining a pattern of DNA methylation and histone modifications (epigenetic status) characteristic of PSCs [12,70]. This way, a new technology was discovered to alter the somatic state of a cell into a pluripotent one: induced pluripotency had emerged.

The advent of iPSCs brought a new set of challenges and hopes to potential clinical application of PSCs given that patient specific iPSCs could be derived to provide a source for autologous cell replacement therapies and disease-specific iPSCs may be use to dissect molecular mechanisms of disease progression and development of new pharmaceuticals. Since 2008, iPSCs have been studied in order to properly understand how the cell can be reset at several levels, including the epigenome, proteome, morphology and biochemistry [71,72,73]. This has been done mostly by comparing iPSCs to ESCs and those studies demonstrated that both cells types share common features in terms of cellular/colony morphology; expression of surface markers, can be kept in culture for long periods of time, and present the same karyotype stability, although iPSC tend to be prone to more chromosomal abnormalities then ESC [68,74]. High telomerase activity was also present in iPSC, which also have the differentiation potential to develop teratomas, form chimeras and give rise to viable embryos. It is important to note, that iPSC lines do present more heterogeneity in terms of differentiation potential then ESC lines [75,76].

Although presently there are different combinations of factors and delivery systems used to form iPSC, there is accordance with the fact that three phases must occur for successful reprogramming: initiation, maturation and stabilization. The initiation phase is characterized by morphological alterations in which it is possible to observe a mesenchymal – to – epithelial transition accompanied by an upregulation of BMP signaling. During the maturation phase, cells that will become PSC will repress the induced transgenes and activate the endogenous pluripotency network, allowing the cells to enter the stabilization phase [71,77].

More importantly, genome wide analyses revealed two major points of gene activity that corroborates with proteomic studies (large scale studies of proteins focusing in particular on their structure and function). In the first point activation of genes involved in proliferation, metabolism and

cytoskeleton organization occurs in parallel with induction in protein levels responsible for RNA processing, chromatin organization, mitochondria, metabolism and cell cycle. These alterations would occur in the initiation phase, and with transition for maturation and stabilization phase, the second major point of gene activity will take place, with the expression of genes for stem cell maintenance and embryonic development, allowing the activation of the core pluripotency network and acquisition of a stable pluripotent state. During this phase glycolytic enzymes have a crescendo augmentation demonstrating that metabolism also needs to be altered in order to achieve pluripotency [72,73,78,79,80,81]. The similarities between iPSCs and ESCs are summarized in table 1.1.

1.5 How stem cells keep themselves pluripotent:

Pluripotency in the embryo is only transient as differentiation progresses and cells become restricted in their developmental potential. In order to understand pluripotency in ESC we should begin with pluripotency in the embryo and briefly explain the role of the three major players in the pluripotency network: Oct4, Nanog, Sox2.

Regarding PSCs, a signaling pathway needs to be activated in order to promote transcription/regulation of these factors or inactivate them if differentiation is to occur.

1.5.1 How the embryo loses pluripotency:

The presence of Oct4 can be detected as early as in fertilized oocytes, zygotic Oct4 expression begins upon the first divisions and uniform amounts of the protein can be observed in all blastomeres. As the embryo begins to polarize which ultimately results in the formation of the blastocyst, Oct4 expression decreases in the outer layer of the morula state and became undetectable in the trophectoderm of a mature blastocyst while in the ICM Oct4 levels are maintained.

It is only when the epiblast and hypoblast are formed that Oct4 presents a different expression pattern, being present only in the first layer of cells. With progressive gastrulation, Oct4 levels start to decrease due to repression on transcription and it will only be detected in the newly established PGCs. These cells will continue to express Oct4 as they proliferate and migrate to form the genital ridges. It is important to note that recent studies have shown that during development, Oct4 will interact alternatively with Sox17 or Sox2 to induce differentiation or maintain pluripotency, respectively [29,82,83,84,85,86].

1.5.2 Extrinsic factors that act in ESC:

As demonstrated in a previous point and noted in table 1.1 the exogenous signals necessary to maintain mESCs and hESCs vary, which in the end will be reflected on the chemical defined media used in the laboratory to culture these cells. mESCs will be addressed first, and when culturing these cells, media must be supplemented with leukemia inhibitor factor (LIF) otherwise cells will differentiate [62].

LIF exerts its function by binding to its heterodimeric receptor LIFR/gp130 promoting the activation of the signal transducer and activator of transcription-3 (STAT3). This activation occurs because the tyrosine kinase Janus [87] is recruited and STAT3 will bind to phosphotyrosine residues on the heterodimeric receptor, then phosphorylated dimers of STAT3 will translocate to the nucleus where it can function as a transcription factor regulating several pluripotency genes. Another activated pathway occurs upon the binding of LIF that will activate the phosphoinositide 3 – Kinase (PI3K) resulting in the activation of AKT leading to the downstream inhibition of the glycogen synthase-kinase 3 (GSK3) [4,88,89]. As a result NANOG and C-MYC (regulates cell cycle, proliferation, growth, differentiation and metabolism) levels will increase, given that they are targets of STAT3. LIF removal from the culture media of mESCs will lead to differentiation and increase in the levels of phosphorylated GSK3 kinase, which promotes c-Myc degradation [64,90].

Regarding how BMP4 functions in order to promote pluripotency there are still some questions, however it is known that in the presence of LIF, BMP4 contributes to the LIF cascade by activating similar to mothers against decapentaplegic homologue 1/5 and 8 (smad) proteins which, in turn, activate the transcription of inhibitors of differentiation genes (Id). An alternative effect of BMP in blocking mESC differentiation is achieved by impairing P38 MAP kinase activity [91,92].

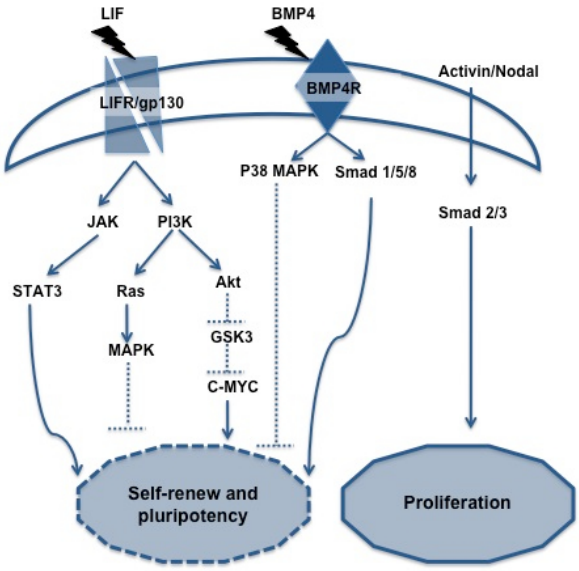

Figure 1.3. Schematic representation of the key signaling pathways required for maintaining pluripotency of mESCs. LIF signaling activates JAK– STAT3 to induce target genes essential for pluripotency, such as c-Myc, which is also regulated negatively by glycogen synthase kinase-3 (GSK3) β via inhibitory phosphorylation. LIF also induces MAP kinase activation, which antagonizes self-renewal. BMP signals potentially function in two ways: activation of Smad1/5/8-Id gene and suppression of p38 MAP kinase. Activin A has been shown to contribute to mESC proliferation but not pluripotency. BMP: bone morphogenetic protein; LIF: leukemia inhibitory factor

Taking hESCs into consideration, we find species related differences regarding the integration of extrinsic factors and activated signaling pathways in order to sustain pluripotency. LIF is not sufficient to maintain pluripotency, and the addition of BMP4 will induce differentiation towards trophectoderm [93]. hESCs rely on a combinated action of bFGF and Activin/ Nodal to maintain pluripotency and self-renewal (table 1.1). It should not be surprising that media composition for hESCs include addition of bFGF, known for increasing the cloning efficiency [94].

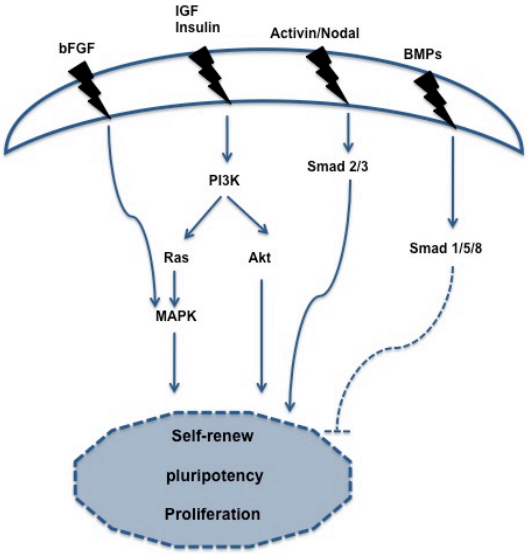

Figure 1.4. Schematic representation of the key signaling pathways required for maintaining pluripotency of hESCs. bFGF is an essential factor for hESCs self-renewal and functions. Also, Activin/Nodal signaling is essential to support hESCs self-renewal via activation of Smad2/3, resulting in upregulation of Nanog and Oct4 transcription. In contrast to mESC, BMP promotes hESC differentiation toward trophectoderm. PI3K–Akt pathway is also essential for hESC self-renewal although down-stream effectors and targets have not been defined. BMP: bone morphogenetic protein; bFGF: fibroblast growth factor.

hESCs have Transforming growth factor beta (TGFβ) type I and type II receptors that respond differently to Activin A, Nodal, TGFβ and BMP4. The first three factors bind specifically to the TGF type II receptors whereas BMP4 binds preferentially to TGFβ type I receptors. If type II receptors are activated, Smad 2 and 3 will be phosphorylated and active, interacting with Smad 4 that will translocate to the nucleus where it will bind to specific elements regulating gene expression towards pluripotency. In contrast, if type I receptors are activated Smad1, 5 and 8 will became active and promote differentiation [95]. It has been demonstrated that an increase in phosphorylated levels of Smad 2/3 is correlated with an enhancement of pluripotency due to an increase in Nanog levels whereas an increase in Smad 1/5

and 8 will lead to Nanog repression. This way it was established that bFGF and TGFβ signaling promote pluripotency through modulation of Nanog levels [90,92,96].

1.5.3 The molecular network of pluripotency:

Now that the role of extrinsic factors in pluripotency has been clarified, it is time to understand how transcription is affected downstream of those signals. First, pluripotency transcription factor (TF) will bind to the regulatory elements of members of the network, including themselves, forming positive feedback loops among the network members promoting pluripotency and repressing differentiation genes [97] (Figure 1.5).

In order to better understand how these TF cooperate with each other and with other pluripotency genes, genome-wide RNA interference (RNAi) screens, genome-wide chromatin immunoprecipitation (ChIP) and microarray high throughput analyses constitute valuable tools to elucidate the role of others TF involved in this network. Recent studies have clarified that the enhancer region of the OCT4 gene can bind at least 14 TF (Oct4, Sox2, Nanog, Sall4, Tcf3, Smad1, Stat3, Esrrb, Klf4, Klf2, Klf5, E2f1, n-Myc and Zfx) while for the NANOG gene, nine TF are known to bind to its enhancer (Nanog, Klf4, Klf2, Klf5, Sall4, E2f1, Esrrb, Stat3 and Tcfcp2l1). These represent key contact points that have a tremendous importance in regulating the pluripotency network, given that genes that bind more TF are usually more transcribed, whereas genes with low levels of occupancy are normally silenced, suggesting the idea of a cooperative mechanism [98,99,100,101,102]. In fact, it is known that some TF depend on Oct4 binding to the DNA for efficient targeting, because this TF has an anchoring function

facilitating the physical interaction with other TF. As an example, this occurs for regulation of Nanog expression. Nanog promoter contains an Oct-Sox binding motif of 170 base pairs upstream from the transcription start site where some Oct4-associated proteins (Sox2, Esrrb, and Dax1) will bind in an Oct4-dependent manner due to this physical anchoring, promoting NANOG transcription [98,103,104].

Recent reports using these extremely sensitive technologies allowed the mapping of TF binding sites in mESC, uncovering two main centers operating in ESC, the Oct4 and Myc centric modules [98]. The Oct4-centric module includes Oct4, Sox2, Nanog, Smad1, Stat3 and Tcf3. These last three are downstream effectors of signaling pathways controlled by BMP, LIF and Wnt respectively. Oct4 will interact biochemically and physically with some of these factors, including Dax1, Nac1, Tcfp2l1, Esrrb and Sox2 acting as an anchor point for the assembly and maintenance of these multi-protein complexes on the DNA. The other module includes c-Myc, n-Myc, E2f1, Zfx, Rex1 and Ronin; which will bind to sites near transcription start sites [98,99]. Their target genes are associated with protein metabolism and because of this it has been proposed a possible role in cancer cells for this module. Another interesting feature of Oct4, Sox2 and Nanog involve their ability to regulate non-coding RNA such as the clusters mir302 and mir290; which are known for repressing key cell-cycle regulators. These clusters are blocked by *let-7* miRNA that in turn is negatively regulated by Lin28 a known target of the core transcription genes [98,105,106,107].

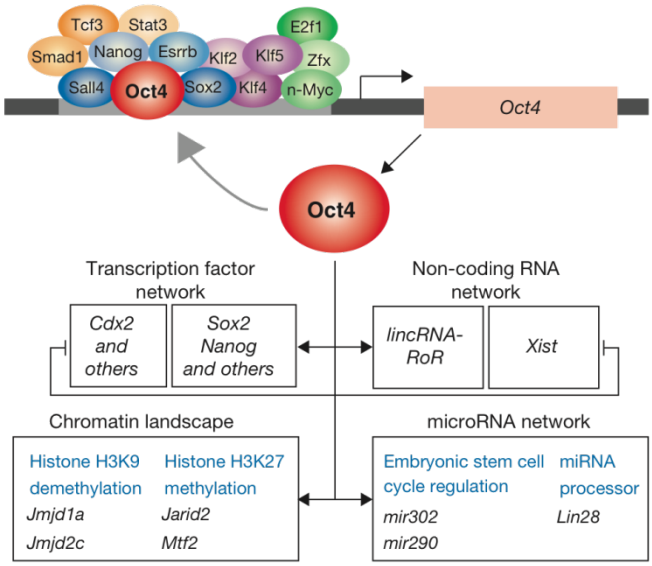

Figure 1.5. Crosstalk between transcriptional regulatory networks in pluripotency. Transcription factor binding site mapping showed that the regulatory regions of the Oct4 gene (light grey) are themselves bound by multiple transcription factors, including Oct4 itself. Oct4 is found to target genes involved in diverse cellular functions (transcriptional regulation, chromatin modifications, and post-transcriptional regulation through non-coding RNAs and microRNAs; bottom).

1.6 Experimental and clinical limitations of PSCs:

There is no doubt that hESC may eventually realize their clinical potential and become the future of tissue replacement therapy, however there are some considerations to point out. Regarding hESC, the fact that in order to derive these cells we will always be dependent on embryos, raises three important questions: the destruction of human embryo; the available number of viable embryos after freezing in fertility clinics and ultimately the quality of the same given that they originate from couples with fertility problems. A secondary problem limiting the use of hESC is the required HLA matching of

the derived cells or tissues to the recipient, requiring a bank of several thousand ESC lines to make tissue therapeutics or gene therapy practical. This last point also raises the question that these cells are difficult to manipulate and most of the differentiation protocols rely on the use of xeno products. Not to mention that if differentiation is not completed for all cells, when transplanted into patients, there is a risk of cancer development. Nevertheless, hESC constitute an extremely valuable system to be used as in vitro models for diseases, early embryonic development studies, drug screening and cancer research.

On the other side, if we consider iPSC, although they represent a major breakthrough because they do not require embryos and it became possible to derive patient specific stem cells (that would limit rejection of the transplanted cells), they also have limitations and some are common with hESC. The xeno products used in culture, the risk of tumurogenesis and the difficulty in maintaining these cells in culture is accompanied by the limitation of the efficiency rate in the process, which is extremely low and expensive. However, it should be noted that induced pluripotency technology allowed the production of iPSC for modeling diseases [108,109].

1.7 Mitochondria and pluripotency:

Present in the majority of eukaryotic cells, mitochondria are dynamic doubled membrane organelles responsible for producing most of the ATP in a cell. Mitochondria are a major regulators of the intracellular energy metabolism, cell death, reactive oxygen species (ROS) production, and signaling pathways. By harboring the oxidative phosphorilative chain (OXPHOS) and the tricarboxilic acid cycle (TCA) as well as the urea cycle, mitochondria has gained a special interest in different research areas related to cancer, metabolic pathologies, aging and more recently in ESC, among others. In this section

some of the main mitochondrial functions will be addressed with particular interest in metabolic regulation by this intriguing organelle [110].

1.7.1 Mitochondrial Structure and functions:

Mitochondria are considered dynamic organelles due to the fact that they can display different morphological arrangements within a cell according to its energetic demands. Therefore, they can present themselves as small individual structures, or an extensive tubular network. No matter what the morphological shape adopted, the most important feature is that they can rearrange this morphological arrangement due to constant fission and fusion events along with cytoskeleton trafficking (mobility events) that alters shape and distribution [111]. There are several proteins involved in this remodeling; the most important ones responsible for fusion are the enzymes Mitofusin1, Mitofusin2 and OPA1. Regarding fission DRP1, a GTPase from the dynamin family is the major key player in this process [112,113,114]. We can distinguish four different mitochondrial structural regions: the outer mitochondrial membrane (OMM) and the inner mitochondrial membrane (IMM) that defines two other compartments: the intermembrane space and the matrix (Figure 1.6B and C). These membranes are completely different from each other. The OMM defines the perimeter and presents a high number of proteins called porins (the voltage-dependent anion channel, VDAC is an example) that are involved in the assembly of transmembrane aqueous channels turning the OMM permeable to the passage of ions and other small molecules. In contrast, the IMM constitutes a very effective barrier and presents a high number of invaginations known as cristae. Most of its weight (76%) is due to the presence of proteins and it is extremely rich in cardiolipin, a lipid that reduces proton permeability and confers fluidity and

stability to the mitochondrial membrane. Its unsaturated nature confers functional specialization and appears to be required for optimal function of many of the proteins and enzymes responsible for mitochondrial energy metabolism [115]. Another very important aspect of the IMM is the protein complexes of the electron transport chain [116] [116] that are responsible for the generation of adenine triphosphate (ATP). Recent studies have shown that cristae organization is more flexible and complex than originally thought, and is directly correlated with ATP demands, meaning that if a cell requires more ATP their mitochondria will have a higher total area of cristae and vice-versa [117,118,119].

Mitochondria present a high degree of genetic and metabolic autonomy although they are integrated as a whole in the cell. This genetic autonomy is characterized by the fact that they have their own genome, mitochondrial DNA (mtDNA) which is maternally inherited and is usually amplified through the maturation process of oocytes [120]. Human mtDNA is a double stranded circular molecule that encodes 13 polypeptides for crucial subunits for the ETC complexes and 22 tRNAs and 2 rRNAs necessary for the translation of these 13 polypeptides (Figure 1.6A). Interestingly, the replication and gene expression of the mtDNA is executed and regulated by enzymes and protein factors encoded by nuclear DNA [14,121].

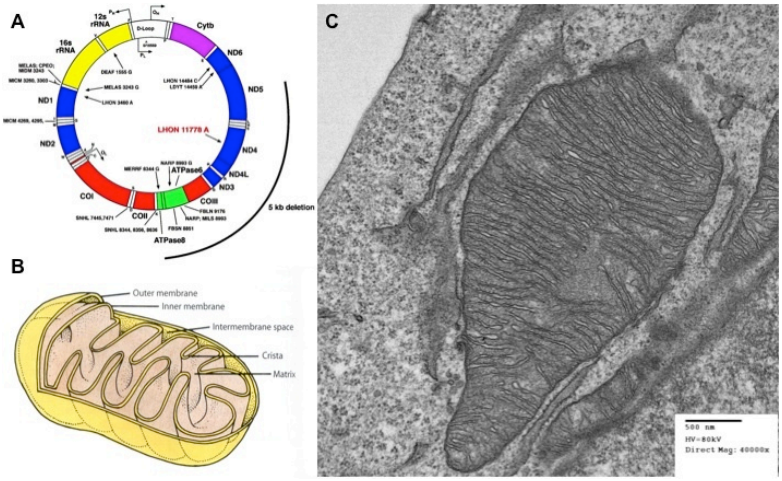

Figure 1.6. Mitochondria structure. A)- Schematic representation of mtDNA. **B)-** Representation of the different compartments found within the mitochondria. **C)-** Electron microscopy picture of mitochondria with extensive number of cristae.

1.7.2 Oxidative phosphorylation (OXPHOS):

Mitochondria are considered the "power houses" of a cell given that they are responsible for providing the majority of cellular ATP through a series of electron transfer processes linked with oxidative phosphorylation (OXPHOS). The cell can up or down regulate this process according to its needs, so it is logical to postulate that each tissue could have its own mitochondrial bioenergetic pattern [122,123]. The mitochondrial OXPHOS system comprises five multi-protein complexes located at the IMM. Complexes I-IV are responsible for electron transfer and compose the mitochondrial respiratory chain. The last complex is Complex V, known as ATP synthase because it produces ATP (Figure 1.7).

Briefly, Complex I (NADH-ubiquinone oxidoreductase) and Complex II (succinate-ubiquinone oxidoreductase) accept electrons from nicotinamide adenine dinucleotide (NADH) and from succinate dehydrogenase-associated $FADH_2$ (reduced flavine adenine dinucleotide), both products from glycolysis and the TCA cycle, respectively. Afterwards the electrons will be delivered to ubiquinone, which is immersed in the membrane. The reduced form of this ubiquinone molecule transfers the electrons to complex III (ubiquinone-cytochrome c oxidoreductase). Cytochrome c then transfers electrons from complex III to complex IV (cytochrome c-oxygen oxidoreductase), where four electrons will reduce molecular oxygen to water (Figure 1.7) [111,124].

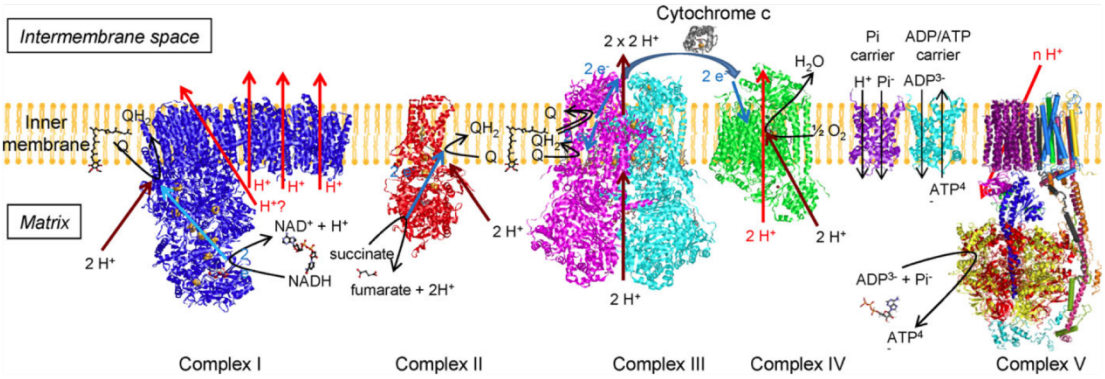

Figure 1.7. Mitochondrial OXPHOS. Pumped protons are in red. Chemical protons are in brown. Electrons transfers are in blue.

The energy transfer involved in this electron transfer pathway allows complexes I, III e IV to pump protons throughout the IMM to the intermembrane space leading to the generation of a proton gradient. This proton gradient forms the protomotive force (Δp) that is composed by two distinct components; one electric (mitochondrial membrane potential-ΔΨm) that results from the charge separation between the two sides of the membrane and one proton concentration-dependent (ΔpH). This proton gradient is then used by the ATP synthase to form ATP [123].

There are other important mitochondrial proteins involved in ATP production, such as the phosphate carrier (phosphate/H^+sinport) and the adenine nucleotide translocator (ANT). This last protein is responsible for the exchange of ADP from the cytosol for ATP [119,124,125,126].

1.7.3 Reactive oxygen species (ROS) and defense mechanisms:

For a normal cellular function, reactive oxygen species (ROS) must be present within a certain physiological range or cellular oxidative stress will occur, so it becomes imperative that ROS production be regulated. ROS include a variety of molecules and free radicals derived from molecular oxygen such as superoxide anion ($O_2^{\bullet-}$) and its conjugated acid hydroperoxyl acid, hydroxyl radical, carbonate radical and peroxyl radical. Although also reactive, hydrogen peroxide (H_2O_2) is a non-radical species as are fatty acid hydroperoxides [127]. ROS and in particular $O_2^{\bullet-}$ can be produced by NADH oxidase, cytochrome P450, lypoxygenase, and mitochondria as byproducts of oxidative phosphorylation. Also, external agents can trigger ROS production. The primary factor governing mitochondrial ROS generation is the redox state of the respiratory chain, which ultimately means that it is governed by the trans-membrane ΔpH and the ΔΨm. $O_2^{\bullet-}$ is formed as a side-product of the respiratory chain by one-electron transfer reactions to molecular oxygen within complex I and complex III. In contrast to complex III, where $O_2^{\bullet-}$ generation is attributed to ubisemiquinone as an electron donor, the site of complex I associated with $O_2^{\bullet-}$ generation is still under discussion, although it is accepted that this complex is the most significant source of $O_2^{\bullet-}$. Moreover, $O_2^{\bullet-}$ is released from complex I to the matrix side of the inner membrane, whereas complex III releases $O_2^{\bullet-}$ to both sides of the inner membrane. The ROS-generating sites have different redox potential, and thus each will respond differently to changes in ΔpH and ΔΨm, resulting in a complex regulation of ROS generation (Figure1.8) [111,128,129].

Excess of ROS can be very problematic, for mtDNA given that it is more sensitive than nuclear DNA to H_2O_2 induced damage, possibly due to the fact that human cells have a limited capacity for repairing mtDNA damage. Because mitochondrial ROS are known to have a higher impact in cellular physiology this section will focus on the production sites of these species [115,129].

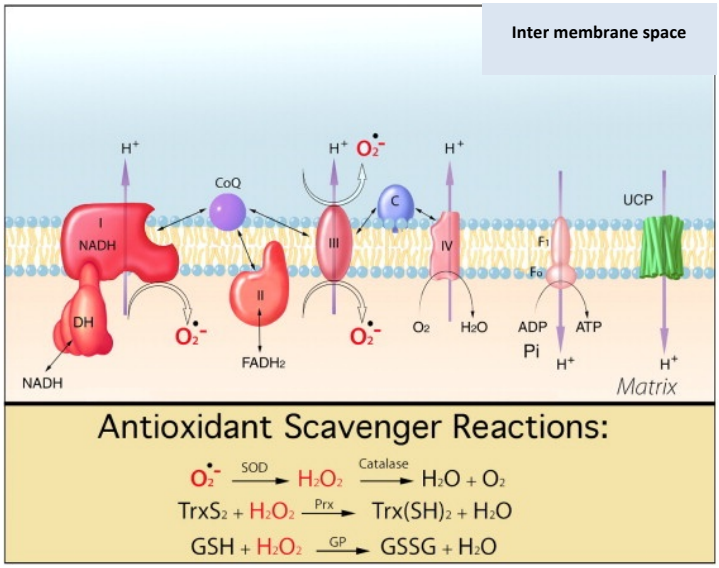

Figure 1.8. ROS Generation in the Mitochondria. The major production sites of superoxide anions are at complexes I and III. Antioxidant enzymes include various isoforms of peroxiredoxin (Prx), superoxide dismutase [130], and glutathione peroxidase (GP). Specific family members of SOD, GP, and Prx are found inside the mitochondria, while other family members localize to the cytosol or extracellular space. The different complexes of oxidative phosphorylation are color coded with regarding the potential for producing ROS, red (complex I) represents the highest and pink (complex IV) the lowest potential. The family of uncoupling protein (UCP), here denoted in green, reduces the overall ΔΨm causing a reduction in ROS formation. Adapted from [127].

Taking into account the physiological importance of ROS homeostasis and the possible harmful effects of ROS, cells have developed antioxidating mechanisms. It is important to note that the low pH of the intermembrane system seems to favor the spontaneous redox reaction in which O_2^- is simultaneously reduced and oxidized to H_2O_2 and O_2 (dismutation of O_2^-), constituting a natural detoxifying mechanism. In terms of enzymatic antioxidant mechanisms, superoxide dismutase [130] [130] exists within the mitochondria and constitutes the primary defense against O_2^-, converting it to H_2O_2. SOD can present different elements in its active side according to its localization, so to detoxify O_2^- in the matrix a SOD that has manganese in its active side (MnSOD) will be needed while at the

intermembrane space the O_2^- will be converted to H_2O_2 by a SOD (also present on the cytoplasm) that contains copper and zinc (CuZn SOD) (Figure 1.8). In mice, inactivation of the mitochondrial SOD, is correlated with a series of disorders such as cardiomyophaty; fibrosis; neurodegeneration; metabolic acidosis; hepatic fat accumulation; DNA oxidative damage, and abnormalities in the ETC and TCA cycle, demonstrating the importance of detoxifying systems. After SOD action, H_2O_2 can migrate to the cytoplasm or stay in the mitochondria. Either way it will be converted to water by catalase or glutathione peroxidase depending on whether it migrates to the cytoplasm or is retained in the mitochondria, respectively [111,127,131].

There are other detoxifying agents besides the ones already described. Cytochrome c for instance, can act as an anti oxidative defense mechanism given that it can be reduced by O_2^-, therefore some of the electrons that escape the ETC can re-reduce cytochrome c. The electron carrier Ubiquinol has been shown to act as a reducing agent when in the presence of succinate and the IMM also contains vitamin E that prevents the propagation of free radical mediated chain reactions. Recently, the mild loss of coupling between the rate of electron transport and ATP production due to the transport of protons back to the mitochondrial matrix (mitochondrial uncoupling), has been suggested as an antioxidant defense given that, by increasing proton leak through the IMM the respiratory chain would act faster, and fewer electrons would theoretically escape. This situation would inhibit ROS production and it would reduce semiubiquinone half-life, which is involved in ROS production. However this mechanism is still controversial [111,119,132].

1.7.4 Fueling the mitochondria: an intricate metabolic network:

The goal of this section is to briefly integrate the different metabolic pathways that keep a cell functioning. In order for OXPHOS to occur properly, mitochondria need NADH and succinate so the complexes can have substrates, but before these substrates become available to the mitochondrial complexes an extensive number of reactions must take place in different cell compartments.

It is important to begin by clarifying the importance of glucose. Glycolysis involves the degradation of glucose in a series of ten reactions yielding two molecules of pyruvate and the energy released during such reactions is converted into ATP and NADH. Another important aspect relies in the fact that glycolysis occurs in both aerobic and anaerobic conditions having two distinct phases. The preparatory phase involves ATP expenditure and begins with activation of glucose by phosphorylation trough Hexokinase action. Resulting D-glucose 6-phosphate is in turn, converted to D- fructose 6-phosphate. Another phosphorylation will convert this last metabolite to D-fructose 1,6- bisphosphate, which will be split to yield two three-carbon molecules of glyceraldehyde 3-phosphate.

Each molecule of glyceraldehyde 3-phosphate will form 1,3-bisphosphoglycerate via the action of glyceraldehyde 3-phosphate dehydrogenase enzyme (GAPDH) and with the conversion of 1,3-bisphosphoglycerate to pyruvate energy will be released, allowing the formation of two molecules of ATP and NADH. This comprises the second phase of glycolysis - called the “payoff” phase because it involves gain of energy in the form of ATP (figure 1.9).

The rate of glycolysis is controlled by several factors, namely: availability of intermediate metabolites and a complex balance between ATP consumption, NADH levels and by regulation of several key enzymes, including Hexokinase which will be addressed in a little bit more detail ahead.

There are three possible routes by which pyruvate can be further metabolized. Under aerobic

conditions, pyruvate is oxidized to yield acetyl-coenzyme A (Acetyl-CoA), which will enter the TCA cycle where the acetyl group is then oxidized completely to CO_2. The second route for pyruvate is its reduction to lactate via lactic acid fermentation and it is usually related with anaerobic situations although this reaction also occurs in aerobic situations such as in erythrocytes or as observed for some type of tumors [133]. This constitutes a way to renovate NAD^+ that is necessary for glycolysis in metabolic situations where oxidative phosphorylation is impaired. This way pyruvate is reduced to lactate by accepting electrons from NADH, resulting in the regeneration of available NAD^+. The third possible route for pyruvate is to be converted to ethanol and CO_2, a process called alcoholic fermentation. All of these represent catabolic processes, however pyruvate can also have an anabolic fate when providing the carbon skeleton for the synthesis of the amino acid alanine [134].

The oxidative decarboxylation of pyruvate into acetyl-CoA is mediated by the pyruvate dehydrogenase complex (PDH) a highly regulated multienzyme complex located in the mitochondria. The PDH complex will also be taken into consideration in more detail in a further section in this introduction in order to provide the framework for this thesis. Acetyl-CoA will then enter the TCA cycle and go through a series of eight cyclic reactions that results in the conversion of this metabolite and oxaloacetate into citrate and two molecules of CO_2 with regeneration of other intermediate metabolites. More importantly, the energy released from these reactions will be conserved in the reduced coenzymes NADH and $FADH_2$/succinate, providing the mitochondrial ETC with electron donors for OXPHOS (Figure 1.9).

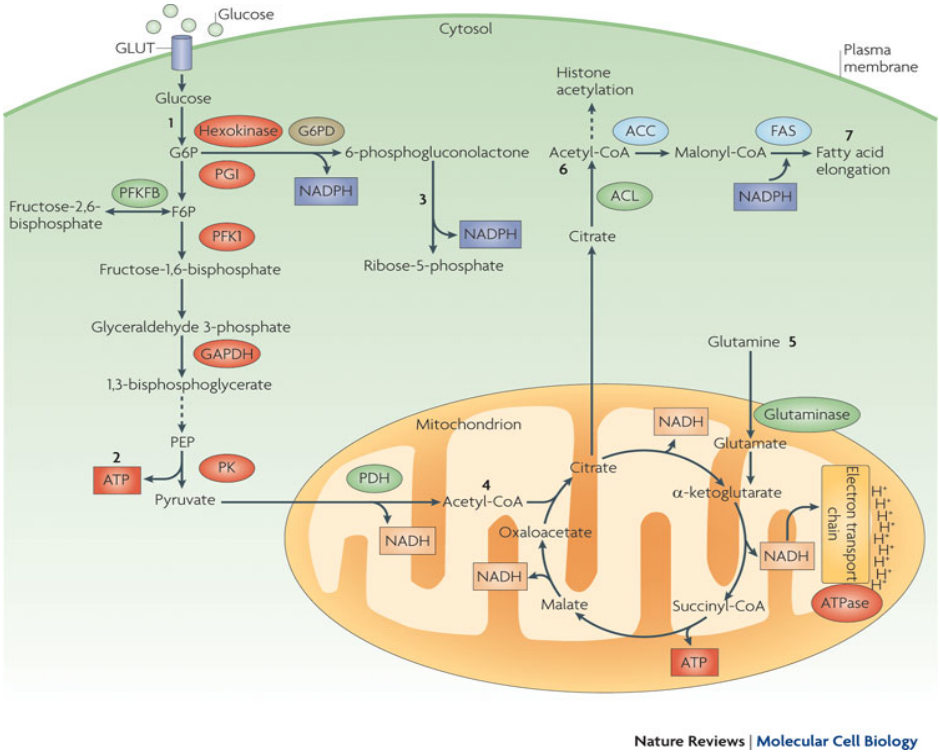

Nature Reviews | Molecular Cell Biology

Figure 1.9. Important metabolic pathways: glycolysis, the tricarboxylic acid (TCA) cycle, the pentose phosphate pathway (PPP) and fatty acid biosynthesis. Glucose enters the cell and is phosphorylated to glucose-6-phosphate (G-6-P) by Hexokinase (1). G-6-P either proceeds through glycolysis to produce ATP, NADH and pyruvate (2), or through the PPP, producing ribose-5-phosphate and NADPH (3). Pyruvate produced by glycolysis is converted to acetyl-CoA, which enters the TCA cycle (4). NADH is then used in mitochondrial oxidative phosphorylation for ATP production. GAPDH, glyceraldehyde-3-phosphate dehydrogenase; GLUT, glucose transporter; F6P, fructose-6-phosphate; FAS, fatty acid synthase; PDH, pyruvate dehydrogenase; PEP, phosphoenolpyruvate; PFK1, phosphofructokinase 1; PFKFB, 6-phosphofructo-2-kinase/fructose-2,6-bisphosphatase; PGI, phosphoglucose isomerase; PK, pyruvate kinase.

1.7.5 Mitochondria in ESC:

There seems to be a paucity of intracellular organization (sometimes discussed as a “stemness” attribute) in ESC colonies, which could also just be a reflection of reduced cytoplasm. Furthermore, it is well accepted that cells in the periphery of the colony are among the first cells to undergo spontaneous differentiation during *in vitro* culture. Interestingly these cells have higher quantities of mitochondria. Although there are line-specific differences it has been shown that, similarly to ICM cells, undifferentiated hESC have few ovoid mitochondria arranged in small perinuclear clusters, and immature morphology, evidenced by the presence of few cristae and low electron lucid matrix [131,135,136]. In general, differentiation involves a shift from small individual oval mitochondria to dynamic tubular networks, with an increase in the number of mitochondrial cristae, suggesting higher OXPHOS activity [121,131].

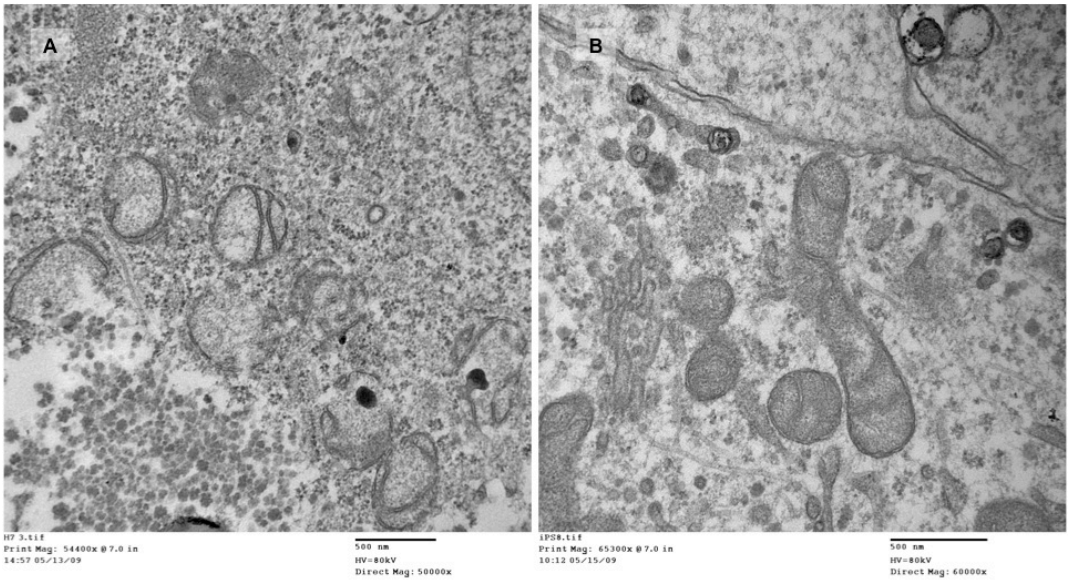

Figure 1.10. Electron microscopy pictures for mitochondria in PSC. The right picture represents the mitochondria found in hESC and it is clear the immature morphology of these organelles in ESC. The picture on the left, represents mitochondria found in iPSC. It is clear that although the mitochondrial morphology is also immature they are not equal to found in ESC.

It has been shown that the proliferative capacity of mESC is strongly correlated with the glycolytic flux and a low oxidative metabolism. Moreover, a study showed that inhibition of mitochondrial respiratory enzyme Complex III with Antimycin A is essential for the maintenance of the pluripotency of ESC [137,138]. Also, it has been demonstrated that hypoxia may facilitate cell growth and pluripotency maintenance [139]. The rationale for using low O_2 tension is related to the conditions found in the female reproductive tract, and thus mimicking physiological conditions for ICM cells. This is not a straightforward issue, because although O_2 may vary throughout the tract, it also seems sufficient to maintain active OXPHOS (see [14] for review). All together, these studies suggest that targeting metabolic pathways may be a promising strategy in the regulation of stem cell physiology.

There is some controversy regarding the polarization of mitochondria in undifferentiated *versus* differentiated ESCs. Undifferentiated mESCs have been reported to have highly polarized mitochondria, which decrease upon differentiation to cardiomyocytes [140]. On the other hand, no differences in MMP between undifferentiated hESCs and differentiated hESCs were also reported [141]. The controversy might be due to the fact that the two groups work with ESCs from different species, mouse and human respectively. In addition, mESCs were specifically differentiated into cardiomyocytes, whereas with hESCs spontaneous differentiation was studied, and as consequence a mixture of cell lineages would be present. Several studies have differentiated ESCs *in vitro* and observed changes in mitochondrial dynamics during differentiation. When ESCs differentiate the number of mitochondria increases and a maturation in morphology can also be observed [121,131,139]. Concomitantly with an

increase of mitochondrial number during ESCs differentiation, the rates of O_2 consumption and ATP production in the cell increase as well, while lactate production decreases [140], suggesting a switch in energy metabolism from glycolysis to oxidative phosphorylation. Similar results have been reported regarding adult stem cells [1,142]. The increase in the number of mitochondria and OXPHOS in differentiated cells also leads to an increase in ROS production [131,141]. This increase in ROS production is important for differentiation of hESCs into cardiomyocytes as demonstrated by Crespo and coworkers providing evidence supporting the role of ROS in the regulation of stem cell differentiation [143].

Given the distinct mitochondrial properties in undifferentiated *versus* differentiated ESCs a role for mitochondria in differentiation may be postulated [14]. In addition, several groups have shown that functional mitochondria are necessary for differentiation. For example, inhibition of mitochondrial respiratory chain complexes I and III, by Rotenone and Antimycin A, respectively, results in reduced cardiomyocyte differentiation, due to an impairment of oxidative phosphorylation [1,140].

Furthermore, glycolytic metabolism is sufficient for maintaining mESCs homeostasis, however, in order for cells to differentiate there must be a switch from glycolysis to the more efficient OXPHOS [140]. Again, several authors have reported a similar role for mitochondria in adult stem cell differentiation [144]. A correlation between MMP, metabolic rate and the differentiation of mESCs has been described, with cells with lower MMP showing more efficient mesodermal differentiation (but low ability to form teratomas), while a population with higher potential behaved in the exact opposite fashion, although both populations were indistinguishable in terms of pluripotency markers [138]. In addition mitochondrial-based apoptosis may also contribute to cell differentiation (see [14]), and mtDNA may also play an important role, given the deficient neuronal differentiation in ESC carrying mtDNA mutations that resulted in severe biochemical deficiency [145]. Regarding mtDNA it was

demonstrated that mtDNA copy number changes as well as the expression levels of crucial factors involved in its replication such as mtTFA (mitochondrial transcription factor A) and DNA polymerase γ (Pol γ) during both spontaneous and retinoic acid-induced differentiation of mESCs [121,146,147].

Regarding iPSCs, there is some recent data that points to the same profile of mitochondrial quiescence in pluripotent iPS cells as has been described for ESCs. This includes similar morphological, metabolic and transcriptomal profiles in terms of mitochondrial-related events and the management of oxidative stress [76,148]. Furthermore, conditions of low mitochondrial activity discussed as being important for pluripotency (such as hypoxia) have been shown to improve the derivation of iPS cell lines [149], and antioxidants such as vitamin C also seem to have a beneficial effect [150,151].

There is also evidence that in iPSCs, both intracellular peroxide and mitochondrial superoxide anions are reduced to the levels similar to those of hESCs and mitochondrial mass, mtDNA copy number, and the expression levels of genes associated with mitochondrial biogenesis are comparable to hESCs. The same can be stated regarding mitochondrial properties and energy metabolism. On the other hand, there is also some information suggesting that inadequate/incomplete reprogramming of somatic cells to a pluripotent phenotype (already described in terms of epigenetics), may also be reflected in mitochondrial properties [76,148,152].

Advances have been achieved regarding metabolic alterations during reprogramming, and they will be considered later in this introduction. However there are still many questions remaining. Although mitochondrial function has become a major point of interest in stem cell biology there are still many issues regarding signaling networks and the possible crosstalk between the mitochondria and the nucleus. However, when we take all of this research together we can definitely infer that repression and activation of mitochondrial function are indeed critical for pluripotency and differentiation of ESCs, respectively.

1.8 Cancer metabolism and clinical strategies:

The main focus of this general introduction is to give the proper frame to understand how a stem cell functions. If on one hand it is relatively easy to find literature for other types of cells regarding mitochondrial function and metabolism, the same is not true for stem cells, in particular ESCs, the main cellular type used throughout the research work presented in this thesis. Mitochondrial morphology and function was already addressed, and if there are still many unanswered questions, when considering cellular metabolism the gap is even bigger. That is why in this next point we will focus on cancer metabolism. The main aim is not to through an extensive review on this topic but instead highlight some key features of this type of cells that share some common characteristics with stem cells.

The cancer cell has only one purpose: to grow and proliferate, doing it so at the expense of its host. Within the classical hallmarks of cancer we can find traits such as: unlimited proliferation potential, self-renewal, self-sufficiency in growth signals, insensitivity to antigrowth signals, evading apoptosis, sustained angiogenesis, tissue invasion and metastasis. All together they make the cancer cell able to survive and proliferate under circumstances that would normally be deleterious [153,154]. Besides the high proliferative potential and self-renewal ability, cancer cells share some cell markers with ESCs (which should be no surprise given that the first stem cells were ECs) and depend on similar signaling pathways [155].

1.8.1 How cancer cells metabolize:

Cancer cells are mostly glycolytic. If we consider that using OXPHOS 36 molecules of ATP are generated against the apparent inefficiency of glucose to lactate conversion, that yields only 2 molecules of ATP it is difficult to understand the reason why a cell would choose this metabolic prolife. As described by Otto Warburg, cancer cells tend to convert most glucose to lactate, even in the presence of sufficient oxygen levels to support mitochondrial oxidative phosphorylation. This phenomenon is labeled “aerobic glycolysis” or the Warburg effect [156].

For the next few paragraphs the advantages of such metabolic profile will be addressed taking into account that the primary purpose of metabolism of a cancer cell must be to facilitate the major purpose of its existence, providing the bioenergetic and synthetic requirements that are important to support growth and proliferation.

The proliferating cancer cells require a net increase in lipids, especially for membrane biosynthesis (lipogenesis/cholesterogenesis). The metabolic shift to lipogenesis in cancer cells is evident from the up-regulation of key lipogenic enzymes, demonstrating its importance for cell growth/proliferation [157]. So, the high rate of aerobic glycolysis has the purpose of providing a readily available source of Acetyl-CoA for mitochondrial synthesis of citrate, implying that not all pyruvate will be converted to lactate. There are two alternatives for mitochondrial citrate it either goes through oxidation, or is exported. Besides citrate oxidation, cancer cells exhibit an increase in the export of citrate from mitochondria, which constitutes an adaptation. The export of citrate is the initiating step of lipogenesis. In the cytosol, citrate is cleaved to Acetyl-CoA, which will be carboxylated for incorporation into fatty acid/cholesterol synthesis. Both citrate oxidation for energy production and citrate export for

lipogenesis will co-exist. In addition, this pathway provides 12 ATP molecules per glucose to meet bioenergetic requirements [134,158].

When considering glycolysis, there are several enzymes involved in this 10 step pathway that are subjected to regulation in order to meet cell demands given that some of the glycolytic intermediates may also serve as carbon sources for the synthesis of macromolecule precursors. One example of enzymes that cooperate with this phenotype is pyruvate kinase (PKM) that catalyzes the conversion of phosphoenolpyruvate (PEP) to pyruvate. There are two isoforms of PKM (PKM1 and PKM2) and cancer cells express the M2 rather than its M1 splice variant. One possible explanation why PKM2 is advantageous to cancer cells takes into account that a slower rate of glycolysis, catalyzed by this isoform allows greater diversion of glycolytic intermediates into subsidiary pathways such as the hexosamine biosynthetic pathway (necessary for cell growth and survival), pentose phosphate, and amino acid biosynthetic pathways, thus supporting cellular biomass increase [159,160].

The pentose phosphate pathway (PPP) produces reduced nicotinamide adenine dinucleotide phosphate (NADPH), a crucial source of reducing equivalents for fatty acid synthesis and for the glutathione, peroxiredoxin, and thioredoxin detoxifying systems. The importance of PPP was demonstrated when fibroblasts deficient in glucose-6-phosphate dehydrogenase, a important enzyme in PPP proliferated less and more importantly had higher levels of oxidative stress [156,161].

Another enzyme that should be taken into consideration is Hexokinase (Hk). This enzyme catalyzes the irreversible first step of the glycolytic pathway where glucose is phosphorylated to glucose-6-phosphate (G-6-P). The basis for this reaction is the entrapment of G-6-P inside the cell for commitment to either the glycolytic pathway or the shunting of this metabolite to the PPP so it can be used mainly for biosynthetic reactions [162,163]. There are four isoforms of this enzyme but this introduction shall focus on Hk2 given that it has been proved to have an essential role in cancer and is

over-expressed in these cells [164]. Hk2 is strategically located on the outer mitochondrial membrane protein VDAC. Here, it gains both preferential access to mitochondrial generated ATP via the mitochondrial adenine nucleotide translocator (ANT), and protection from inhibition by its product G-6-P. Thus, tumors have cleverly overexpressed Hk2 in order to bypass regulatory mechanisms forcing glycolysis and biosynthetic metabolic pathways to function at an enhanced capacity, providing the optimal support for uncontrolled proliferation. In addition to being critical for this unique metabolic profile in many type of cancers, Hk2 and mitochondrial interactions are now believed to be crucial also for promoting cancer survival via modulation of signaling events related to apoptosis by mobilization of the anti-apoptotic Bcl2 member Bcl-XL to VDAC in the OMM [165,166].

Another important adaptation of these cells relies on glutamine (Gln) metabolism. Indeed, recent evidence demonstrates that some cancer cells rely on Gln to support anabolic processes that fuel proliferation [167]. It is clear that even with limited amounts of pyruvate entering the TCA cycle, cancer cells continue to produce limited energy via OXPHOS. However, as an alternative to pyruvate, these cells can use amino acids, such as Gln, as carbon sources for the TCA cycle. Gln is a great carbon source because in high concentrations their passive diffusion into cells is facilitated, being more easily converted into intermediates of the TCA cycle. Before Gln can be used as a carbon source it is first converted to glutamate by phosphate-activated glutaminase (PAG) and then into α-ketoglutarate by glutamate dehydrogenase (GDH) [167,168].

In conclusion it is reasonable to say that cancer cells present a heterogeneous metabolism that has been reported to function not only as an ultimate adaptation for survival and uncontrolled proliferation, but also and most interesting to promote a “metabolic symbiosis”. This symbiosis takes into account that within a tumour, there is heterogeneity between cells that rely on aerobic glycolysis

and OXPHOS so, when excess of lactate produced by hypoxic cells is secreted it can be up-taken by aerobic cancer cells that are closer to blood vessels [169].

1.8.2 The molecular circuits of cancer metabolism:

In normal cells, a critical response to hypoxia is the induction of the hypoxia-inducible transcription factor 1 alpha (Hif-1α), a basic–helix-loop-helix (bHLH) transcription factor that binds to DNA and increases the expression of important genes that encode glycolytic enzymes as well as genes important for angiogenesis [170,171]. In addition to alterations in oxygen tension, changes in glucose concentration can also activate many glycolytic enzyme genes, which will have an impact on both MYC and HIF-1 genes. It is important to note that c-Myc is responsible for regulating cell proliferation and metabolism and inducing the expression of enzymes involved in glycolysis, in PPP and amino acid metabolism. This factor is known to be altered in several types of cancer [107,172].

The transcriptional activation of key genes encoding metabolic enzymes, comprises: Hk2; lactate dehydrogenase A (LDHA), which converts pyruvate to lactate and PDHK1, encoding pyruvate dehydrogenase kinase 1, which inactivates PDH thereby shunting pyruvate away from the mitochondria [173]. Moreover Hif-1α, is also responsible for up-regulating the expression of GLUT1, a glucose transporter; and to induce a transcriptional program by stimulating angiogenesis through the induction of vascular endothelial growth factor A (VEGF-A) and angiopoietin-2 [160,170,174]. Interestingly, another target for Hif-1α is the gene coding for PKM2. This enzyme can also be found in the nucleus where it can interact with Hif-1α promoting its expression [175]. Hif-1α and p53 transcription factors were located on the promoter of Hk2 and functional analysis revealed modulation of this gene promoter

by glucose, hypoxia, cAMP analogs, and insulin [170,175,176], unveiling the crosstalk between different signaling pathways that promotes the metabolic profile observed in cancer cells. Another important interaction mediated by this central transcription factor regards p53: as stated above it has been shown that both have a role on metabolism but most interestingly is the ability of Hif-1α to stabilize p53 [170,177,178].

Together c-Myc and Hif-1α have a primary role in promoting the cancer metabolic profile. More importantly, as it will be discussed ahead, many of these adaptations and key players in signaling pathways are emerging as having similar roles in the metabolism of ESC.

1.8.3 Metabolic targets for cancer therapy:

Science continues to be challenged to find reliable and effective targets for cancer therapy. The objective of this topic is to introduce two compounds that were used in the research work presented in this thesis. They were chosen because currently they are used in research and in clinical trials as possible therapeutic drugs against cancer. Both compounds will be properly addressed in the results chapters.

Both compounds inhibit metabolic enzymes and there is evidence that targeting metabolic pathways will give extra advances in cancer therapy [179,180,181,182]. Some of the potential candidates are over expressed in certain cancer types and were chosen with the premise that by disrupting the metabolism in cancer cells they will not be able to maintain their phenotype and therefore will be more prone to cell death.

These candidates include inhibition of lactic acid efflux by silencing or inhibiting lactate transporters (via interfering RNA), promoting the influx of pyruvate into mitochondria by inhibiting

pyruvate dehydrogenase kinase (PDHK) via dichroloacetic acid or dichroloacetate (DCA), inhibition of tumor expressed LDH [183] isoforms via RNA interference. The same experimental approach could be used to switch between isoforms of PKM in tumor cells in order to alter the kinetics of pyruvate synthesis. Inhibiting the first step of glycolysis by chemical inhibition of Hk2 with 3-Bromopyruvate (3BRP) is another promising strategy [184]. It is important to keep in mind that although hopeful it is difficult to choose the correct metabolic target given the heterogeneity of tumors and also because such strategies would interfere with the metabolism of "healthy" cells. Regarding the last point, promising advances in nanomedicine could overcome such limitations regarding drug delivery directly to targeted cells [185,186].

1.9 Metabolism in PSCs: Is there a parallelism between a cancer and a stem cell?

Throughout this introduction the main concern is to create the appropriate framework to understand the different properties and characteristics of PSCs. Regarding metabolism however, the task is a little bit more complicated given that metabolism became a hot topic in the stem cell field in the recent years and there are still many loose ends. The reason for introducing cancer cells is due to fact that recent papers have demonstrated some similarities between these two types of cells and the purpose of this section is to summarize the current knowledge about metabolism in ESCs.

As previously stated ESCs harbor mitochondria with an immature morphology, which correlates with a reduced oxidative capacity and a glycolysis dependent metabolic profile [131,140,187,188]. While the stimulation of glycolysis in ESCs, either through hypoxia [189], will promote stemness its inhibition

will impair proliferation and precipitate cell death [188]. In fact recent studies show that mESCs, hESCs and iPSCs have a high dependency on glycolysis under aerobic conditions demonstrating a similar metabolic profile with cancer cells. If in the latter cells the PPP is important it has been proved that in mESCs the PPP must also be highly active to promote cell survival under oxidative stress and to control cell fate upon differentiation [190]. As observed for cancer cells, ESCs also rely on citrate and other intermediate metabolites for lipid and amino acid biosynthesis [80].

The core pluripotency circuitry, including the Oct4, Sox2, and Nanog subset, shares points of convergence with signal transducer and activator of transcription 3 (STAT3), a master metabolic regulator controlling the oxidative to glycolytic switch [191]. Specifically, the stemness factor Oct4 has a number of targets associated with energy metabolism, which may impact the balance between glycolysis and OXPHOS [192,193]. Also, it was demonstrated that PKM2 interacts with β-catenin and Oct4, highlighting it diverse roles [194,195]. Chromatin modifiers, such as polycomb repressor complexes, which promote pluripotency, also target metabolic enzymes within their active gene sets [196]. Similarly, Hif-1α participates in the maintenance of stem cell identity, namely by interacting with pluripotency core transcriptional factors [197,198,199]. Respiration and energy production are less coupled in PSC similar to what was demonstrated in cancer cells. In PSCs UCP2 must be repressed during the differentiation process to allow metabolic maturation because uncoupling suppresses differentiation [200,201].

Taking iPSC into consideration if we keep in mind that these cells resemble closely ESCs it is reasonable to assume that somatic cells reprogrammed to pluripotency should become dependent on glycolysis. Indeed iPSCs show a high glycolysis rate and increased decoupling of respiration from ATP production in mitochondria [187,200]. Recent papers show an increase in reprogramming efficiency if the starting somatic cells present a metabolic profile closer to the glycolytic than OXPHOS energy

metabolism [202], which could suggest a type of ‘‘metabolic memory’’ [203].

Other studies have revealed that in order for reprogramming to occur a metabolic resetting must occur, and therefore metabolism could control reprogramming efficiency. Indeed, by inhibiting glycolysis, through incubation of somatic cells with; 2-deoxyglucose to compete for glucose uptake; or with 3BRP to block Hexokinase II, or with DCA to impair PDHK1, reprogramming efficiency was diminished, whereas promoting glycolysis with D-fructose-6-phosphate or by PDK1 activation enhances iPSCs reprogramming efficiency [187,199,202,204]. Also, during reprogramming an increase in the expression of specific glycolytic genes precedes the gain of expression of genes that regulate self-renewal and pluripotency [187]. Interestingly, some reprogramming factors directly regulate metabolism, such is the case of c-Myc that promotes glycolysis and represses respiration. However, its absence does not block reprogramming [73].

All together it is clear that PSC share many similarities with cancer cells with common key players mediating this metabolic profile and alterations. Nevertheless, the molecular mechanisms that regulate energy metabolism in PSC are just now starting to be exposed and it seems reasonable and tempting to follow clues from cancer cells.

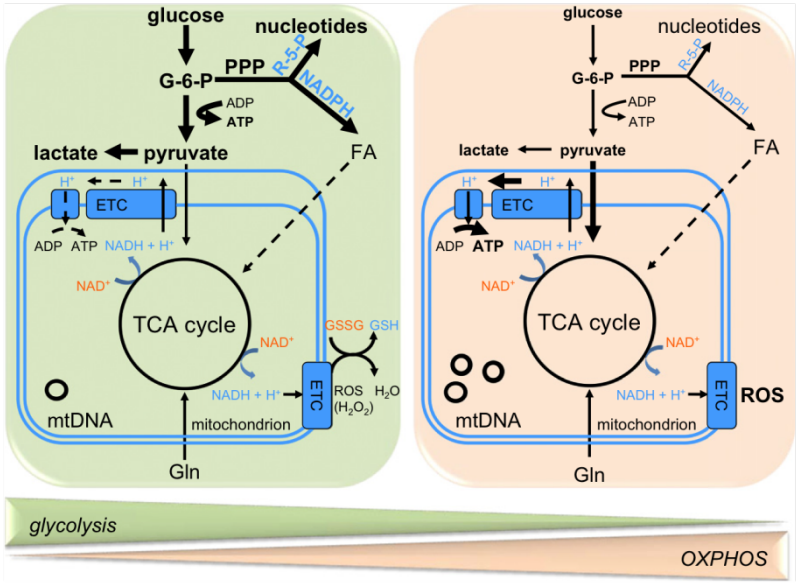

Figure 1.11. Key Differences in Metabolism between PSCs and Differentiated Cells. Energy metabolism shifts from glycolysis to OXPHOS with differentiation, or from OXPHOS to glycolysis with reprogramming to pluripotency. Glycolytic flux is elevated in PSC (left panel) to provide ATP and intermediate metabolites through the PPP for nucleotide and lipid biosynthesis, also because respiration is lower and less coupled to energy production than in differentiated cells. Pyruvate entry into mitochondria is limited by an inactive PDH or by high expression of UCP2. Less ROS are produced from lower respiration and elevated antioxidant enzymes. These features establish a reduced cellular redox environment that becomes more oxidative with differentiation. The TCA cycle in PSC provides intermediate metabolites such as citrate and α-ketoglutarate that are siphoned for lipid and amino acid biosynthesis. ETC, electron transport chain; FA, fatty acid; G-6-P: glucose-6-phosphate; GSH; glutathione; GSSG, glutathione disulfide; mtDNA, mitochondrial DNA; NAD: nicotinamide adenine dinucleotide; NADP: nicotinamide adenine dinucleotide phosphate; PPP, pentose phosphate pathway; R-5-P, ribose-5-phosphate; ROS, reactive oxygen species; TCA, tricarboxylic acid cycle. Elevated metabolic pathways are indicated with bold letters and arrows [73].

1.10 Main hypothesis and goals of this thesis:

The main hypothesis to be tested was if pluripotency could be modulated by metabolism and mitochondrial activity. It should be taken into consideration that when this research work began little was known about mitochondrial function or metabolic status of ESC, which lead to the subdivision into three main goals in order to pursue our hypothesis:

The first goal (*chapter 3*) was to access mitochondrial function and clarify the metabolic profile of hESC comparing it with differentiated cells. At the same time to clarify if the reprogramming process was indeed complete to the same metabolic profile of ESC, a comparison with iPSC was also made. In order to pursue this objective several hESC and different fibroblasts lines were cultured in order to perform electron microscopy analysis, metabolic arrays, determination of oxygen consumption rates as well as lactate production levels and measurement of ATP levels. At the same time different iPSC were subjected to the same methodologies and experimental design in order to compare with the hESC lines. Our main goal was to determine some possible key metabolic enzymes in hESC metabolism, by assessing the mitochondrial function as well as the metabolic status of hESC and their differentiated counterparts.

Once we have established the metabolic profile of ESC **the second goal (*chapter 4*)** was to infer if by blocking the first step of glycolysis this metabolic profile would become altered and pluripotency would be affected, trying to clarify a possible role for Hk2 in metabolic modulation with consequences for pluripotency. A pharmacological approach was chosen and in order to inhibit Hexokinase II, 3BRP a chemical compound used in clinical trials for cancer treatment, was applied to mESC. Given the absence of reports applying 3BRP to these cells, careful toxicology analysis was performed recurring to viability assay, determination of total cell number and morphological analysis. The pluripotent state of these

cells was also evaluated by western blot analysis and RT-PCR. Also, mitochondrial function and concentration of some metabolites was determined in order to clarify Hk2 inhibition effects.

The results obtained in the **first goal** pointed out an inactive PDH, which would divert pyruvate to lactate conversion instead of promoting the TCA cycle. So our **third goal (*chapter 5*)** was to assess if this inactive state of the PDH was essential for pluripotency and if PDH was a good target for metabolic modulation in ESC. For that, cells were treated with another compound used for cancer treatment DCA, which inhibits PDHK, the kinase responsible for inactivation of PDH. This way we should promote a more active PDH and therefore pyruvate would be more easily converted to acetyl-CoA promoting a more active TCA cycle and possibly OXPHOS. Due to the fact that to date, there is no literature available on the effects of DCA in ESC, a toxicology analysis was performed as in chapter 4. Pluripotency was assessed by Elisa and RT-PCR as well as mitochondrial function. MMP was determined and ROS production was assessed. The PDH active/inactive state was also determined by western blot and RT-PCR analysis. In order to shed some light into possible similarities between ESC and cancer cells we determined the protein levels for some key players in metabolic pathways.

Material and Methods

Chapter 2

2.1 Material and Methods for human embryonic stem cells:

2.1.1 Cell culture:

In this work we used hESC lines WA07, WA09 and WA01 (WiCell Research Institute, Madison, WI), human iPSC lines HFF1 iPS, IMR-90 iPS (WiCell Research Institute) and AE iPS (derived in our laboratory). In terms of differentiated fibroblasts, both the IMR-90 human diploid fibroblast and the human foreskin fibroblast (HFF1) strains were obtained from American Type Culture Collection (ATTC, Manassas, VA); these lines were reprogrammed to form the IMR-90 iPS and HFF1 iPS lines noted above, respectively. Finally, differentiated H7TF fibroblasts were isolated from a WA07 ESC-derived teratoma, following injection of WA07 hESCs into immunocompromised mice.

HESC and iPSC lines were cultured in mTeSR ™ (STEMCELL Technologies, Vancouver, BC, Canada) on matrigel (BD Biosciences; San Jose, CA) coated dishes. Both H7TF and HFF1 were cultured in CF1 medium containing: 90% Dulbecco's Modified Eagle's medium; 10% fetal bovine serum (FBS); 1% MEM non-essential amino acids; 1% penicillin/streptomycin (Pen/Strep) and 1% 2mM L-glutamine (all from Invitrogen, Carlsbad, CA). The IMR-90 line was cultured in 90% Eagle's minimal essential medium (ATTC, Manassas, VA), 10% FBS and 1% Pen/Strep. All lines were maintained at 37°C, 21% O_2 and 5% CO_2. Throughout the work WA07, IMR-90 iPS, H7TF and IMR-90 lines were used in the majority of the experiments in order to compare cell lines that have the same genetic background. The other lines were used in key experiments to consolidate the results trying to avoid any artifact that could be line specific or culture derived.

2.1.2 Transduction of pluripotent and differentiated cells using a baculovirus system:

Mitochondria GFP labeling was performed using the organelle lights Mito reagent (CellLight™ Mitochondria-GFP by Molecular Probes/Invitrogen). This system is a baculovirus system that contains a leader sequence for the E1 alpha pyruvate dehydrogenase fused with GFP protein. Cells were plate on coverslips and cultured for three days or 24 hours, for pluripotent and differentiated cells, respectively. Cells were rinsed with Dulbecco's Phosphate Buffered Saline (D-PBS), and incubated in D-PBS containing 82% organelle lights reagent during 30 minutes at room temperature with gentle shaking. Organelle lights mixture was removed and cells were incubated with appropriated media containing 0.1% enhancer solution (provided) for two hours at 37°C. Enhancer solution was removed and replaced by cell culture media. Although the transfection efficiencies were low, 20 hours later, GFP protein could be observed in the mitochondria. Cells were then fixed with 4% paraformaldehyde (Sigma-Aldrich) and imaged using a TCS-SP@ laser scanning confocal microscope (Leica, Microsystems, Gmbh, Wetzlar, Germany).

2.1.3 Electron Microscopy:

Cells were cultured on matrigel or matrix free conditions for pluripotent cells or differentiated cells, respectively. Cells were rinsed with PBS and fixed with 2.5 % glutaraldehyde in PBS, pH 7.4, for 1 hour at room temperature. The fixative was removed and samples were washed 3 times with PBS at room temperature for 10 minutes each. Samples were post-fixed for 1 hour at 4°C in 1% osmium

tetroxide with 1% potassium ferricyanide, followed by three washes with PBS (10 minutes each). Afterwards, samples were dehydrated using a graded ethanol series (30%, 50%, 70%, and 90%-10 minutes) with three changes in 100% ethanol (15 minutes each). Samples were then incubated three times with a 100% Epon solution (1 hour each). Finally, samples were incubated for 1 hour with Epon solution, maintained overnight at 37°C and afterwards at 60°C for 2 days. Sections were made using an ultra microtome and imaged in a 1011 CX Transmission electron microscope (JEOL, Tokyo, Japan).

2.1.4 RNA extraction, DNA clean up and Glucose RT^2 profiler PCR array:

Total RNA isolation using the TRIzol reagent (Invitrogen) and genomic DNA was eliminated with DNA-free kit (Ambion, Austin, TX) as previously described [137]. An additional step of DNA clean up was performed using the genomic elimination kit from SABiosciences (Frederick, MD). In brief, 1µg of RNA was incubated with genomic DNA elimination mixture (containing 2µl of 5X genomic DNA elimination buffer and nuclease free water) for 5 minutes at 42°C. The first cDNA strand was synthesized by incubating the product of the genomic DNA elimination reaction with 10µl of the Reverse transcriptase (RT) mixture (5 x reverse transcriptase (RT) buffer, RT, primers and external control, and nuclease free water) for 15 minutes at 42°C. Reactions were immediately stopped by heating at 95°C for 5 minutes. RT products were further diluted with 91µl of nuclease free water. cDNA samples were then loaded in the glucose gene expression panel (SABiosciences), run in a 7900HT Real Time system (Applied Biosystems, Foster City, CA) accordingly to the following thermal cycle conditions; 95°C for 10 minutes, and 40 cycles at 95°C for 15 seconds and 60°C for one minute. Each array contained wells that allowed us to control for genomic DNA contamination, and first cDNA synthesis efficacy. Twelve genes (*ALDO B*, *FBP1*, *FBP2*, *G6PC*, *GCK*, *GYS2*, *HK3*, *PCK1*, *PDK4*, *PGK2*, *PKLR* and *PRPS1L1*) were not considered in the analysis, as their Ct value was above 30. Gene expression differences were calculated using the -ΔΔCt method. Gene

expression was normalized to the housekeeping gene β-actin and fold change was calculated relative to the hESC line WA07. p values were determined using online software provided by SABiosciences.

2.1.5 High Performance liquid Chromatography (HPLC):

Pluripotent cells were cultured as mentioned above for seven days, whereas differentiated cells were cultured for two days. Cells were enzymatically dissociated with Accutase (Millipore) or TripLe Express (Sigma-Aldrich, St. Louis, MO) for pluripotent cells and differentiated cells, respectively. Adenosine triphosphate (ATP) was extracted with 0.6 M perchloric acid (Sigma) supplemented with 25mM EDTA-Na (Sigma) followed by centrifugation. Supernatants were neutralized with 3M potassium hydroxide in 1.5M Tris. ATP separated by HPLC. The detection wavelength was 260nm and the column was a Licrosphere 100 RP108 5µm (Merck). The elution buffer for was 100mM phosphate buffer (pH 6.5) supplemented with 1% methanol. Standard for ATP was purchased from Sigma- Aldrich.

2.1.6 Lactate Production:

Lactate levels were determined using the Lactate assay kit (Biovision). In this assay lactate is enzymatically oxidized and the product of this reaction reacts with a lactate probe (provided) and emits fluorescence at Em=587nm. Both pluripotent and differentiated cells were plated and cultured for 48 hours. At this point, fresh media was added to the cells. Twenty-four hours later, 500µl of medium was collected, and cell numbers were determined. Medium samples were processed following manufacturer's instructions. Fluorescence was determined using a microplate reader (Spectra Max M2; Molecular Devices, Sunnyvale, CA). Lactate concentrations were normalized to cell number.

2.1.7 Western blotting:

Cells were maintained on matrigel or matrix free conditions for pluripotent cells or fibroblasts, respectively. Pluripotent cells were dissociated using Accutase (Millipore), whereas for differentiated cells Triple E (Sigma-Aldrich) was used. Total cell extracts were lysed in RIPA buffer (Sigma) supplemented with 1mM phenylmethylsulphonyl fluoride (PMSF) (Sigma-Aldrich) and 2x Halt phosphatase inhibitor cocktail (Pierce, Rockford, IL). Mitochondrial extracts were isolated using mitochondria isolation kit (Sigma-Aldrich), as previously described by Wieckowski and colleagues [205]. In brief, cells were washed once with PBS, and incubated on ice with the extraction buffer supplemented with cell lysis detergent (1:200) and PMSF (1:200) for 5 minutes. Samples were resuspended every minute. Afterwards, we added 2v/v of extraction buffer and centrifuged twice, at 4°C, for 10 minutes, at 2000g. Pellets containing the cytosolic fraction were stored at -80°C. Supernatants were transferred to a new tube and centrifuged, at 4°C for 10 minutes, at 11000g. Supernatants were discarded and the pellets containing the mitochondrial fraction, were washed with extraction buffer, and centrifuged at 4°C, for 20 minutes, at 11000g. The debris fraction (supernatant) was stored, as well as, the mitochondrial fraction at -80°C. Protein quantification was carried out using the Bradford assay (Bio-Rad laboratories, Inc., CA) and 7µg of protein were separated in 4%-15% SDS Page gels (Bio-Rad laboratories). The primary antibodies used were: anti - Oxphos complex kit (1:500, Invitrogen); anti-PDH (1:500, Cell Signaling and Technologies); anti- PDHK1 (1:500, Cell Signaling and Technologies); anti-phospho PDH-E1α Ser ^{293} (1:250, EMD); anti-hexokinase II (1:500, Cell Signaling and Technologies), and anti-Nanog (1:500, Kamiya Biomedical Company, Seattle, WA), ECL Advanced Western Blot Detection kit (Amersham Biosciences, Piscataway, NJ) was used for detection.

2.1.8 Immunocytochemistry (ICC):

Cells were cultured on coverslips for six days or two days for pluripotent and differentiated cells respectively. Cells were fixed in 2% formaldehyde, rinsed in D-PBS, permeabilized with PBS 0.1 % Triton and incubated with blocking solution (containing 0.3% Bovine Serum Albumin (BSA), 1x D-PBS and 5% of normal serum from the specie of the corresponding secondary antibody) for an hour at room temperature. The primary antibody used was anti-Hexokinase II (1:500, Cell Signaling and Technologies). Antibody was incubated overnight at 4°C, followed by three washes of 15 minutes in PBS 0.15% Triton. Respective secondary antibody was incubated for one hour at 37°C, followed by three washes in PBS 0.1% Triton. Coverslips were assembled in slides using the fluorescence mounting media Vectashield with DAPI (Vector Labs, Switzerland). Slides were imaged using a TCS-SP2 laser scanning confocal microscope (Leica).

2.1.9 Oxygen consumption rates:

O_2 consumption was determined using Seahorse XF24 extracellular Flux analyzer as previously described by Qian and Van Houten [206]. Briefly, cells were seeded in the 24-well XF24 cell culture plate in the respective culture media. For pluripotent cells, matrigel coated plates were used and cells were allowed to grow for three days, whereas for differentiated cells 300 000 cells were seeded and allowed to grow for 24h. Thirty minutes prior to the run, culture media was replaced by unbuffered DMEM and plates were incubated at 37°C for 30 minutes for pH and temperature stabilization. Three mitochondrial inhibitors; oligomycin (1µM), FCCP (300mM) and rotenone (1µM) were sequentially injected after

measurements, 2, 4, and 6, respectively. After all the measurements were completed, cells were dissociated and counted.

2.1.10 Statistical analysis:

Means and standard error of the mean (SEM) were calculated and statistically significant differences were determined by One-way ANOVA followed by Dunnett's Multiple Comparison test. n refers to sample size. Statistical significance was determined at $p<0.05$. The p values for the Glucose array were calculated using SABiosciences online software. The test used was a two-tailed Student's t-test, and statistical significance was determine at $p<0.05$.

2.2 Material and Methods for mouse embryonic stem cells:

2.2.1 Cell culture conditions:

In this study experiments were performed using the cellular line mESC E14. Dr. Martin Hooper derived this well characterized cell line from the mouse strain 129/Ola in 1985 [207,208]. Cells were maintained in feeder free conditions using Knockout-DMEM media (Gibco® Life Technologies) supplemented with 15% of KSR (Knockout serum replacement - Gibco® Life Technologies), 1% of MEM Non-Essential Amino acids (Sigma-Aldrich), 1% Penicillin/Streptomycin, 1% L-glutamine (2mM) (both from Gibco® Life Technologies) and β-Mercaptoethanol (Sigma-Aldrich). In order to maintain pluripotency LIF (ESGRO® mLIF Millipore) was added at a final concentration 10U/L. Media was changed 12hours after splitting and plating the cells and every 24hours until the cells presented the right confluence for passage. Cells were maintained at 37°C, 20%O_2 and 5% CO_2.

2.2.2 Passaging and platting mESCs:

E14 mESCs were passaged when the right confluence was achieved, usually two or three days after platting. Briefly, 0.1% gelatin (Sigma-Aldrich) was added to plates and allowed to coat for ten minutes at 37°C. Afterwards, the excess was removed and supplemented Knockout-DMEM media was added. To passage the cells, media was removed and rinsed once with D-PBS (Sigma-Aldrich). The enzyme accutase (Gibco® Life Technologies) was added and incubated for 5 minutes at 37°C to allow a gentle detachment of the cells. Afterwards 1ml of media was added in order to inactivate accutase. Cells were collected and subjected to centrifugation for 5 minutes at 1200 rpm. Supernatant was discarded and the pellet was gently ressuspended with media (the volume was adjusted to pellet size) in order to

obtain a single cell suspension. 10μl from that cell suspension were mixed with 10μl of Trypan Blue (Sigma-Aldrich) in order to access cell number and viability using the Neubaeur chamber. Only viable cells were counted and taking that into account, cells were plated at a final density of 5000cells/cm.

2.2.3 Experimental design for 3-Bromopyruvate (3BRP):

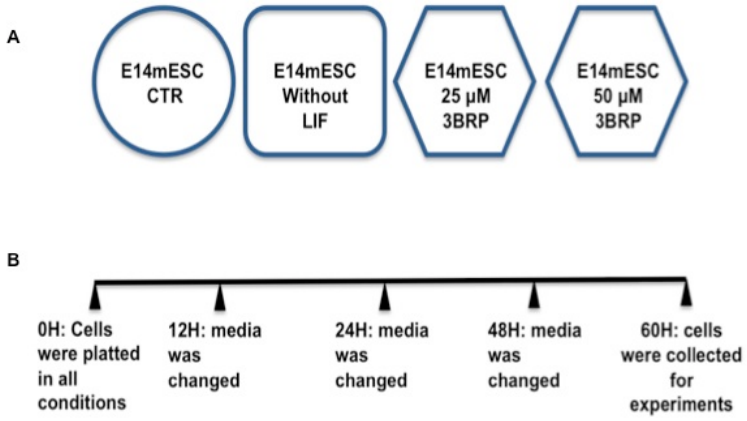

Figure 2.1. Experimental design for 3BRP: (A) and time line that the cells were subjected to (B).

mESCs were platted for the four conditions, according to the experimental design (figure 2.1A). Therefore, cells were platted in control conditions, in the absence of LIF and in the presence of the drug. The chemical compound 3BRP (Sigma-Aldrich) was freshly prepared and added at all time points when the media was changed (figure 2.1B). Experiments were conducted after 60hours of incubation for all the experimental conditions.

2.2.4 Experimental design for Dichloroacetic acid (DCA):

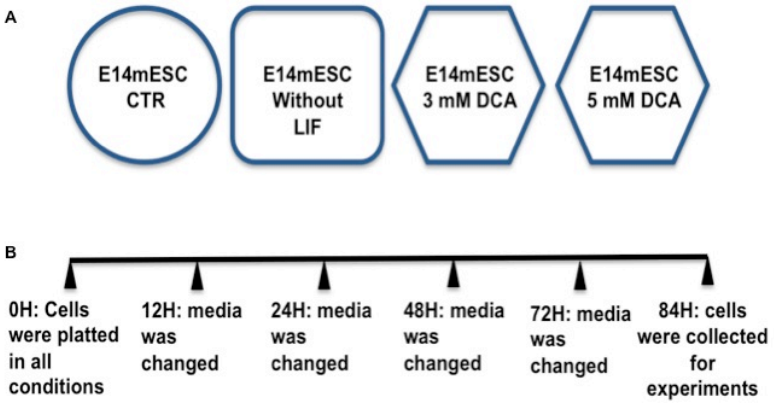

Figure 2.2. Experimental design for DCA: (A) and time line (B) that the cells were subjected to.

mESCs were platted for the four conditions, according to the experimental design (figure 2.2A). This way, cells were platted in control conditions, in the absence of LIF and in the presence of the drug. The chemical compound DCA (Sigma-Aldrich) was freshly prepared and added at all time points when the media was changed (figure2.2B). Experiments were conducted after 84hours of incubation for all the experimental conditions.

2.2.5 Viability:

In order to determine the effect of the experimental conditions on cell viability, the LIVE/DEAD® Kit from Invitrogen was used. The Kit consists of two DNA binding fluorescent dyes: SYBR® 14 which is membrane permeable staining the nucleus green for all cells, and IP (propidium iodide). This last dye, although a DNA stain, will only enter cells with compromised membrane integrity, thus staining the nucleus of dead cells red. Cells were collected at the 60 and 84 hour time point by enzymatic

dissociation with accutase, and centrifugation for 5 minutes at 1200rpm. The supernatant was discarded and the pellet ressuspended in D-PBS. 6μM of SYBR® 14 and 0.48mM of PI were added to the cell suspension that was then incubated for 20 min at 37°C, 20%O_2 and 5% CO_2. Viability was assessed by counting 100 cells. Green fluorescent cells without red fluorescence were counted as live cells and a cell with both stains as dead cells using a Leica fluorescent microscope.

2.2.6 Thiazolyl Blue Tetrazolium Bromide (MTT) assay:

MTT was reconstituted according to the manufacturers' instructions (Sigma-Aldrich) and was used at a final concentration of 0.5mg/ml. This assay is routinely used as an assay for cell proliferation/metabolic activity. This is due to the fact that MTT is reduced by cellular dehydrogenases (of both NADPH and NADH) present in the cells, and this will produce violet formazan crystals that are soluble in acidified isopropanol [209]. Cells were plated and incubated for 60 and 84 hours, afterwards media was changed so that the assay did not take place in the presence of 3BRP or DCA. Formazan crystals (violet) formed after a 5 hour incubation at 37°C, 20%O_2 and 5% CO_2 were solubilized with 300 μl of isopropanol with HCl 0.04M. Violet color intensity was measured colorimetrically at 570 nm. Metabolic activity was normalized to the control condition and then to total cell number for each condition.

2.2.7 Alkaline phophatase assay:

Although alkaline phosphatase (AP) positive staining is not considered the best pluripotency marker it is well accepted that stem cells that are self renewing and pluripotent present high levels of AP [22]. As a first approach to monitor pluripotent status the AP assay (using the Alkaline Phosphatase Detection Kit from Milipore) was performed for each experimental condition. Briefly, cells were cultured in a 24 well plate for 60hours (3BRP) and for 84hours (DCA), media was removed and cells were rinsed with D-PBS and then fixed with 4% paraphormaldeide for one minute. Cells were then washed for 5minutes with TBST and the alkaline phosphatase reagent (prepared according to the manufacturers' instructions) was added. After a 20 minute incubation at room temperature (RT) in the dark the reagent was removed and D-PBS was added and colonies were counted using an optical microscope.

2.2.8 High Resolution enzyme-linked immunosorbent assay (ELISA):

To further assess the pluripotent status of our experimental conditions, mESCs were plated in a 24 well plate and at the collection time point cells were rinsed with D-PBS and then fixed for 30minutes with paraformaldehyde (PFA) at 4%. A permeabilization step was performed with a 1% Triton X-100 solution and cells were incubated with a 3% H_2O_2 solution for 5minutes to stop endogenous peroxidase activity. Cells were blocked for 1hour at room temperature with a 3% BSA, 0.25 Triton X-100 in PBS solution and incubation with primary antibody against Oct4, Nanog and Gapdh (1:500 was the dilution for all the antibodies) occurred overnight at 4°C. For each experimental condition a negative control was performed in which no primary antibody was added. Prior to incubation with the proper HRP-conjugated secondary antibodies (1:1000) cells were washed 3 times for 5minutes with D-PBS. To detect HRP activity, cells were incubated for 10minutes with the chromogenic substrate tetramethylbenzidine (TMB-Sigma-Aldrich). The reaction was stopped with the addition of 1M H_2SO_4 and color quantification

was done at 450nm in a microplate reader [210]. In order to normalize our results total mass quantification was performed using sulforhodamineB (SRB, Sigma-Aldrich) [211]. Briefly after the HRP reaction cells were washed with D-PBS until the entire colorimetric product was washed out. Cells were allowed to dry at room temperature and then incubated for 1hour at 37°C with SBR (0.5% w/v solution in 1% acetic acid solution). A 1% acetic acid solution was used to wash the excess of SRB that did not bound to the cells and subsequently SRB that bound to the cells was extracted with a 10mM Tris solution (pH=10) and transferred to a 96well plate and optical density was determined at 450nm with the microplate reader.

2.2.9 Flow cytometry methods:

2.2.9.1 Evaluation of mitochondrial membrane potential:

Fluorescent dyes have been commonly used to monitor mitochondrial membrane potential and there are several available options [212]. In this study we used tetramethylrhodamine methyl (TMRM-Invitrogen) a lipophilic cationic fluorescent dye that, due to its positive charge, will accumulate in the mitochondria accordingly to membrane potential. Thus, mitochondria that are more polarized will accumulate more TMRM. We evaluated the TMRM signal by flow citometry (BD FACSCalibur) in the FL2 channel with the proper positive and negative controls. Cells were collected as described, centrifuged and a wash was performed with D-PBS in order to remove all media. Cells were incubated with 20µM of TMRM for 20 minutes at 37°C, 20%O_2 and 5% CO_2 in the dark in 1ml of D-PBS. Afterwards cells were centrifuged for 5 minutes at 1200rpm to remove excess TMRM [138,213]. Pellets were ressuspended

with 300µl of PBS, kept on ice and analyzed. In order to define the proper gates for an accurate analysis we used cells without TMRM as a negative control and TMRM labeled cells incubated with 250µM of CCCP, a potent mitochondrial uncoupler, for 5 minutes as a positive control. 20000 cells were analyzed per condition with the Cell Quest Pro Acquisition software.

2.2.9.2 Superoxide Anion Quantification:

To evaluate the intracellular amounts of the superoxide anion in our experimental conditions we used MitoSOX Red (Molecular Probes) that fluoresces after selectively reacting with superoxide in mitochondria. After cell dissociation, cells were centrifuged and pellets were reconstituted in fresh media. MitoSOX Red was prepared according to the manufacturers' instructions and cells were incubated for 30 minutes at 37°C in the dark with a final concentration of 3µM of the probe. After incubation, cells were centrifuged and reconstituted in 300µl of D-PBS for flow cytometry analysis. MitoSox red was excited at 488nm and the data collected in the 585/42 channel. To properly define the analysis gates we used cells without the probe as a negative control and cells that were incubated with Antimycin A (100µM) as a positive control. Antimycin A, a potent mitochondrial complex III inhibitor was used in order to increase ROS production so that we could assess the maximum amount of ROS production in our cells [214,215,216]. Once more, 20000 cells were analyzed per condition with the Cell Quest Pro Acquisition software.

2.2.9.3 mESCs proliferation assay:

To infer the effect of our experimental conditions in cell proliferation we examined the expression of the proliferating cell nuclear antigen (PCNA). It has been shown that this antigen has a role in DNA replication and repair and is highly expressed in cells that are rapidly proliferating [217]. mESCs were maintained according to the experimental design and were collected as previously described, fixed with 70% ethanol and stored overnight at -20°C. The next day cells were washed with D-PBS and subjected to an acidic denaturation step with 2N HCl and then washed once more with PBS. Afterwards cells were incubated for 1hour with primary antibody against PCNA (1:100), washed with D-PBS and FITC-conjugated secondary antibody was added (1:100) and allowed to incubate for 1hour in the dark [218]. Cells were washed to remove excess of the secondary antibody and cells staining positive for PCNA were analyzed using the FACSCalibur cytometer and data acquisition/analysis was performed with the CellQuest Software (BD Biosciences). 20000 cells were analyzed per condition and cells without antibodies (to access auto-fluorescence), as well as cells with the only primary antibody and cells incubated only with the secondary antibody were used as controls.

2.2.10 Adenine nucleotides content analysis by High Performance liquid chromatography (HPLC):

Cells were cultured accordingly to the experimental design and collected as previously described. Total number of cells was counted using a Neubaeur chamber. Cells were then centrifuged for 5 minutes at 1200rpm and the pellets were ressuspended with 1ml of D-PBS and centrifuged once

again. Afterwards 100μl of D-PBS at 4°C was added and samples were mixed with a vortex for 10 seconds. 100μl of the extraction solution (0.6 M perchloric acid supplemented with 25mM EDTA-Na - Sigma) was added on ice, to allow for the extraction of the adenine nucleotides. Samples were centrifuged at 13000rpm for 2 minutes at 4°C and the supernatants containing the adenine nucleotides were neutralized with 3M KOH in 1.5M Tris followed by centrifugation (13000rpm for 2 minutes at 4°C). Samples were stored at -80°C until assayed by HPLC. The elution buffer was composed by 100mM phosphate buffer (pH 6.5) and supplemented with 1% methanol. Retention times were determined using standards for ATP, ADP and AMP (Sigma-Aldrich): Adenylate Energy Charge was calculated according to the following formula: ATP+0.5xADP/(ATP+ADP+AMP) [219,220].

2.2.11 Real Time Polymerase chain reaction (RT-PCR):

2.2.11.1 Total RNA isolation:

Cells were collected enzimatically with accutase and centrifuged for 5minutes at 1200rpm. Afterwards supernatants were discarded and the pellet ressuspended with 1ml of TrIzol reagent (Invitrogen). Samples were subjected to vortex for 10 seconds and 200 μl of chloroform was added. Cells were again mixed by vortex for 30 seconds and then centrifuged at 2500g for 5 minutes in order to obtain a separation between an aqueous phase and the protein phase. Approximately 600 μl of the aqueous phase (transparent) was collected and the protein phase was discarded. In order to precipitate RNA 600μl of isopropanol (Sigma-Aldrich) was added and samples were stored overnight at -20°C. After RNA precipitation samples were centrifuged for 30 minutes at 16000g at 4°C supernatants were discarded and 600μl of 75% ethanol was added to the pellets. Samples were then centrifuged at 16000g

for 10 minutes at 4°C and once again supernatants were discarded and the pellets left to dry at RT for 5 minutes. The RNA pellets were dissolved in 20-30μl of nuclease free water (depending on pellet size).

2.2.11.2 DNA clean up:

The RNA samples were subjected to a DNA clean up step using the DNA-free Kit from Ambion. The kit was used following kit instructions, briefly 0.1v/v of DNase I buffer was added to our dissolved pellets mixed well, by pippeting, and incubated for 30 minutes at 37°C, the reaction was stopped with the addition of 0.1 v/v of DNase inhibitor. Samples were incubated for 2 minutes at RT and then centrifuged at 9500g for 1.5 minutes. Afterwards RNA was collected and concentration as well as quality of the RNA was determined using NanoDrop 2000 (Thermo Scientific). Samples presenting a 260/280 ratio under 1.8 were discarded. Samples of total RNA were stored at -80°C until use [137].

2.2.11.3 Preparing first strand cDNA:

cDNA was obtained using the iScript™ cDNA Synthesis Kit from Bio Rad according to the protocol established from the manufacturer. Each PCR reaction was prepared in 0.2ml PCR tubes according to table 2.1. Afterwards, samples were placed in the thermal cycler (S1000™ Thermal Cycler) programmed with the following reaction protocol: 5 minutes at 25°C; 30 minutes at 42°C; 5 minutes at 85°C and hold at 4°C for 1hour. For the negative control we prepared duplicates of the PCR reactions for each sample but instead of the iScript reverse transcriptase, nuclease free water was added.

Table 2.1. PCR mixture for the synthesis of the first cDNA strand using iScript™ cDNA Synthesis Kit.

Components	Volume per Reaction
5x iScript reaction mix	4µl
iScript reverse transcriptase	1µl
Nuclease free water (x corresponds to the sum of the other components volumes minus 20µl)	Xµl
RNA template (y corresponds to 1.5µg)	yµl

Total volume = 20µl

2.2.11.4 RT-PCR:

RT-PCR was performed to quantify gene expression for OCT4; NANOG; GAPDH, PDH, PDHK1, PDHK2, HEXOKINASEII AND HEXOKINASEI with β-ACTIN used as housekeeping gene for data normalization. The primers that were used for RT-PCR are described in table 2.3 and were obtained from a primer bank data base (http://pga.mgh.harvard.edu/primerbank/) and ordered from Integrated DNA Technologies (IDT). SsoFast™ EvaGreen® Supermix (Bio-Rad) was used to perform RT-PCR analysis. Briefly, the mixture was prepared as described in table 2.2, each gene was quantified in duplicate with a negative control in which SsoFast™ EvaGreen® Supermix was substituted by water. 1µl o cDNA of each sample was loaded to the 96 well reaction plate (Bio-Rad) and afterwards 19µl of the supermix was added to each well. Samples were run in CFX96 Touch™ Real-Time PCR Detection System and mRNA fold change was calculated using the -ΔΔCt method.

Table 2.2. Quantitative PCR mixture using SsoFast™ EvaGreen® Supermix.

Components	Volume per Reaction
SsoFast™ EvaGreen® Supermix	10µl
Forward Primer	2µl
Reverse Primer	2µl
Nuclease free water (x corresponds to the sum of the other components volumes minus 20µl)	Xµl
cDNA template	1µl

Total volume = 20µl

Table 2.3. List of primers nucleotide sequences for RT-PCR analysis.

Gene	Primer Bank ID		Nucleotide Sequence 5'-3'
OCT4	356995852c3	Forward (FW)	CGGAAGAGAAAGCGAACTAGC
		Reverse (RV)	ATTGGCGATGTGAGTGATCTG
NANOG	31338864a1	FW	TCTTCCTGGTCCCCACAGTTT
		RV	GCAAGAATAGTTCTCGGGATGAA
GAPDH	6679937a1	FW	AGGTCGGTGTGAACGGATTTG
		RV	TGTAGACCATGTAGTTGAGGTCA
HEXOKINASEII	7305143a1	FW	TGATCGCCTGCTTATTCACGG

		RV	AACCGCCTAGAAATCTCCAGA
HEXOKINASE I	309289a1	FW	CGGAATGGGGAGCCTTTGG
		RV	GCCTTCCTTATCCGTTTCAATGG
PDH	6679261a1	FW	GAAATGTGACCTTCATCGGCT
		RV	TGATCCGCCTTTAGCTCCATC
PDHK1	27369966a1	FW	GGACTTCGGGTCAGTGAATGC
		RV	TCCTGAGAAGATTGTCGGGGA
PDHK2	19526816a1	FW	AGGGGCACCCAAGTACATC
		RV	TGCCGGAGGAAAGTGAATGAC
β-ACTIN	6671509a1	FW	GGCTGTATTCCCCTCCATCG
		RV	CCAGTTGGTAACAATGCCATGT

2.2.12 Total Protein Extracts and protein quantification:

In order to obtain protein extracts for western blot analysis mESCs were dissociated using accutase, centrifuged and washed once with D-PBS. The pellets were lysed with 100µl of RIPA buffer (Sigma-Aldrich) supplemented with 2mM of phenylmethylsulphonyl fluoride-PMSF (Sigma-Aldrich) and 2x Halt phosphatase inhibitor cocktail (Pierce, Rockford, IL). The pellet was subjected to vortex and incubated on ice for 5 minutes. Afterwards samples were centrifuged at 500g for 15 minutes and supernatants were collected and stored at -80°C. Protein quantification was performed using the Pierce™ BCA (Bicinchoninic Acid) Protein Assay Kit and following the protocol in the kit datasheet. Both samples and calibration curve were determined with duplicates.

2.2.13 Western Blot protocol:

Protein samples for western blot were prepared by diluting 10µg of protein in Laemmli sample buffer (Bio-Rad) and water, given that the volume of sample buffer had to contain 10µg of protein (water was used to adjust the volume). A total volume of 30µl per sample was prepared and denatured at 95°C in a dry bath. After this step samples were loaded into 12% Acrilamide Tris-HCl gel and electrophoresis was performed in a Mini protean tetra cell Bio-Rad apparatus for 1hour at constant amperage (60mA) on ice. The running buffer was also acquired from Bio-Rad. After protein size separation in the gel, proteins were blotted into a PDVF membrane (Bio-Rad) using a transfer buffer (25mM Tris; 190mM glycine and 20% methanol) at constant voltage (100mV) for 1hour and 30 minutes at 4°C and on ice. Membranes were then blocked for 1hour using a solution of 5% powder milk (Bio-Rad) in Tris-Buffered Saline with Tween (TBST) (5mM Tris; 15mM Nacl; 0.1% Tween 20) at RT. Afterwards, membranes were washed in TBST for 3minutes to remove the blocking solution excess and incubated overnight at 4°C with the primary antibody. The list of antibodies and respective dilutions is shown in table 2.4. Membranes were washed 3 times in TBST for 15 minutes (each wash) and then incubated for one hour at room temperature with the correct HRP-conjugated secondary antibody. Before detection, membranes were washed 3 times for 15 minutes in TBST. Proteins were detected using the Clarity Western ECL Substrate (Bio-Rad). Briefly, equal volumes of enhanced luminol reagent and the oxidizing reagent were mixed. The mixture was applied onto membranes for 1 minute at room temperature. Excess mixture was removed from membranes using filter paper and membranes were developed using the VersaDoc Imaging system (Bio-Rad). Protein quantification was performed using Quantity One software and results were normalized to β-Actin levels for each condition.

Table 2.4. List of antibodies used for Western Blot protocol.

Antibody	Source	Dilution
Nanog anti-mouse	Santa Cruz Biotechnology	1:500
Oct4 anti-rabbit	Cell Signaling Technology	1:1000
P53 anti-mouse	Cell Signaling Technology	1:1000
PDH anti-rabbit	Cell Signaling Technology	1:1000
PDHK1 anti-rabbit	Cell Signaling Technology	1:1000
Phospho-PDH anti-rabbit	EMD Millipore	1:1000
HIF 1 alpha anti-mouse	Thermo Scientific	1:1000
c-MYC anti-rabbit	Cell Signaling Technology	1:1000
GAPDH anti-rabbit	Cell Signaling Technology	1:2000
PKM 1/2 anti-rabbit	Cell SignalingTechnology	1:1000
Hexokinase I anti-mouse	Cell Signaling Technology	1:500
Hexokinase II anti-mouse	Cell Signaling Technology	1:500
β-Actin anti- mouse	Sigma-Aldrich	1:3000

2.2.14 Lactate Production:

We determined lactate levels in the extracellular media using the Lactate assay kit from Biovision. This assay is based on the enzymatic oxidation of lactate, the product of which will react with a probe provided with the kit and emit fluorescence. The protocol was carried out according to Biovision instructions. Briefly, 700µl of media from our experimental conditions was collected reflecting the lactate that is exported from the cells in the last 24hours of incubation. The collected media was centrifuged in filtered eppendorfs so we could remove dead cells and stored at -80°C until use. Fluorescence (Ex/Em=535/590 nm) was determined using a microplate reader. Total number of cells was determined in order to normalize lactate concentrations that were calculated following the formula C=La/Sv (La corresponds to lactate levels in nmol from our samples and Sv the added volume of media to each well in the plate assay).

2.2.15 Pyruvate Production:

Pyruvate levels secreted into the media were determined using the EnzyChromTM Pyruvate Assay Kit (BioaAssay Systems). 700µl of media from our experimental conditions was collected, centrifuged in filtered eppendorfs so we could remove dead cells and stored at -80°C until use. Protocol was followed according to the manufacturers' instructions. Briefly, a standard curve was performed and media was added to wells containing the working reagent (provided in the kit). Optical density of the colorimetric product was measured at 570nm using a microplate reader. Pyruvate concentration (µM)

was calculated using the formula C=(ODsample-ODmedia without cells)/Slope. OD stands for optical density values [221].

2.2.16 Statistical Analysis:

Means and standard deviation of the mean, were calculated and statistically significant differences were determined by One-way ANOVA followed by Dunnett's Multiple Comparison test. n refers to sample size. Statistical significance was determined at $p<0.05$. The p values for the Glucose array were calculated using SABiosciences online software. The test used was a two-tailed Student's t-test, and statistical significance was determine at $p<0.05$.

Energy Metabolism in Human Pluripotent Stem Cells and Their Differentiated Counterparts

Chapter 3

Based on:

Varum S*, Rodrigues AS*, Moura MB, Momcilovic O, Easley CA IV, Ramalho-Santos J, Van Houten B, Schatten G. (2011) Energy Metabolism in Human Pluripotent Stem Cells and Their Differentiated Counterparts. PLoS ONE 6(6): e20914. doi:10.1371/journal.pone.0020914

* Joint first authors

Abstract

Human pluripotent stem cells have the ability to generate all cell types present in the adult organism, therefore harboring great potential for the in vitro study of differentiation and for the development of cell-based therapies. Nonetheless their use may prove challenging as incomplete differentiation of these cells might lead to tumoregenicity. Interestingly, many cancer types have been reported to display metabolic modifications with features that might be similar to stem cells. Understanding the metabolic properties of human pluripotent stem cells when compared to their differentiated counterparts can thus be of crucial importance. Furthermore recent data has stressed distinct features of different human pluripotent cells lines, namely when comparing embryo-derived human embryonic stem cells [1] and induced pluripotent stem cells (IPSC) reprogrammed from somatic cells. We compared the energy metabolism of hESC, IPSC, and their somatic counterparts. Focusing on mitochondria, we tracked organelle localization and morphology. Furthermore we performed gene expression analysis of several pathways related to glucose metabolism, including glycolysis, the pentose phosphate pathway and the tricarboxylic acid (TCA) cycle. In addition we determined oxygen consumption rates (OCR) using a metabolic extracellular flux analyzer, as well as total intracellular ATP levels by high performance liquid chromatography (HPLC). Finally we explored the expression of key proteins involved in the regulation of glucose metabolism. Our results demonstrate that, although the metabolic signature of IPSC is not identical to that of hESC, nonetheless they cluster with hESC rather than with their somatic counterparts. ATP levels lactate production and OCR revealed that human pluripotent cells rely mostly on glycolysis to meet their energy demands. Furthermore, our work points to some of the strategies which human pluripotent stem cells may use to maintain high glycolytic rates, such as high levels of Hexokinase II and inactive pyruvate dehydrogenase (PDH).

3.1 Introduction:

Although they can be differentiated into any somatic cell lineage pluripotent Human embryonic stem cells (hESCs), cannot be genetically matched to putative patients in possible cell replacement therapies. However, it has been recently shown that human somatic cells can be reprogrammed into hESC-like pluripotent stem cells, the so called induced pluripotent stem cells (iPSCs), using a variety of approaches [68,69,222]. The differences and similarities of hESCs and iPSCs have been studied at several levels, namely differentiation potential, global gene expression, and epigenetic status. The various analyses have revealed that despite the high level of resemblance in terms of pluripotency these cell types are not identical [75,223,224,225,226]. Namely, gene expression profiling revealed that, while iPSCs are highly similar to ESCs, a unique gene expression signature appears in iPSCs regardless of their origin [223]. Furthermore, DNA methylation analysis revealed that the methylome of certain developmental genes in iPSCs was intermediate between that found in differentiated cells and ESCs. In other cases, the methylation pattern in iPSCs was exclusive, differing from both ESCs and differentiated cells [224], suggesting both the occurrence of abnormal methylation during reprogramming and that some “epigenetic memory” from the reprogrammed somatic cells may linger in iPSCs, with unknown consequences [227], although the extent of this phenomenon is questioned [228]. Recent data suggests that iPSCs may be more prone to genetic mutation and instability [229,230,231]. Recently, Zhao et al. [232] demonstrated immunogenicity differences between authentic ESCs and iPSCs. Given the potential of these cells, further studies are needed to scrutinize these differences and to understand their impact on differentiation potential and possible therapeutic applications.

The mammalian embryo resides in a hypoxic environment prior to implantation [230]. During the early stages of embryonic development there is a metabolic shift from oxidative phosphorylation (OXPHOS) to glycolysis, and oxidative metabolism is only fully reinstituted after implantation [233].

Similarly to ICM cells, embryonic stem cells rely mostly on glycolysis for energy supply. Furthermore, the mitochondria in these cells are rather immature with perinuclear localization. As human pluripotent stem cells differentiate they acquire more mature mitochondria and undergo a metabolic switch from glycolysis to OXPHOS [14,76,131,136]. In agreement with these findings several authors have reported that hypoxia is beneficial for the maintenance of hESCs in a pluripotent state [189,198]. In addition low O_2 tensions have been reported to increase the reprogramming efficiency of both mouse and human somatic cells [149].

It is known that glycolysis and OXPHOS function in a coordinated fashion, and that the former generates 18 times more ATP per molecule of oxidized glucose than the former [234]. The first glycolytic reaction is crucial as glucose is captured within the cell by conversion to glucose 6-phosphate. This is one of the rate limiting steps in glycolysis and is catalyzed by hexokinases. Cell types with high glycolytic rates have been reported to have high expression levels of hexokinases [235,236]. Glucose 6-phosphate can be further metabolized in glycolysis producing two molecules of pyruvate, NADH and ATP. In normoxic conditions pyruvate enters mitochondria and links glycolysis to aerobic respiration by entering the TCA cycle (which provides the mitochondrial electron transfer chain (ETC) with reducing agents for ATP synthesis) as acetyl-coA. However under low O_2 tensions or in the presence of dysfunctional mitochondria pyruvate will be converted to lactate.

The pyruvate dehydrogenase (PDH) complex, localized in the mitochondrial matrix is the link between glycolysis and the TCA cycle. It is composed of several copies of three catalytic proteins (E1, E2 and E3) that catalyze the irreversible decarboxylation of pyruvate to acetyl-coA and NADH [237,238].

The E1-alpha subunit is considered the on/off switch of the PDH complex, as its phosphorylation by one of the four pyruvate dehydrogenase kinase isoforms (PDHK1-4) leads to PDH complex inactivation, whereas removal of one phosphate group by one of the two pyruvate dehydrogenase phosphatases (PDP1 and PDP2) activates the complex [237,238].

The exact mechanism by which hESCs maintain an anaerobic metabolism even in the presence of oxygen remains largely elusive. However, there is a certain putative parallelism with what has been described for cancer cells, which also maintain glycolysis as a key metabolic pathway under normoxia, in detriment to OXPHOS, the so-called Warburg effect [239]. Furthermore it has been recently shown that some cancer lines cultured under hypoxia acquire an undifferentiated phenotype similar to that of ESCs [240]. The aerobic glycolysis feature of cancer cells may involve the regulation of PDH function, at least in some cases, and indeed modulation of PDH function has been therapeutically considered in cancer [241]. However these analogies must be considered with great care, as there are considerable metabolic variations between cancer cell lines [242,243].

Additionally, it would be of interest to determine if and how iPSCs acquire a more glycolytic metabolism upon reprogramming, or if they instead maintain the metabolic features of the original somatic cell type that was reprogrammed. In this study our aim was to answer these questions by further characterizing the energy metabolism of both hESCs and human iPSCs when compared with their differentiated somatic counterparts. Towards that goal we analyzed mitochondrial morphology, glucose-related gene expression, OCR, intracellular ATP levels, lactate production and protein levels of regulatory enzymes relevant in metabolism. We believe that the obtained results help to answer some questions regarding some of the mechanisms that human pluripotent cells use to maintain high levels of glycolysis under normoxia.

3.2 Results:

3.2.1 Mitochondrial localization and morphology:

In order to determine mitochondria morphology and localization within the cell in pluripotent *versus* differentiated cells we transduced hESCs (WA07 line) and fibroblasts cells (H7TF, IMR-90 and HFF1) with a baculovirus system containing a leader sequence for PDH E1 alpha subunit fused with the GFP protein. Mitochondria in the hESC line WA07 showed perinuclear localization (Fig. 3.1A, top left) whereas the mitochondria of their differentiated counterparts (H7TF) were distributed in the cytoplasm (Fig. 3.1A, top right). This might be a consequence of the high nuclear-cytoplasmic ratio observed in the hESCs. Furthermore, the mitochondria in WA07 cells showed a globular shape, whereas mitochondria in the H7TF line were mainly elongated and formed extensive reticular networks. Similarly, the mitochondria of the somatic lines HFF1 and IMR-90 were also distributed in the cytoplasm rather than clustered around the nucleus; their shape was mostly tubular and they formed extensive networks (Fig. 3.1A, bottom left and right).

In order to better characterize mitochondrial morphological features in pluripotent versus differentiated somatic cells we performed transmission electron microscopy [244] for hESCs (WA07 line), iPSCs (IMR-90 and HFF1 iPSC lines) and fibroblasts cells (H7TF, IMR-90 lines) (Fig.3.1B). TEM analysis demonstrated that mitochondria in hESCs have few cristae and electron-lucid matrix (Fig. 3.1B, top left). These results are in accordance with previous reports [76,131]. TEM of cells obtained after differentiation of W07 hESCs (H7TF) revealed mitochondria with an elongated shape, and with a higher number of cristae, as well as a denser matrix (Fig.3.1B. bottom, left). Similar to H7TF, IMR-90 and lung fibroblasts (LF) showed mature mitochondria with numerous cristae and electron dense matrix (Fig. 3.1B. bottom center and right, respectively). Interestingly, both IMR-90 and HFF1 iPSCs showed a mix of both elongated and

globular mitochondria. Furthermore, the matrix of the mitochondria resembled that of differentiated cells (Fig.1B top, center and right, respectively).

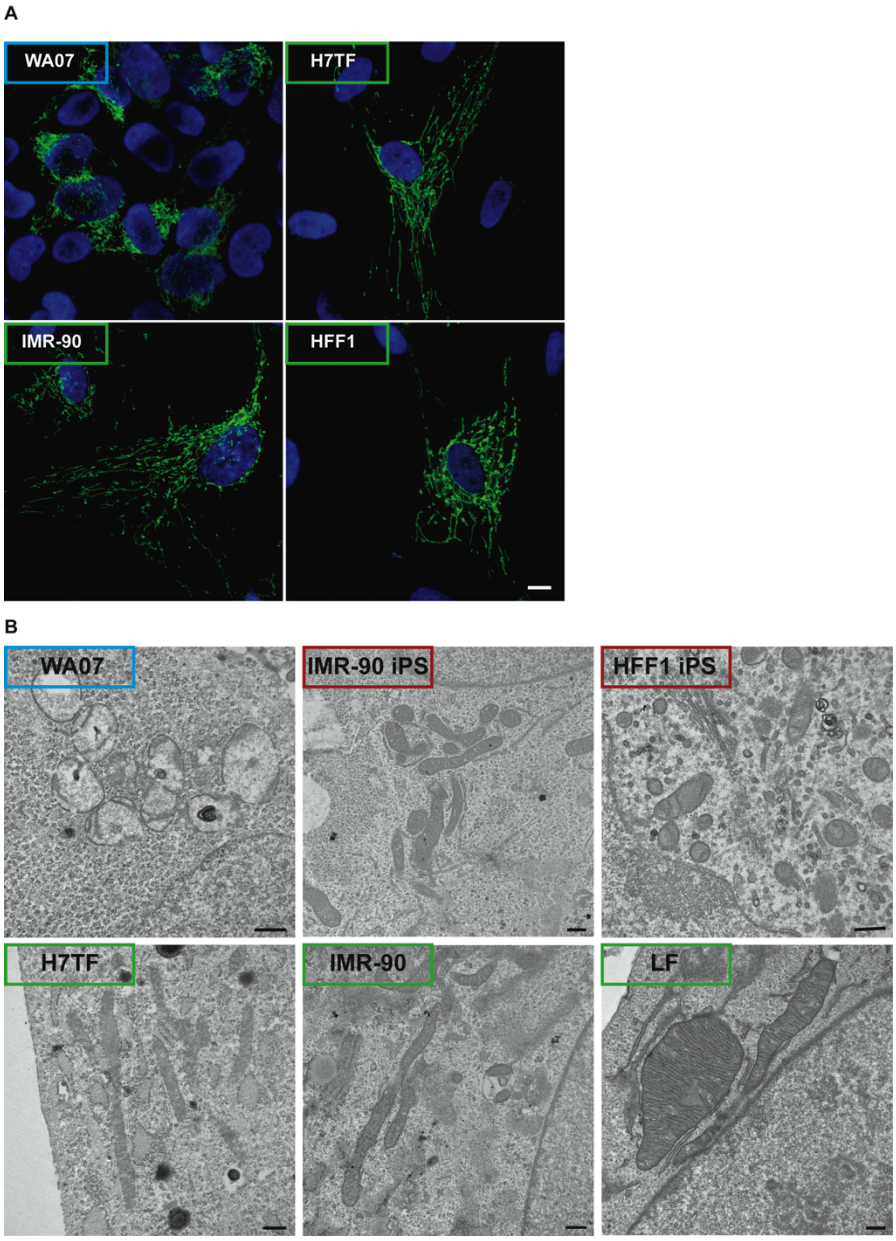

Figure 3.1. Mitochondrial morphology and localization in human pluripotent stem cells vs. differentiated cells. A) Transduction of hESCs (WA07 line,) and differentiated cells (H7TF, HFF, and IMR-90 lines) with organelle lights MitoGFP was used investigate mitochondria morphology and localization within the cell. Blue: DAPI; Green: pyruvate dehydrogenase GFP. Scale bar: 10µm **B)** Transmission electron microscopy [244] was used to investigate mitochondria morphologic features in hESCs (WA07 line), IPSCs (HFF1 and IMR-90 IPSC lines), and fibroblast cells (H7TF, IMR-90 and HFF1). Scale bar: 500 nm.

These results suggest that mitochondria morphology in human iPSCs is not identical to that found in hESCs, but iPSCs seem to have a mixed phenotype between that found in hESCs and differentiated cells. It would be of interest to perform histomorphometric analysis in order to fully validate this assumption.

3.2.2 Metabolism-related gene expression in human pluripotent stem cells vs. differentiated cells:

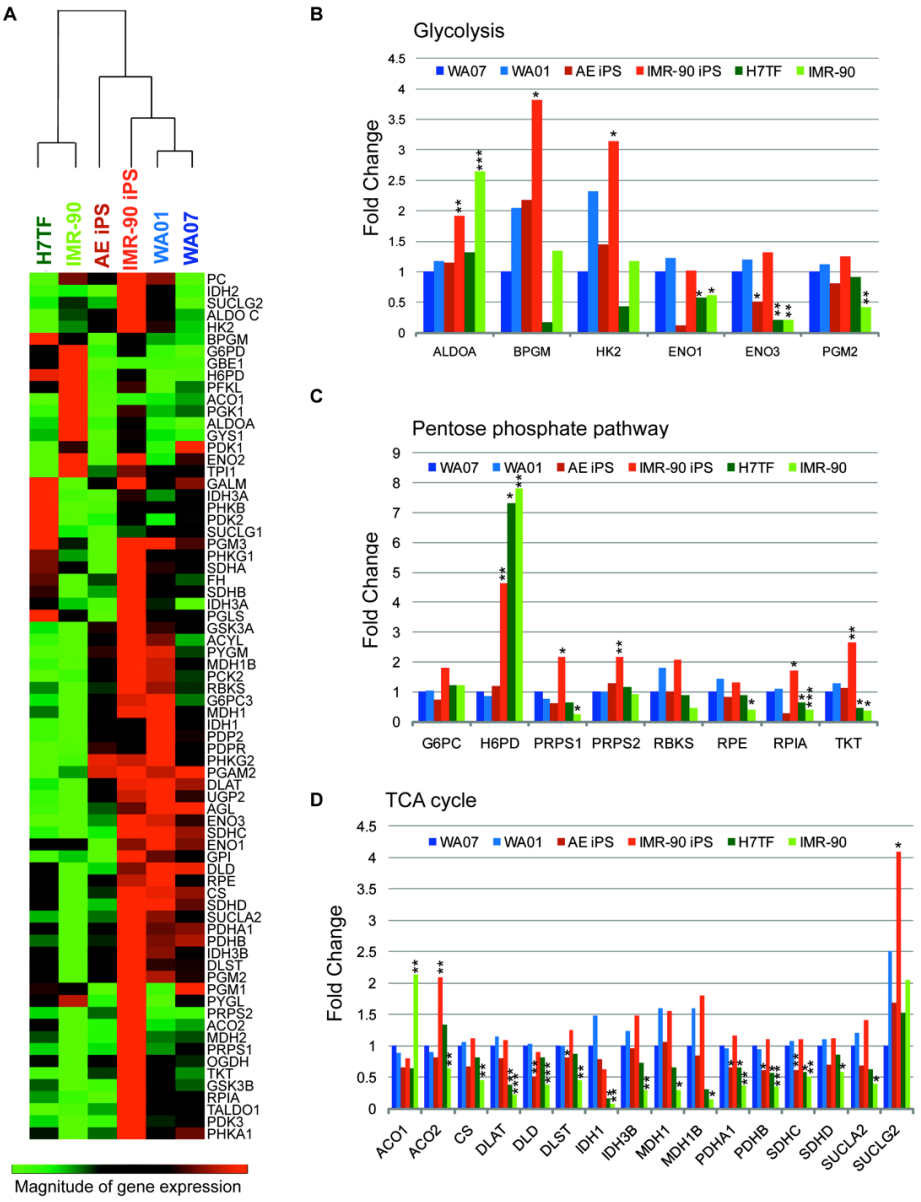

Figure 3.2. Metabolism-related gene expression in human pluripotent stem cells vs. differentiated cells. A) Heat map of average gene expression. Gene expression is represented as $\log_{10}$ of Ct values. An increase in gene expression is depicted in red, whereas a decrease in gene expression is represented by the green color. No differences in expression are depicted in black. Clustering was performed using SABiosciences online software. The various genes were grouped accordingly to their participation in different metabolic pathways. **B)** Glycolysis-related genes with at least two fold difference when compared to the WA07 line. **C)** Pentose phosphate pathways-related genes with at least two fold differences when compared to the WA07 line. **D)** TCA cycle- related genes with

at least two fold differences when compared to the WA07 line. Fold changes were calculated using the -ΔΔCt method relative to the WA07 line. hESC lines are represented in blue, IPSC lines in red and somatic cell lines in green . The values represent means of three independent experiments. Statistical analysis was performed using Student's t test (SABiosciences online software) and significance was determined at $p<0.05$. Statistically significant differences are represented in Table 3.1.

To further investigate the metabolic pathways used by human pluripotent stem cells and differentiated somatic cells we used two hESC lines (WA07 and WA01), two iPSC lines (IMR-90 iPS and AE iPS), and two somatic lines (WA07 teratoma fibroblasts-H7TF, and IMR-90 fibroblasts) and performed the SABiosciences human glucose metabolism RT^2 profiler PCR array. This array contains 84 key genes involved in the regulation of glucose and glycogen metabolism, along with five housekeeping genes. Overall we observed that pluripotent lines tend to cluster together rather than with their somatic counterparts (Fig. 3.2A, heatmap). Furthermore, we observed that there are no significant differences in gene expression between the two hESC lines (WA07 and WA01) used in this study (Table 3.1). Statistical analysis showed that when compared to WA07 cells, IMR-90 iPSCs showed 25 genes with significantly different expression, whereas in AE iPSCs there were 14 such genes (Table 3.1). For differentiated cells when compared the WA07 cell line; the IMR-90 cells showed 44 differentially expressed genes whereas for H7TF cells there were 18 genes (Table 3.1). We further focused our analysis on 60 genes known to be involved in glycolysis, the pentose phosphate pathway and the TCA cycle (Figure 3.2, Table 3.1). Due to their pleiotropic nature some of the genes were included in more than one group. Only genes that were differentially expressed at least two fold when compared with the WA07 line, and with $p<0.05$ where considered in the analysis.

Regarding the glycolytic signature, six genes among all lines were either up regulated or down regulated when compared with the WA07 line (Fig. 3.2 B and Table 3.1). Among these differentially expressed genes, *ENO 1* and *ENO 3* were downregulated (2.02 and 1.98 fold, respectively, $p<0.05$) in AE

iPSC. The IMR-90 iPSC line displayed up regulation of *BPGM* (3.82 fold, p<0.01), and *HK2* (3.15 fold, p<0.05) (Figure 3.2B, Table 3.1). Both H7TF and IMR-90 lines showed down regulation of *ENO 3* (4.72 fold, p<0.05 and 4.73 fold, p<0.01, respectively) (Figure 3.2B, Table 3.1). In addition, the IMR-90 line showed decreased expression of *PGM2* (2.38 fold, p<0.01) and up regulation of *ALDO A* (2.64 fold, p<0.001).

In terms of the pentose phosphate pathway seven genes were differentially expressed among all the lines when compared with the WA07 line. No differences were observed between the WA07 line and both the WA01 and AE iPSC lines. The IMR-90 iPSC line showed up regulation of *H6PD* (4.65 fold, p<0.01), *PRPS1* (2.18 fold, p<0.05), *PRPS2* (2.17 fold, p<0.01), *TKT* (2.67 fold, p<0.01). Both the H7TF and IMR-90 lines displayed increased expression of *G6PD* (1.96 fold, p<0.001 and 2.82 fold, p<0.001, for H7TF and IMR-90, respectively) *H6PD* (7.33, p<0.05 and 7.82, p<0.01, respectively), and decreased expression of *TKT* (2.13 fold, p<0.05 and 2.65 fold, p<0.05, respectively). In addition the IMR-90 line showed decreased expression of *PRPS1* (3.96 fold, p<0.05), *RPE* (2.50 fold, p<0.05) and *RPIA* (2.52 fold, p<0.05).

Regarding the TCA cycle signature we observed that 17 genes were differentially expressed when compared to the WA07 line (Figure 3.2D, Table 3.1). Again no significant differences were observed between the two hESC lines. When compared to the WA07 line, the AE iPSC line displayed decreased expression of *DLD* (1.98 fold, p<0.05) (Figure 3.2C). The IMR-90 iPSC line showed increased expression of *ACO2* (2.09 fold, p<0.01), and *SUCLG2* (4.08 fold, p<0.05) (Figure 3.2C). Both the H7TF and IMR-90 lines showed down regulation of *DLAT* (2.65 fold, p<0.01 and 4.65, p<0.001, respectively) and *IDH1* (6.34 fold, p<0.05 and 14.13 fold, p<0.01, respectively) (Figure 3.2C, Table 3.1). In addition, the IMR-90 line demonstrated decreased expression of *CS* (2.21 fold, p<0.01), *DLD* (4.65 fold, p<0.001), *DLST* (2.22 fold, p<0.05), *IDH3B* (3.44 fold, p<0.01), *MDH1* (3.43 fold, p<0.05), *MDH1B* (6.52 fold, p<0.05),

PDHA1 (2.78 fold, p<0.01), *PDHB* (2.88, p<0.001), *SDHC* (1.96, p<0.01) and *SUCLA2* (2.52, p<0.05), and up regulation of *ACO 1* (2.13 fold, p<0.01).

With respect to genes involved in the regulation of the TCA cycle no significant differences were detected between the WA07 line, the WA01, AE iPSC and iMR-90 iPSC lines (Table 3.1). Both differentiated lines showed down regulation of *PDP2* (3.52 fold, p<0.05 and 4.55 fold, p<0.01 for H7TF and IMR-90, respectively). In addition the IMR-90 displayed decreased expression of *PDK3* (5.32 fold, p<0.01).

Table 3.1. - p values and fold change values for gene expression comparing cell lines. p values and fold change were determined relative to the WA07 line, values for the WA01 were omitted given the absence of statistical differences. p values represented in red correspond to genes that are significantly up regulated, whereas p values depicted in green represent genes that are significantly down regulated. p values above 0.05 are represented in black.

		AE iPS	IMR-90 iPS	H7TF	IMR-90
Glycolytic signature in human pluripotent stem cells and differentiated cells					
Glucan (1,4-alpha-), branching enzyme 1	p value	0.182796	0.401636	0.059971	0.003255
(GBE1)	fold change	0.7054	1.1367	4.7209	8.495
Glycogen synthase 1 (muscle)	p value	0.305042	0.073519	0.361399	0.006032
(GYS1)	fold change	0.811	1.9655	1.1979	2.5033
UDP-glucose pyrophosphorylase 2 (UGP2)	p value	0.583771	0.349007	0.009063	0.00436
	fold change	0.8944	1.9655	1.1979	2.5033
Amylo-1, 6-glucosidase, 4-alpha-glucanotransferase (AGL)	p value	0.005425	0.192293	0.003653	0.000895
	fold	0.4876	0.8313	0.3105	0.2598

	change				
Phosphoglucomutase 2 (PGM2)	p value	0.234121	0.248629	0.699586	0.002456
	fold change	0.8094	1.2579	0.912	0.4195
Phosphorylase kinase, alpha 1 (muscle) (PHKA1)	p value	0.046949	0.322249	0.283362	0.011132
	fold change	0.5629	1.2064	0.6188	0.2989
Phosphorylase kinase, gamma 1 (muscle) (PHKG1)	p value	0.004105	0.098563	0.538787	0.712081
	fold change	0.693	1.2688	1.1493	0.8383
TCA signature in pluripotent stem cells and differentiated cells					
Aconitase 1, soluble (ACO1)	p value	0.079385	0.17169	0.083256	0.001386
	fold change	0.6574	0.8055	0.6382	2.1317
Aconitase 2, mitochondrial (ACO2)	p value	0.089029	0.006734	0.15926	0.006435
	fold change	0.8176	2.0941	1.3357	0.6398
Citrate synthase (CS)	p value	0.052026	0.45459	0.548219	0.003514
	fold change	0.6765	1.1202	0.822	0.4525
Dihydrolipoamide S-acetyltransferase (DLAT)	p value	0.369543	0.531728	0.001807	0.000145
	fold change	0.8036	1.0924	0.3766	0.2149
Dihydrolipoamide dehydrogenase (DLD)	p value	0.027963	0.493081	0.671359	0.004943
	fold change	0.5042	0.9001	0.8158	0.3774
Dihydrolipoamide S-succinyltransferase (E2 component of 2-oxo-glutarate complex) (DLST)	p value	0.019154	0.018305	0.726826	0.036226
	fold change	0.8177	1.2538	0.8764	0.4507
Isocitrate dehydrogenase 1 (NADP+), soluble (IDH1)	p value	0.38673	0.274658	0.0133	0.009346
	fold	0.7855	0.6221	0.1576	0.0708

	change				
Isocitrate dehydrogenase 2 (NADP+), mitochondrial (IDH2)	p value	0.7786	0.031926	0.983299	0.759598
	fold change	0.9283	1.9134	1.0082	1.0896
Isocitrate dehydrogenase 3 (NAD+) beta (IDH3B)	p value	0.753791	0.063038	0.271417	0.002515
	fold change	0.956	1.4816	0.736	0.2906
Isocitrate dehydrogenase 3 (NAD+) gamma (IDH3G)	p value	0.888987	0.020491	0.160844	0.22335
	fold change	1.0302	1.9212	1.604	1.2025
Malate dehydrogenase 1, NAD (soluble) (MDH1)	p value	0.888013	0.220693	0.24667	0.032701
	fold change	1.0678	1.551	0.6616	0.2919
Malate dehydrogenase 1B, NAD (soluble) (MDH1B)	p value	0.520214	0.113153	0.126206	0.019708
	fold change	0.8393	1.7995	0.3061	0.1533
Malate dehydrogenase 2, NAD (mitochondrial) (MDH2)	p value	0.076133	0.030813	0.960944	0.012102
	fold change	0.8325	1.6313	0.9978	0.7057
Oxoglutarate (alpha-ketoglutarate) dehydrogenase (lipoamide) (OGDH)	p value	0.383583	0.033559	0.773533	0.003039
	fold change	1.0779	1.797	1.0241	0.5878
Pyruvate carboxylase (PC)	p value	0.486329	0.070307	0.698611	0.144088
	fold change	1.8306	3.2082	1.0055	2.7399
Phosphoenolpyruvate carboxykinase 1 (soluble) (PCK1)	p value	0.046384	0.011521	0.331536	0.339268
	fold change	0.7211	1.7918	1.2305	1.215
Pyruvate dehydrogenase (lipoamide) alpha 1 (PDHA1)	p value	0.041691	0.395379	0.045818	0.00137
	fold change	0.6524	1.1575	0.6586	0.3597

Pyruvate dehydrogenase (lipoamide) beta (PDHB)	p value	0.012731	0.486834	0.018482	0.000693
	fold change	0.6072	1.1068	0.5688	0.3472
Succinate dehydrogenase complex, subunit A, flavoprotein (Fp) (SDHA)	p value	0.053203	0.04001	0.445353	0.210469
	fold change	0.0924	1.5081	1.2054	0.8044
Succinate dehydrogenase complex, subunit B, iron sulfur (Ip) (SDHB)	p value	0.151871	0.250403	0.557484	0.01685
	fold change	0.7772	1.3079	1.1108	0.6016
Succinate dehydrogenase complex, subunit C, integral membrane protein, 15kDa (SDHC)	p value	0.009183	0.168632	0.033296	0.002187
	fold change	0.6088	1.0997	0.5814	0.5113
Succinate dehydrogenase complex, subunit D, integral membrane protein (SDHD)	p value	0.059517	0.463437	0.475622	0.011049
	fold change	0.7036	1.1243	0.8578	0.5881
Succinate-CoA ligase, ADP-forming, beta subunit (SUCLA2)	p value	0.193395	0.129939	0.172629	0.014183
	fold change	0.682	1.405	0.6284	0.3963
Succinate-CoA ligase, alpha subunit (SUCLG1)	p value	0.025023	0.153357	0.198642	0.045376
	fold change	0.5737	0.7974	1.2925	0.6963
Succinate-CoA ligase, GDP-forming, beta subunit (SUCLG2)	p value	0.465278	0.01718	0.621296	0.237038
	fold change	1.6929	4.0889	1.5243	2.0461

3.2.3 Mitochondrial contribution to the energy metabolism of human pluripotent stem cells and differentiated cells:

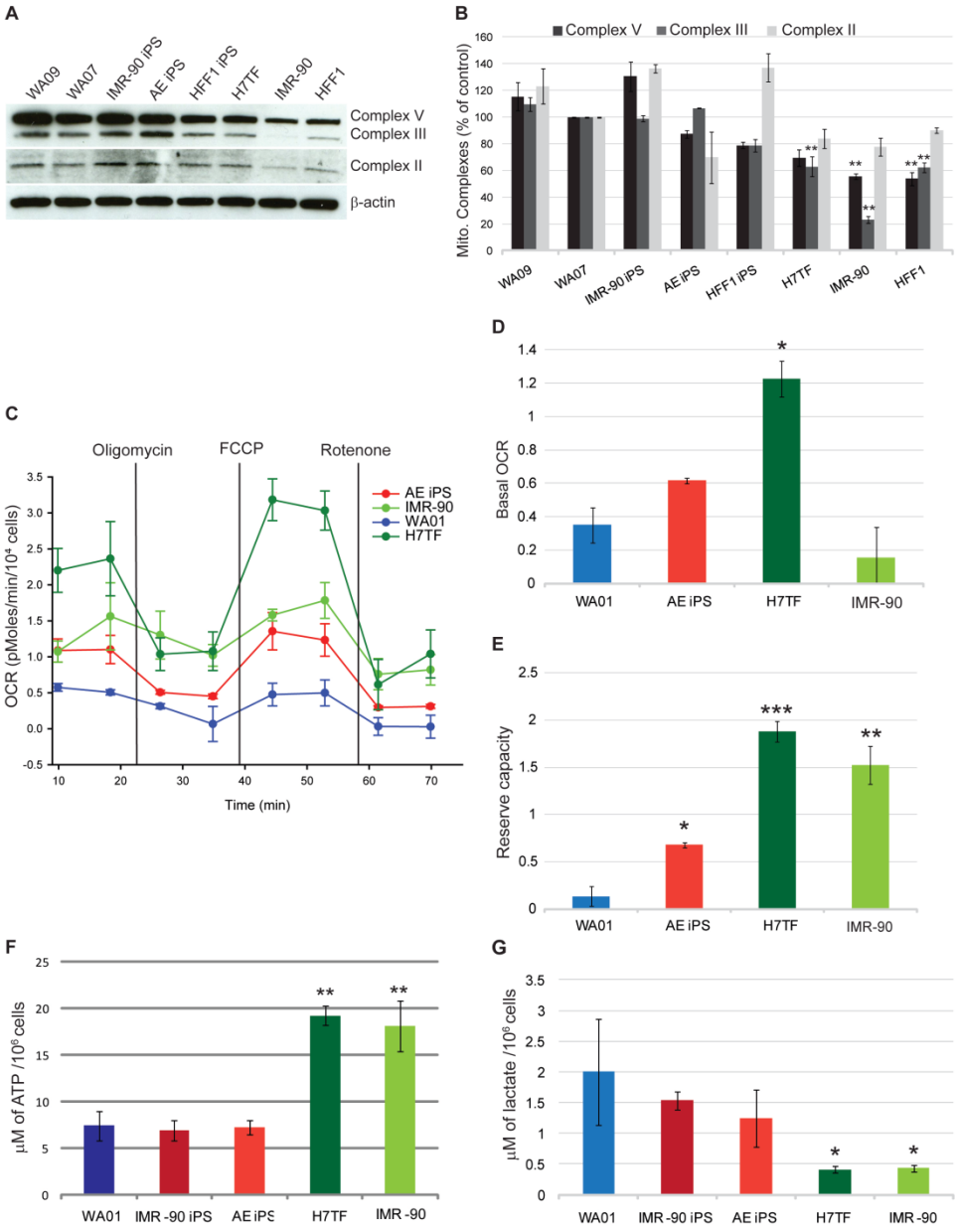

Figure 3.3. Mitochondrial contribution to the energetic metabolism of human pluripotent stem cells and differentiated cells. A) Western blotting analysis of mitochondrial complexes II, III and V. β-actin was used as a loading control. **B)** Quantification of mitochondrial complexes II, III and V protein levels relative to the WA07 line. **C)** Oxygen consumption rate (OCR) was determined by Seahorse XF24 analyzer. The three mitochondrial inhibitors were sequentially injected (after measurement points, 2, 4, and 6, as indicated) and the final concentrations of

each were: oligomycin (1μM); FCCP (300mM); rotenone (1μM) **D)** Basal OCR (represents the mean of the first two measurements minus the mean of measurements 3 & 4). **E)** Reserve capacity (FCCP induced levels, measurements 5 & 6 minus the basal level). **F)** Intracellular ATP levels determined by HPLC. **G)** Lactate levels secreted into the medium. The values are averages of three independent experiments. Statistical significance was determined by one-way ANOVA followed by Dunnet's multiple comparison test. Statistical significance was determined at $P<0.05$. Error bars: SEM.

To further understand mitochondrial contribution to the energy metabolism of pluripotent cells we analyzed protein expression of mitochondrial complexes II, III and V in pluripotent *vs.* differentiated somatic cells. We observed no statistical significant differences in mitochondrial complexes II, III and V between the various pluripotent lines. Intriguingly, we observed that pluripotent cells even have higher protein levels of mitochondrial complexes II, III and V than differentiated cells (Fig. 3.3A, B). Indeed, when compared to the WA07 line, mitochondrial complex V protein levels were decreased by 45% and 46% in IMR-90 and HFF1 fibroblasts, respectively ($p<0.01$ Fig. 3.3A,B). Furthermore, complex III protein levels were decreased by 76.8%, 38% and 27% in IMR-90, HFF1 and H7TF fibroblasts, respectively ($p<0.01$, Fig. 3.3A,B). Although, we observed a decreased expression trend for mitochondrial complex II in differentiated cells, it was not statistically significant.

In order to determine if the differences observed in mitochondrial complex expression could be translated in terms of higher mitochondrial activity in pluripotent cells we determine O_2 consumption rate (OCR) using the Seahorse XF24 extracellular flux analyzer. We have used a pharmacological profiling approach, by combining the use of three mitochondrial inhibitors (rotenone, FCCP and oligomycin) and the Seahorse instrument as previously described by Qian and Van Houten [206]. The OCR response to the chemical compounds were analyzed in one hESC line (WA01), one iPSC line (AE) and two differentiated cell lines (H7TF and IMR-90).

The basal OCR (measure of OXPHOS) is the amount oxygen consumption that is linked to ATP synthesis in the mitochondria, and represents the mean basal levels of oxygen consumption minus the mean of the two values following oligomycin treatment (measurements 3 and 4). Oligomycin inhibits ATP synthase by binding to the oligomycin sensitivity-conferring protein (OSCP) at the F_0 subunit of the ATP synthase. This blocks the proton conductance resulting in loss of electron transfer and O_2 consumption. Addition of oligomycin resulted in decreased levels of OCR in all cell types (Fig. 3.3C). Nonetheless the kinetics and relative intensity of response varied among the various cell types with hESCs having the slowest and less pronounced response followed by IMR-90, AE IPSC and finally H7TF (Fig.3.3C).

The H7TF cells showed higher basal O_2 consumption rates when compared to the other cell types (Fig. 3.3C and 3.3E). The lowest basal OCR was observed for hESCs (WA01) and the differentiated line IMR-90 (Fig. 3.3C and 3.3E). The AE IPSC line displayed intermediate basal OCR levels between those found for the H7TF and WA01 line (Fig. 3.3C and 3.3D). Likewise to what was observed in glucose-related gene expression there were marked differences between the IMR-90 and H7TF with respect to their basal OCR. Because H7TF cells are derived from teratomas one could question whether the OCR levels of these cells are representative of other differentiated lines. In order to address that question we performed OCR measurements for a normal diploid human skin fibroblast line (NDHF). We observed that OCR levels in these cells are similar to those observed in H7TF rather to those observed in the IMR-90 cells (Figure 3.4)

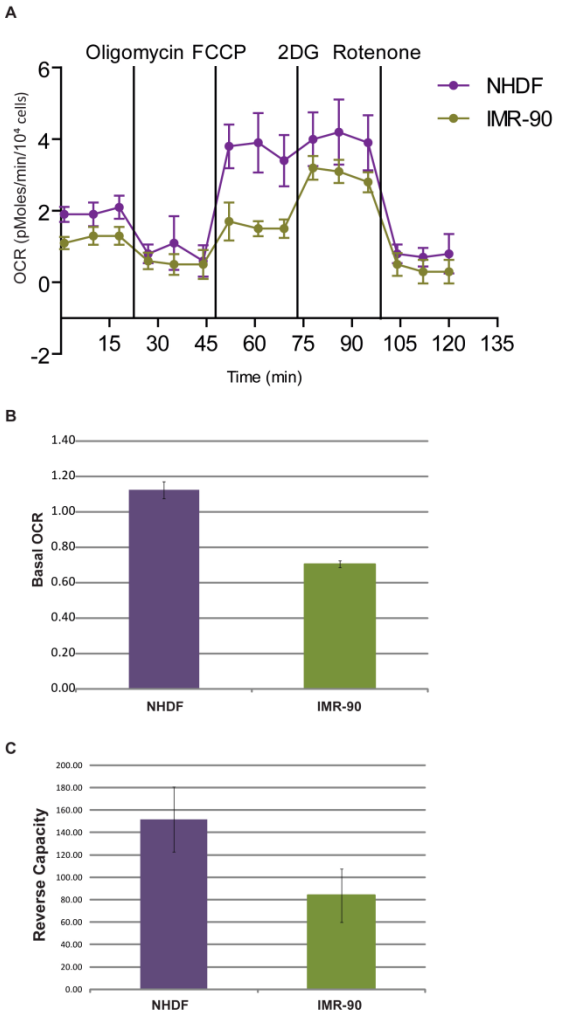

Figure 3.4. Comparison of OCR in two differentiated cell lines. A**)** Oxygen consumption rate (OCR) was determined by Seahorse XF24 analyzer for IMR-90 and NHDF lines, the former also listed in Figure 3.3. The mitochondrial inhibitors were sequentially injected at specific time points as illustrated in the figure. **B)** Basal OCR (represents the mean of the first three measurements minus the mean of measurements 4, 5 & 6). **C)** Reserve capacity (FCCP induced levels, measurements 7, 8 & 9 minus the basal level). Measurements show that NHDF cells show higher values than IMR-90 cells, similarly to what is described for the other differentiated cell line (H7TF) listed in Figure 3.3.

FCCP is a mitochondrial uncoupler that dissipates the proton gradient, and therefore uncouples electron transport and mitochondrial respiration from ATP synthesis. FCCP treatment has been shown to increase O_2 consumption to its maximum in various cell types. In fact FCCP resulted in an increase of

OCR levels in all cell types, with the most pronounced response being observed in H7TF, followed by IMR-90, AE IPS and WA01 cells (Fig. 3.3C). The difference between FCCP OCR and basal OCR is a good measure of respiratory capacity (also designed of reserve capacity) of these cells. Indeed we observed that the respiratory capacity of differentiated cells is higher than that observed for pluripotent lines (Fig.3.3E).

Rotenone is a mitochondrial inhibitor that prevents electron transfer from complex I to ubiquinone by blocking the ubiquinone binding site [245]. Treatment with rotenone decreased OCR levels in all cells types although H7TF fibroblasts showed a more pronounced response to the treatment. Overall our results suggest that both hESCs and iPSCs have lower reliance in OXPHOS when compared to the H7TF cells. Interestingly IMR-90 fibroblasts showed low basal O_2 consumption rates, but when challenged with FCCP had the ability to increase OXPHOS rates to a similar extent to that observed in other differentiated cell types (H7TF and NDHF). In contrast both hESCs and iPSCs showed a considerably reduced response to FCCP than differentiated cells (H7TF and NDHF). These results suggest that mitochondria in pluripotent cells, although functional, present a low activity rate, and that the differences in mitochondrial content noted previously do not directly account for differences in activity.

Total ATP levels are originated both from anaerobic and aerobic respiration. In order to determine intracellular ATP levels in human pluripotent stem cells and differentiated cells we performed HPLC (Fig. 3.3F). Our results showed that somatic cells have elevated intracellular ATP levels when compared to differentiated cells. In addition we measure lactate secretion to media (a good measure for glycolysis that does not add to the TCA cycle) in human pluripotent stem cells and differentiated cells (Fig.3.3G). As expected human pluripotent cells displayed higher lactate levels than differentiated cells. Overall these results suggest that human pluripotent stem cells rely mostly on glycolysis to meet their energy demands.

3.2.4 Hexokinase II expression in human pluripotent stem cells and differentiated cells:

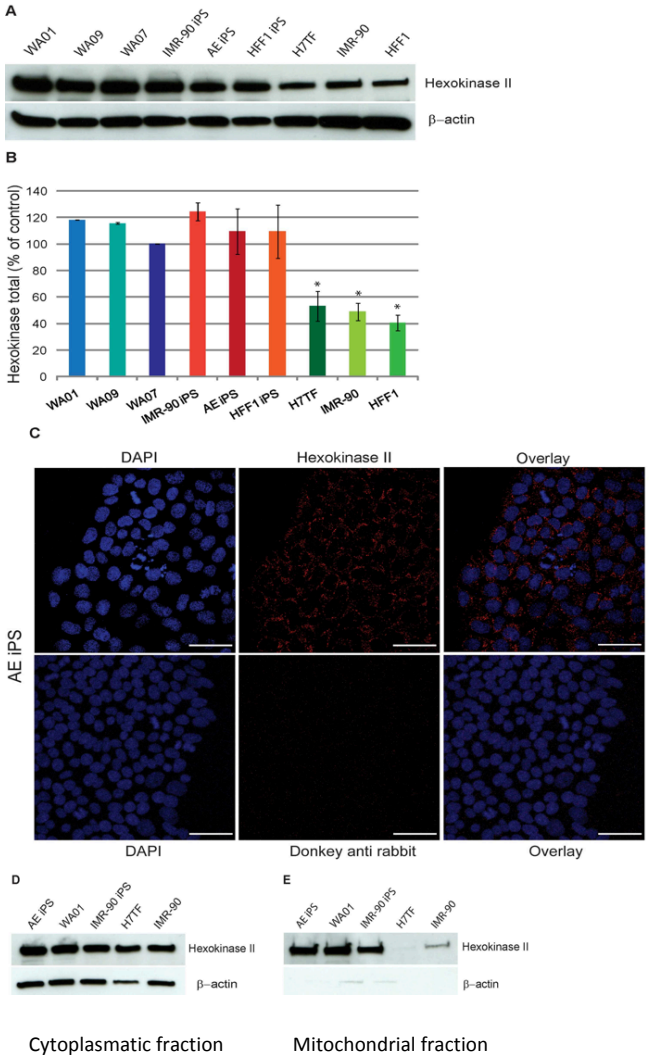

Figure 3.5. Hexokinase II expression in human pluripotent stem cells and differentiated cells. A) Western blotting analysis for Hexokinase II protein levels. **B)** Quantification of Hexokinase II protein levels relative to the WA07 line. **C)** Localization of Hexokinase II in AEIPS cells; **D-E**) Hexokinase II protein levels in the cytoplasmic and mitochondrial fractions, respectively. β-actin was used as a loading control. Values are means of three independent experiments. Statistical significance was determined at $p<0.05$ by one-way ANOVA followed by Dunnet's multiple comparison test. Error bars: SEM

Mammalian tissues harbor four Hexokinase isoforms (I- IV) with particular kinetics and tissue specificity. Both Hexokinase I and II have an N-terminal hydrophobic domain that allows binding to the outer mitochondrial membrane. Pedersen and colleagues have shown that mitochondrial-bound Hexokinase II is responsible for the high glycolytic profile of rat hepatoma cells [235,236]. In order to determine if Hexokinase II could play a role in the maintenance of high glycolytic rates in pluripotent cells we performed western blotting analysis for Hexokinase II in three hESC lines (WA01, WA07 and WA09), three IPSC lines (IMR-90 IPSC, AE IPS and HFF1 IPSC) three differentiated lines (H7TF, IMR-90 and HFF1). We observed that pluripotent cells overexpress Hexokinase II when compared to differentiated cells (Fig 3.5A, B). We next isolated the cytoplasmic and mitochondrial fractions of hESCs (WA01 line), IPSCs (AE IPS and IMR-90 IPS) and fibroblasts cells (H7TF and IMR-90) and determined Hexokinase protein levels in both fractions (Fig. 3.5C, D, respectively). We observed that Hexokinase II in differentiated cells is preferentially localized in the cytoplasm, whereas pluripotent cells display high levels of Hexokinase II in both cytoplasmic and mitochondrial fractions.

2.3.5 PDH complex regulation in human pluripotent stem cells and differentiated cells:

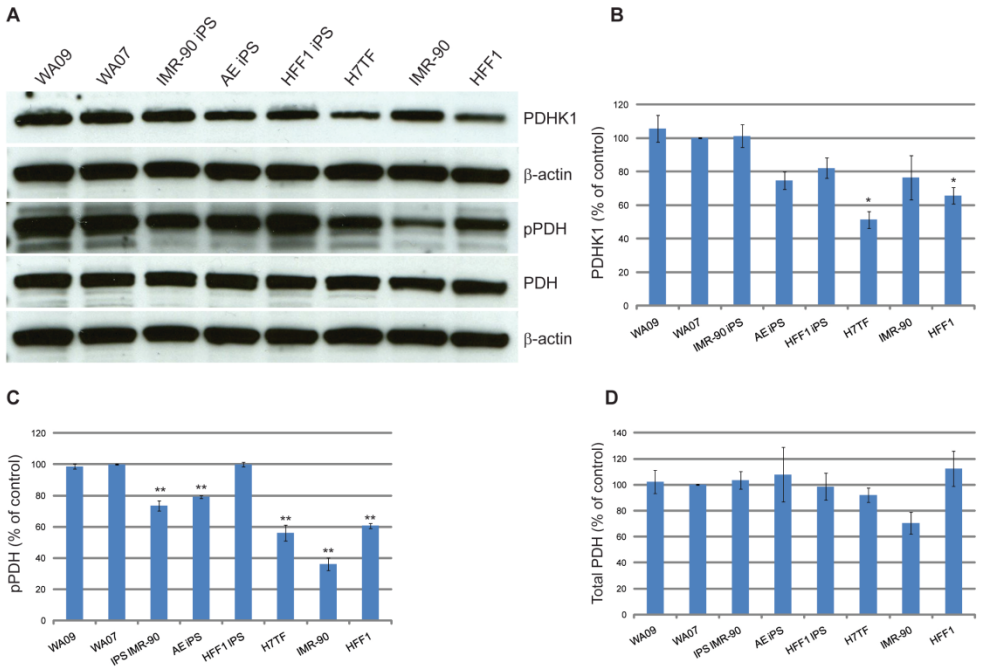

Figure 3.6. Pyruvate dehydrogenase regulation in human pluripotent stem cells and differentiated cells. **A)** Western blotting analysis of PDHK1, pPDH and total PDH protein levels. β-actin was used as a loading control. **B-D)** Protein levels quantification relative to the Wa07 line of PDHK1, pPDH and PDH, respectively. Values are means of three independent experiments. Statistical significance was determined at $p<0.05$ by one-way ANOVA followed by Dunnet's multiple comparison test. Error bars: SEM Abbreviations: PDHK1, pyruvate dehydrogenase kinase one; pPDH: phospho Ser ^{293} pyruvate dehydrogenase subunit E1α; PDH: pyruvate dehydrogenase.

Key metabolic regulation in terms of glycolysis versus OXPHOS involves the PDH complex. We therefore analyzed PDHK1, phosphorylated PDH (phosphoPDH) and total PDH protein in pluripotent stem cells and differentiated cells. We observed that PDHK1 protein levels are upregulated in pluripotent cells when compared to differentiated cells (Fig.3.6 A, B). Statistical analysis revealed that there are no significant differences between the WA07 hESC line and the other pluripotent lines (Fig. 3.6B). Although, there was a decrease in PDHK1protein levels between the WA07 line and both H7TF and HFF1 fibroblast lines (49% and 34% decrease for H7TF and HFF1, respectively; $p<0.05$) no significant

differences were observed for the IMR-90 line (Fig. 3.6B). This result suggests that PDHK1 protein stabilization differs between pluripotent and differentiated cells. Consistent with higher PDHK1 protein levels, pluripotent cells also displayed higher phosphoPDH levels when compared to differentiated cells (Fig. 3.6 A and C). All three differentiated lines showed lower phosphoPDH protein when compared with the hESC line WA07 (44%, 64% and 39% decrease for H7TF, IMR-90 and HFF1 fibroblast, respectively; $p<0.01$; Fig. 5C). Interestingly, both AE and IMR-90 iPSCs showed lower levels of phosphoPDH than the WA07 line (20% and 26% decrease for AE iPSCs and IMR-90 iPSCs, respectively; $p<0.01$; Fig. 5C). No significant differences were found for total PDH levels. These results suggest that the lower mitochondrial activity observed in pluripotent cells might, at least partially, be attributed to high levels of phosphoPDH. Our results further suggest that besides PDHK1 other PDHKs are regulating the activity of the PDH complex in these cells, as no significant differences were observed for the PDHK levels in IMR-90 cells but these cells displayed higher levels of phospho PDH

3.3 Discussion:

In this study we sought to understand the energetic metabolism of pluripotent stem cells and their differentiated counterparts. We started by looking at mitochondrial morphology and localization in human pluripotent stem cells (both hESCs and iPSCs), and somatic cells. In agreement with previous reports our results demonstrate that mitochondria in hESCs appear immature with fewer cristae, and low electron density matrix, when compared to differentiated somatic cells [14,131]. Interestingly iPSCs displayed a mixed mitochondrial phenotype that still resembles the somatic cells of origin and is not quite that of ESCs. Analyzing distinct mitochondrial features during the reprogramming process and how they compare with the acquisition and stabilization of pluripotency characteristics would therefore be of interest, and might provide novel insights into mitochondrial activity and metabolic shifts during reprogramming.

Glucose-related gene expression analysis revealed that both hESC lines analyzed in this study have identical glucose-related metabolism signatures. In contrast iPSCs are not identical to hESCs, although they cluster together, rather than with their somatic counterparts. Interestingly both iPSC lines analyzed in this study showed different metabolic gene expression signatures, with IMR-90 iPSCs having higher transcripts levels. It should be noted that that the cocktail of transcription factors used for the reprogramming of both lines differ [222]. However recent papers [228] established a genome-wide map for DNA methylation and gene expression for a considerable number of iPSC lines generated using several somatic cells and various methodologies, demonstrating some cell-line differences in gene expression that are probably not due to a single factor. It would be interesting to determine if these differences are also reflected in terms of functional metabolic studies.

Regarding the glycolytic signature of human pluripotent stem cells and somatic cells we observed that H7TF fibroblasts displayed similar glycolytic signature to their pluripotent counterpart the WA07 hESC line, with only four genes significantly downregulated. Interestingly the IMR-90 fibroblasts displayed 10 genes differentially expressed (six genes significantly downregulated and four genes up regulated when compared to the WA07).

Cell division requires not only ATP but also biosynthetic precursors derived from glycolysis, the pentose phosphate pathway and the TCA cycle. For instance, glucose 6-phosphate can be diverted from the glycolytic pathway to the pentose phosphate pathway in order to generate ribose 5-phophate for *de novo* nucleotide synthesis. The pentose phosphate pathway can be divided in two major branches, an oxidative branch and a non-oxidative branch [87]. Our gene expression analysis demonstrated that both *G6PD* and *H6PD* are significantly up regulated in differentiated cells. The enzymes encoded by these genes catalyze the first step in the oxidative branch of the pentose phosphate pathway that involves the conversion of glucose 6-phosphate to 6-phosphogluconate with concomitant production of NADPH. Besides its role as a cofactor in many biosynthetic reactions, NADPH is essential to regenerate reduced glutathione from glutathione disulfide [246]. Hence *G6PD* and *H6PD* transcripts levels may reflect high requirement for NADPH, either as reducing agent for biosynthetic pathways or instead as a cofactor in the cell antioxidant defense. The latter hypothesis is supported by the fact that differentiated cells have a higher mitochondrial activity and therefore a higher potential for ROS production. Furthermore, we observed that human pluripotent cells have higher expression levels of genes related to the non-oxidative branch, such as *TKT*, and *RPIA.* These results suggest that human pluripotent cells preferentially use the non-oxidative branch of the pentose phosphate pathway in order to obtain ribose-5 phosphate that is important for nucleotide synthesis. A similar pattern has been previously described for cancer cells [247,248,249].

Interestingly, the TCA cycle signature revealed that most of these genes are downregulated in differentiated cells, when compared to pluripotent lines. Besides its role in oxidative catabolism of carbohydrates and fatty acids, the TCA cycle provides precursors for many biosynthetic pathways, including precursors for amino acid and nucleotide synthesis. It is possible that upregulation of TCA cycle-related genes in human pluripotent stem cells is related to the high proliferative rates and concomitant need for nucleotides rather than need for reducing agents for mitochondrial activity. This issue needs to be explored further. Regardless, higher levels of genes encoding TCA cycle proteins might be indicative of increased electron transport capacity and cellular respiration. Consistent with increased level of genes encoding proteins of the TCA cycle we observed that pluripotent lines have higher levels of mitochondrial electron transport complexes than differentiated cells. The transcription factor c-Myc is crucial for the maintenance of embryonic stem cell self-renewal and its ectopic expression allows the reprogramming of somatic cells to an embryonic stem cell like state [69,222]. In addition this transcription factor has been previously described to up regulate the expression of several glycolytic enzymes as well as to promote mitochondrial biogenesis [250,251,252,253]. Hence higher levels of complex II, III and V may be due to higher c-Myc levels in pluripotent cells and may not be representative of high mitochondrial activity. In accordance with this hypothesis our OCR results showed that pluripotent lines consume lower levels of O_2 than the differentiated line H7TF. However, IMR-90 fibroblasts displayed similar basal OCR levels than those found in pluripotent lines. These results could be related to the fetal origin of the IMR-90 fibroblasts, as the fetal lung is exposed to a rather hypoxic environment [254]. In agreement with this notion, when we induced mitochondrial respiration by the use of FCCP (reserve capacity) IMR-90 fibroblasts could increase OCR to similar levels to those found in H7TF. Importantly, human pluripotent stem cells did not display a strong response to FCCP treatment suggesting that aerobic respiration in these cells is somewhat impaired. Consistent with less active mitochondria, human pluripotent cells showed reduced ATP levels when compared with differentiated

cells. In addition these cells secreted higher lactate levels indicative of higher glycolytic rates. Thus despite higher levels of genes encoding proteins from the TCA cycle and higher content in mitochondrial electron transport chain complexes, human pluripotent cells seem to have lower overall OXPHOS activity. It remains to be established why this is the case, but our data suggests some possibilities.

Hk2 catalyzes the first reaction of glycolysis and it has been previously demonstrated that its expression is restricted to the inner cell mass of the blastocyst, and that Hk2 knock down results in mouse embryonic lethality around E.D. 7.5 [255,256]. Although we did not observe significant differences at the mRNA level, the total protein levels of Hk2 were significantly elevated in human pluripotent stem cells. These results suggest that Hk2 protein stabilization might be increased in human pluripotent lines. Higher levels of mitochondrial Hk2 can be advantageous for glycolytic metabolism in two ways: first binding of Hk2 the outer mitochondrial membrane allows this enzyme to escape inhibition by its product glucose-phosphate; and second it allows the enzyme to gain access to newly synthesized ATP required for the phosphorylation of glucose [166,257]. In addition Hk2 plays a key role in the prevention of cell death by binding to VDAC, therefore representing a link between glucose metabolism and apoptosis [258,259]. Hence it is possible that Hk2 plays a role in preventing human pluripotent stem cell apoptosis as well.

On the other hand, the PDH complex is a crucial step in regulation of metabolism since it constitutes the link between anaerobic metabolism and the TCA cycle. Phosphorylation of the PDH E1α subunit leads to inactivation of the PDH complex and consequently results in lower levels of acetyl CoA to enter the TCA cycle. Tellingly, pluripotent lines have higher levels of phosphorylated PDH E1α. Phosphorylation of PDH complex can be carried out by four PDHKs and in this study we analyzed PDHK1 expression levels. Although we did not observe an increase in PDHK1 gene expression in pluripotent lines when compared to differentiated cells we did observe an increase in PDHK1 protein levels in

pluripotent cells. These results suggest that PDHK1 protein stability differs between pluripotent and differentiated cells. Papandreou and colleagues have previously demonstrated that under hypoxic conditions hypoxia inducible factor (HIF-1) up regulation resulted in increased expression of PDHK1 leading to inactivation of the PDH complex. This in turn resulted in reduced substrate availability to enter the TCA cycle and led to decreased oxidative phosphorylation [260]. HIF-1α might therefore be considered a good target for future work, given that we observed that some of its targets are involved in the maintenance of this glycolytic profile.

Overall our results demonstrate that human pluripotent cells have a greater reliance on glycolysis than differentiated cells. In addition our study suggests that this can be mediated by increasing Hexokinase II levels and inactivation of the PDH complex. Interestingly these metabolic strategies involving features of anaerobic metabolism under normoxia are also found in many types of tumor cells [133,243], and parallel assays in both pluripotent and tumor lines would be extremely interesting Importantly we demonstrate that despite the fact that both hESCs and iPSCs rely on glycolysis, these cell types are not identical in terms of glucose-related gene expression, mitochondrial morphology, and O_2 consumption. This suggests that iPSC somatic cell reprogramming to iPSC may result in differences at the metabolic level, when compared to the pluripotent standard of hESC. While epigenetic and transcriptomic differences have been mentioned above [227,228] other significant genetic changes in iPSCs when compared to hESCs and differentiated cells were also recently described [229,230], including higher mutation rates and copy number variation. Interestingly, recent data suggests that iPSC mitochondria retain significant developmental plasticity upon IPSC generation, and somatic cell re-differentiation. [261].

In addition we also observe that not all the differentiated lines display the same metabolic profile and this might have an impact in the reprogramming efficiency of various somatic cell types, and

on the characteristics of differentiated cells obtained from different iPSC lines. Indeed recent reports have confirmed this hypothesis and also that during reprogramming a shift in metabolism, to glycolysis, occurs before the intrinsic pluripotency network is activated [80,187]. Overall, our results stress the importance of the complete characterization of these cell lines, and suggest that there may be other links to tumor cells besides those already described.

Effect of 3-Bromopyruvate on mESC pluripotency

Chapter 4

Abstract

Our previous results have highlighted Hexokinase II as an important enzyme for the glycolytic profile of ESC. This key enzyme, which phosphorylates glucose (G-6-P) trapping it inside the cells, has four different isoforms in mammalian tissues (Hk1-4) with different affinities for glucose and different localizations inside the cell. The scope of this chapter focuses on the clarification of the possible importance of Hk2 in pluripotency. To accomplish our goal mESCs were treated with 3-brompyruvate (3BRP), a chemical compound analog to pyruvate and a potent inhibitor of Hk2. Also, as a positive control for differentiation, we grew cells without LIF, which is essential for pluripotency. Overall our results demonstrate that inhibition of Hk2 has deleterious effects on pluripotency. There seems to be a tendency for alterations in metabolism given that cells become less glycolytic with some alterations in mitochondrial function. A negative effect on key players in maintaining the glycolytic profile, such as Hif-1α, p53 and c-Myc was also observed. Interestingly, our positive control for differentiation allowed the distinction between 3BRP effects and alterations associated with differentiation. Our results improved the current knowledge about which possible metabolic players could be involved in differentiation and more importantly it was demonstrated that a normal function of Hk2 is important for pluripotency.

4.1 Introduction:

The previous results (presented in chapter 3) have shown that besides the glycolytic phenotype and silent mitochondria, human pluripotent stem cells (hPSCs) present some putative strategies common to some types of tumor cells in order to maintain high glycolytic rates. These include high levels of Hexokinase II (Hk2) linked to the outer mitochondrial membrane and a PDH cycle promoting the conversion of pyruvate into lactate rather then Acetyl-CoA.

Hexokinase is the key enzyme that phosphorylates glucose (G-6-P) trapping it inside the cells. This G-6-P either will enter glycolysis or it will enter the phosphate penthose pathway. There are four different hexokinases in mammalian tissues (Hk1-4) with different affinities for glucose, and with different localizations inside the cell. Its role in metabolism of cancer cells was already addressed in chapter 1 and as a proof of principal there are some reports in which depletion of Hk2 in tumor cells increased sensitivity to cell death. Also, the work of Wolf et al. [262] showed that stable depletion of Hk2 inhibited aerobic glycolysis and led to an increase in normal oxidative glucose metabolism.

3-brompyruvate (3BRP) is a chemical analog of pyruvate that presents some chemical properties that allows for a selective and potent inhibition of HKII leading to an impact on the metabolic activity of this enzyme. Lately this compound has been used as an anti-cancer drug in some clinical trials and in innumerous research projects. Papers by Ko et al and Cho et al [131,263] demonstrated that 3BRP induces cell death in a tumor, consequently reducing its size. The exact mechanism by which this compound is acting as an anti-tumural drug is not completely described, however it has been shown that a shift in metabolism occurs after 3BRP treatment, and that mitochondrial function is altered in terms of ROS production and mitochondrial membrane potential, leading to cell death.

If we take into account that ESCs are also highly proliferative and that they share some common features with tumor cells we wondered if Hexokinase II could have a role in maintaining the glycolytic metabolism in these cells, and if this activity was associated with pluripotency. Furthermore, when we consider metabolism networks other players should be taken into consideration, such as Hypoxia inducible factor-1a (Hif-1α), c-Myc and p53 [160]. It has already been described that tumor aggressiveness and tumor progression is correlated with a hypoxic microenvironment due to the high activity of Hif-1α [264]. Also, this hypoxic status alters the metabolism of cancer cells turning them more glycolytic with a reduced mitochondrial activity, which occurs due to the fact that Hif-1α will induce the transcription of genes coding for glycolic enzymes and other important signaling pathways such as Notch and BMP pathways [157,160,171]. Tumors therefore become highly de-differentiated and fast growing, supporting the idea that Hif-1α is related to maintenance of an undifferentiated cell state and to inhibition of cell differentiation [171]. Another important player is the oncogene c-Myc, commonly found in high levels in transformed cells [195] and known for having an important role in integrating cellular metabolism with proliferation rates [265]. Alterations in the c-Myc levels contribute to promoting the Warburg effect usually observed in cancer cells, where glucose is metabolized via glycolysis although there is enough oxygen to support oxidative phosphorylation.

All of these molecular characteristics ultimately will influence each other, due to fact that many of the downstream targets are common, and the same is true for p53 and its role as a decisive player in the life or death decisions within cells. However p53 has other possible exciting roles in a cell, specifically by responding to metabolic changes through the activation of AMP-activated protein Kinase or its role in ROS production by activating genes responsible for lowering oxidative stress [177,266,267]. The goal of our work was to determine if Hk2 has a role in mESCs metabolism and pluripotency, and if so, to identify which players from known metabolic pathways are involved.

4.2 Results:

4.2.1 Effect of 3BRP on total number of cells, morphology and viability:

As a first approach, and given that 3BRP is known for inducing cell death in glycolytic cells [268], we started by analyzing possible drug effects in terms of total cell number, morphology and viability on E14 mESC. We observed that cells incubated with this compound had an inferior total number of cells when compared to our control. However, cell number was more affected in our negative control (cells grown without LIF) meaning that, although 3BRP was affecting the total number of cells in our culture the absence of the pluripotency inducer LIF ($P<0.05$) has a more deleterious effect (figure 4.1A). In terms of morphology, alterations in our experimental conditions were observed: while in the control, bright tightly packed round colonies growing as a dome could be seen, cells growing without LIF no not longer contain perfect colonies. Instead, we have higher levels of differentiation translated into cells with more cytoplasm and that can be perfectly distinguished within a colony. On the other hand, in cells grown in the presence of 3BRP, while showing more differentiation in comparison with the control, we can still observe well-defined round colonies. Interestingly these colonies are smaller when compared to control colonies (Figure 4.1B). Given that we were observing an effect in terms of total cell number we accessed the viability of the cells in culture. Results with the LIVE/DEAD® Kit (Invitrogen) clearly showed that although there are fewer cells for some experimental conditions, there are no differences in the percentages of live cells (Figure 4.1C). Fluorescent images obtained after counting (Figure 4.1D) clearly show that the vast majority of cells present green fluorescence.

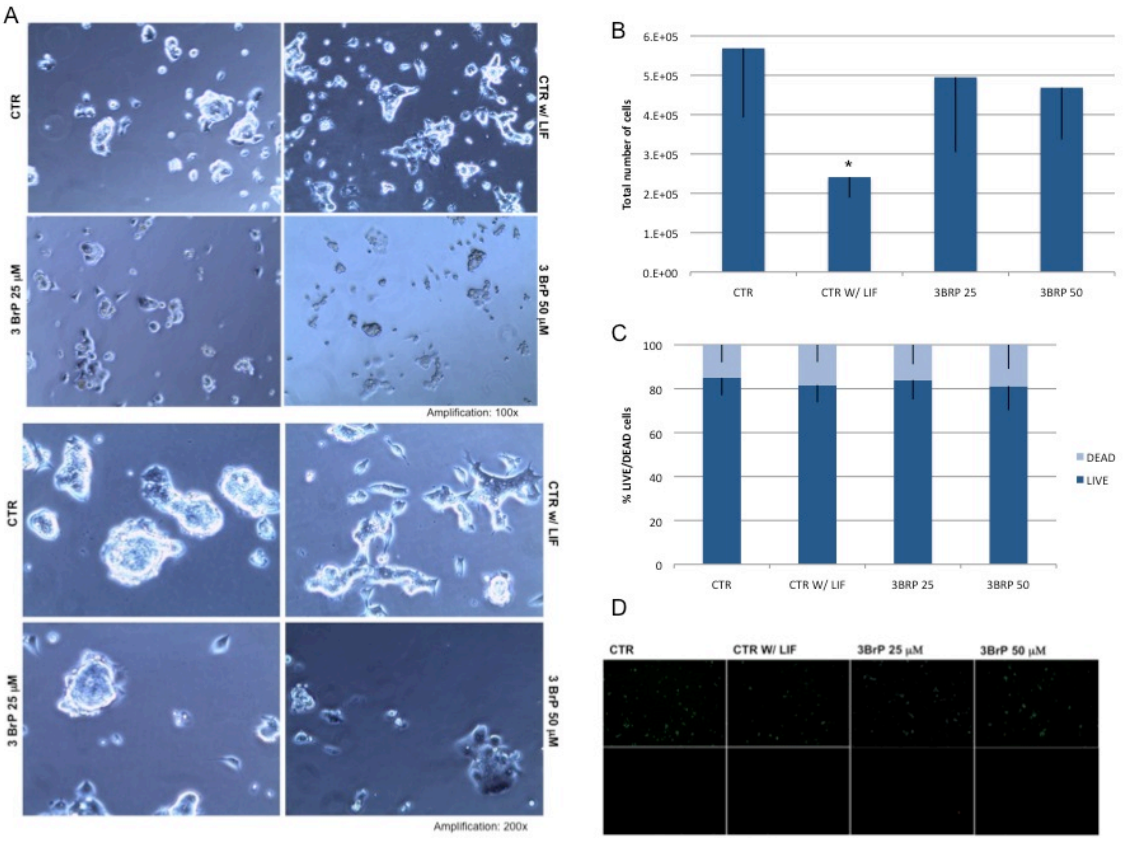

Figure 4.1. Effect of 3BRP on total number of cells, morphology and viability. A) Phase microscopy photographs of the colonies in all conditions. The upper panel represents an amplification of 100x and the lower of 200x. **B)** Total number of cells counted upon collection for experiments. N=20 **C)** Percentage of viable cells *versus* dead ones. Cells stained green were counted as live while IP positive cells were counted as dead. 100 cells were counted per condition N=8 **D)** Fluorescence images of the cells in order to confirm that the vast majority is indeed alive and there are no major differences between groups.

4.2.2 Effects of 3BRP on pluripotency:

We began pluripotency analysis using an Alkaline Phosphatse (AP) assay, which exploits the fact that pluripotent cells present high levels of AP, resulting in colonies stained red, that are AP positive. This

characteristic has been proven to positively correlate with a pluripotent state [22,269]. We used a kit provided by Millipore and colonies that presented the red color typical of the AP staining were counted as positively marked, while colonies with no red staining were counted as non-AP positive. All colonies in the 24 wells were counted and normalized to 100%, and experiments were performed in duplicates for all experimental conditions.

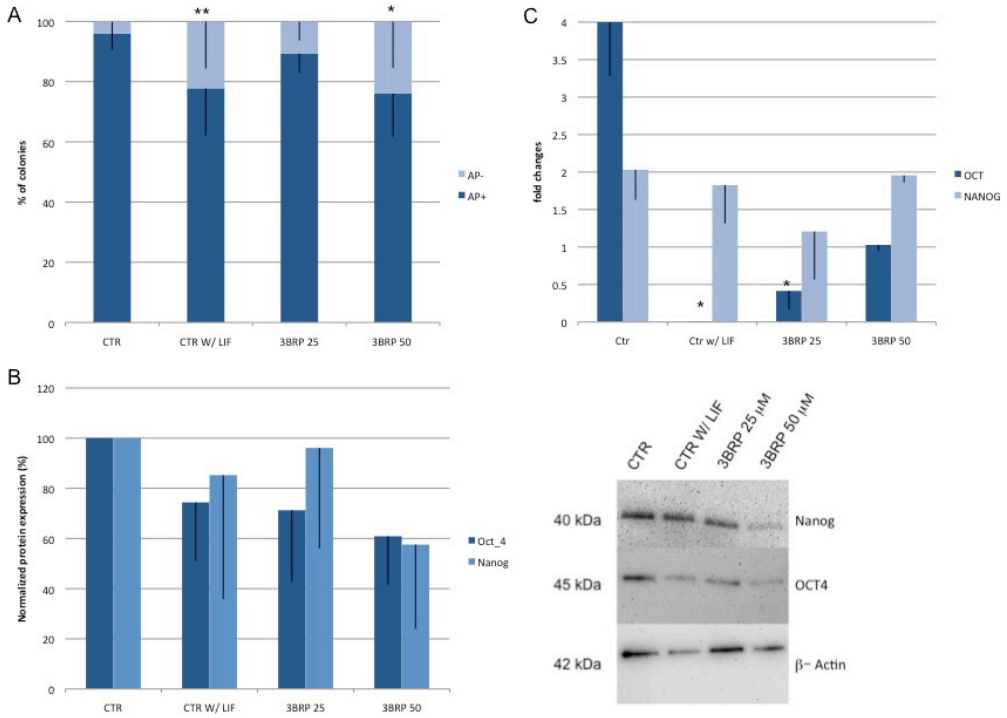

Figure 4.2. Effects of 3BRP on pluripotency. A)- Alkaline phosphatase assay. Colonies stained red were counted as positive (AP+) pluripotent colonies whereas colonies with no staining were counted as negative for pluripotency (AP-). N=10 **B).** Western Blot quantification for Oct4, and Nanog, results are presented as percentage relative to the CTR and were normalized for β-actin. N=3 **C)**- RT-PCR analysis for the Oct4 and Nanog, results are represented as fold changes. N=3, results are expressed as means with Standard deviation of means.

Our results demonstrate that, as expected, cells in the control condition have a high percentage of AP+ colonies (over 90%) while cells growing without LIF have a lower percentage of AP+ colonies

(P<0.01). Interestingly, we observe a similar decrease when we interpret results obtained with the higher concentration of 3BRP (P<0.05) while the effect of 25μM 3BRP was not statistically significant (Figure 4.2A). Our AP results points to a possible negative effect of 3BRP on pluripotency.

We then analyzed protein levels for the major regulators of the pluripotency network: Oct4 and Nanog. Both western Blot (Figure 4.2B) and RT-PCR (Figure 4.2C) analysis demonstrate a tendency for a negative effect of 3BRP on pluripotency, given that both protein and mRNA levels seem diminished in cells grown in the presence of this compound. Once more the most deleterious effect was observed in our negative control (CTR W/ LIF). Interestingly, the negative effect is more accentuated in terms of mRNA levels for Oct4, specially for the CTR W/ LIF and 3BRP 25μM that are statistically different (P<0.005), when compared with protein levels meaning that if we continued to culture our cells under these conditions higher levels of differentiation would probably be detected.

4.2.3 mESCs proliferation under the influence of 3BRP:

Next we analyzed proliferation rates in our experimental conditions. It has been described that 3BRP has an effect in tumor cell proliferation, mainly due to the induction of apoptosis, but an effect in the cell cycle cannot be ruled out. Given that we observed an effect in total cell number and that the cells are viable, we explored the possibility that 3BRP could be disrupting mESCs proliferation rate. To quantify cell proliferation we evaluated levels of PCNA by flow cytometry, normalizing data to the control. Results for 50μM 3BRP showed a significant decrease in cell proliferation is seen (p<0.05), which could explain the decrease in cell number, and the fact that colonies are smaller under these conditions (Figure 4.3).

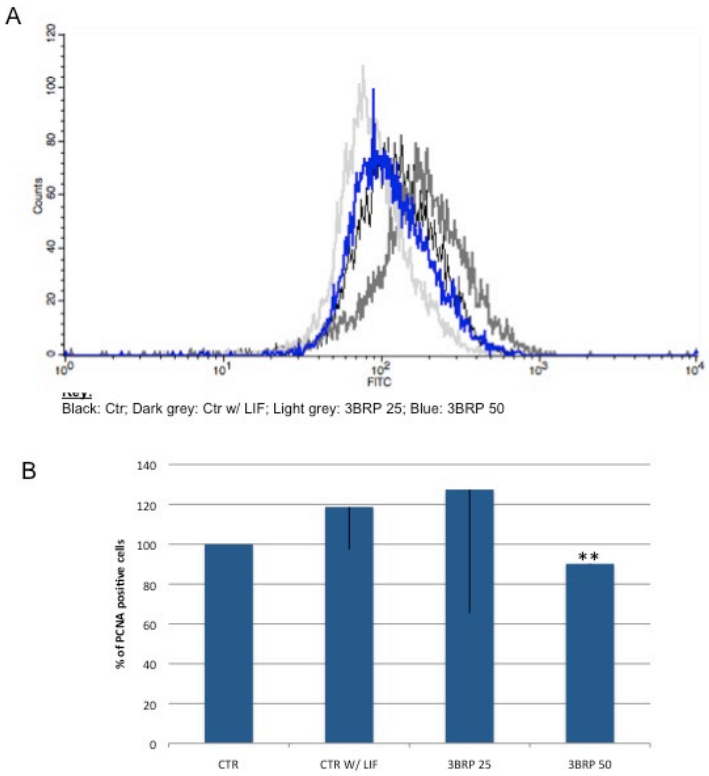

Figure 4.3. mESCs proliferation under the influence of 3BRP. A)- Schematic representation of the shift during the flow cytometry analysis of each population. **B)-** Quantification of the proliferation rates accessed by PCNA levels in the cells. Results are presented as percentage relative to the control and represent the average of 20000 cells for each condition. N=3, results are expressed as means with Standard deviation of means.

4.2.4 Mitochondrial function and Energetic status of mESCs:

Given the importance of mitochondrial function in cell differentiation as discussed in the previous chapter and at chapter 1, we first accessed mitochondrial membrane potential with the TMRM dye since it has been described that 3BRP leads to mitochondrial depolarization [182] and that differentiated cells would have a higher mitochondrial membrane potential (MMP). Interestingly, our

results demonstrate a trend to an increase in MMP, although with no statistical difference, except for 50μM 3BRP (P<0.05), the experimental condition presenting the highest values for MMP (Figure 4.4C).

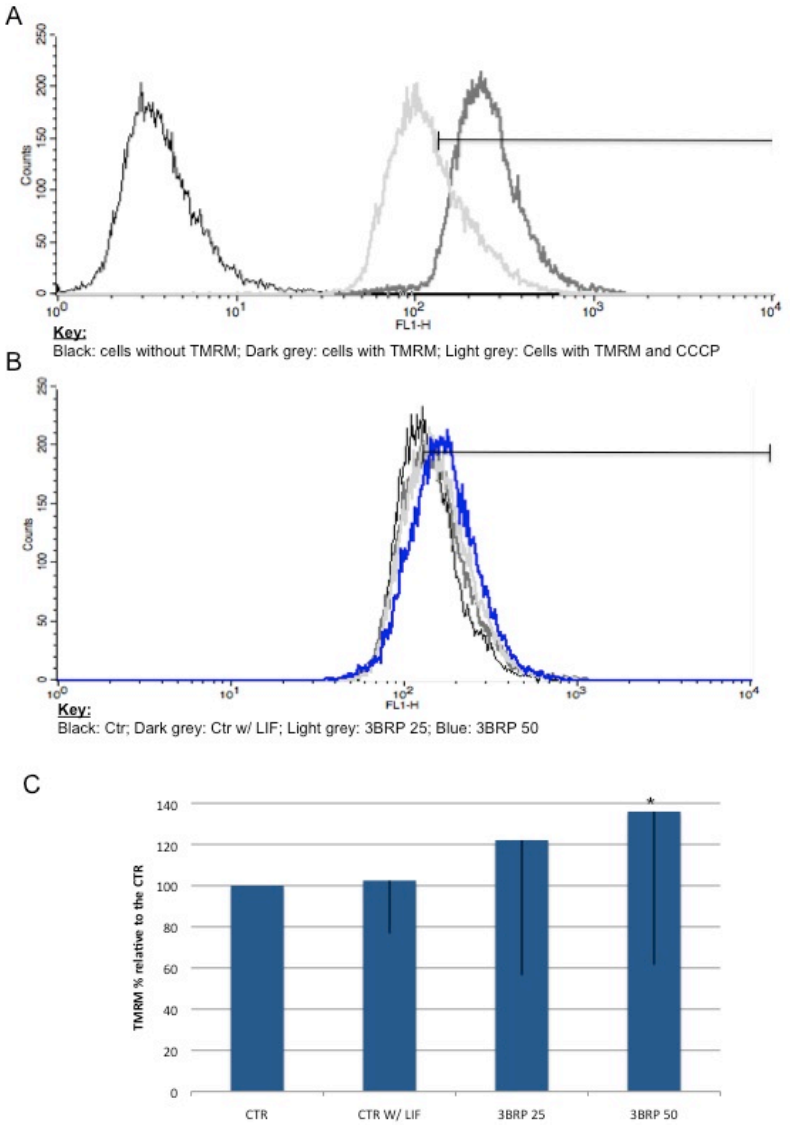

Figure 4.4. Assessment of the mitochondrial membrane potential by flow cytometry with the TMRM dye. A)- Schematic representation of the populations used for defining population gates. Cells without TMRM as negative CTR, CTR cells with dye and CTR cells with CCCP, an uncoupler, to determine the lowest MMP potential possible in these cells. **B)-** Schematic representation of the experimental conditions populations obtained by flow cytometry. **C)-** Quantification of the MMP potential using TMRM dye, results are expressed as percentage relative to the CTR, 20000 cells were evaluated for each population. N=4, results are expressed as means with Standard deviation of means.

We then analyzed mitochondrial ROS production as another indicator of mitochondrial activity. The trend was once again that the experimental conditions presented higher levels of superoxide anion production when compared to the control cell, although there were no statistically significant differences (Figure 4.5C).

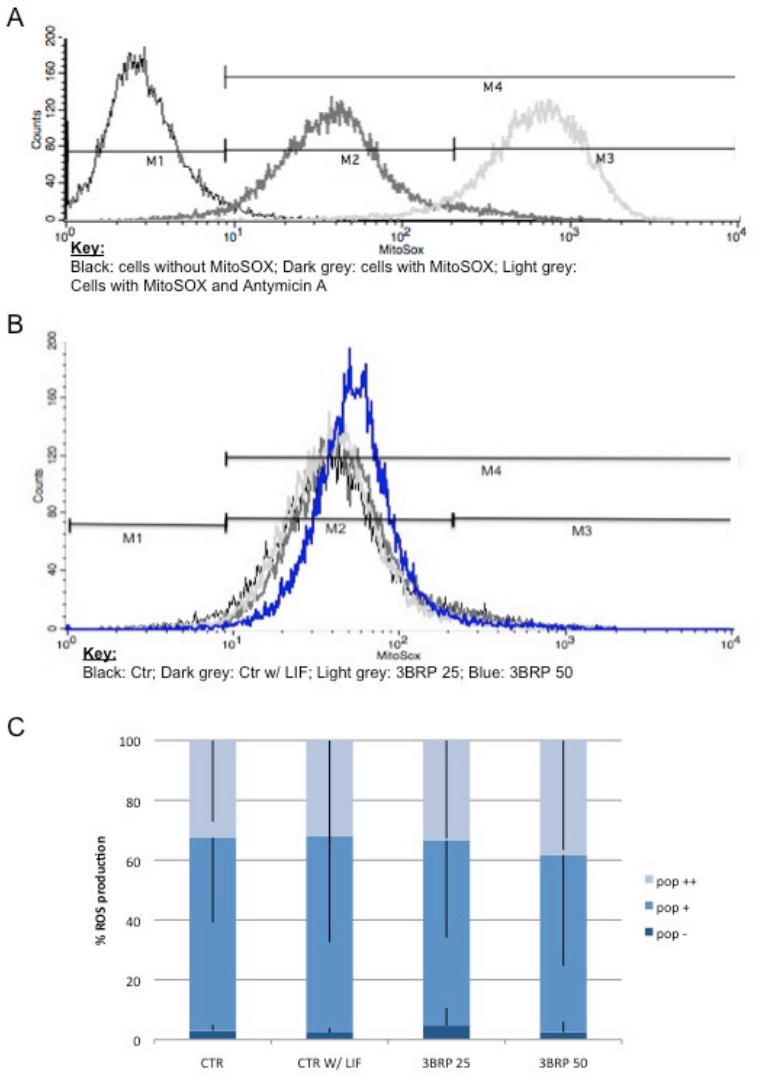

Figure 4.5. Flow cytometry analysis ROS production quantified by MitoSOX Red dye. A)- Schematic representation of the populations used for defining population gates. Cells without MitoSOX as negative CTR, CTR cells with dye and CTR cells with Antimycin A, an inductor of ROS production, as a positive CTR, to determine the highest levels of ROS production in these cells. **B)-** Schematic representation of the experimental conditions populations obtained by flow cytometry. **C)-** Quantification of ROS production, results

are expressed as percentage relative to the CTR, 20000 cells were evaluated for each population. N=4, results are expressed as means with Standard deviation of means.

For each experiment, we used a negative (cells without MitoSOX) and a positive control (cells with MitoSOX and Antimycin A an inhibitor for the mitochondrial complex III that causes an increase in ROS production) in order to properly set the analysis gates. We obtained three different populations: a negative one (M1/pop-) consisting of cells that are producing low quantities of ROS, a positive population of cells producing normal quantities of ROS (M2/pop+) and a third population (M3/pop ++) that represents cells that are producing higher amounts of ROS. Interestingly, cells grown with the higher concentration of 3BRP presented a decrease in the pop- gate and an increase in the pop ++ gate. Cells grown with 25 μM 3BRP had a higher percentage of cells in the pop- population. Although our results only demonstrates a tendency, they are in accordance with the literature describing that 3BRP exposure leads tumor cells to increase ROS production [270].

To address the energy status of mESCs following 3BRP treatment, adenine nucleotides were quantified (Figure 4.6A). In accordance with previous data, a tendency for a decrease in ATP levels in cells treated with 50μM 3BRP is observed. However, this was not significant. No differences were observed for ADP concentration while for AMP the same was not true, given that cells without LIF and treated with 50μM 3BRP presented an increase in AMP when compared to the control cells ($P<0.05$). Energy charge results (Figure 4.6B) show that our experimental conditions are inducing a lower energy charge in our cells when compared to the control, with the more significant decreases observed for cells without LIF and exposed to 50μM 3BRP ($P<0.01$ and $P<0.05$, respectively). While for the ATP/ADP ratio (Figure 4.6C), there were no changes, when we take into consideration the AMP/ATP ratio (Figure 4.6D) there is a significant increase for cells without LIF and exposed to 50μM 3BRP ($P<0.01$ and $P<0.05$, respectively), when compared to the control.

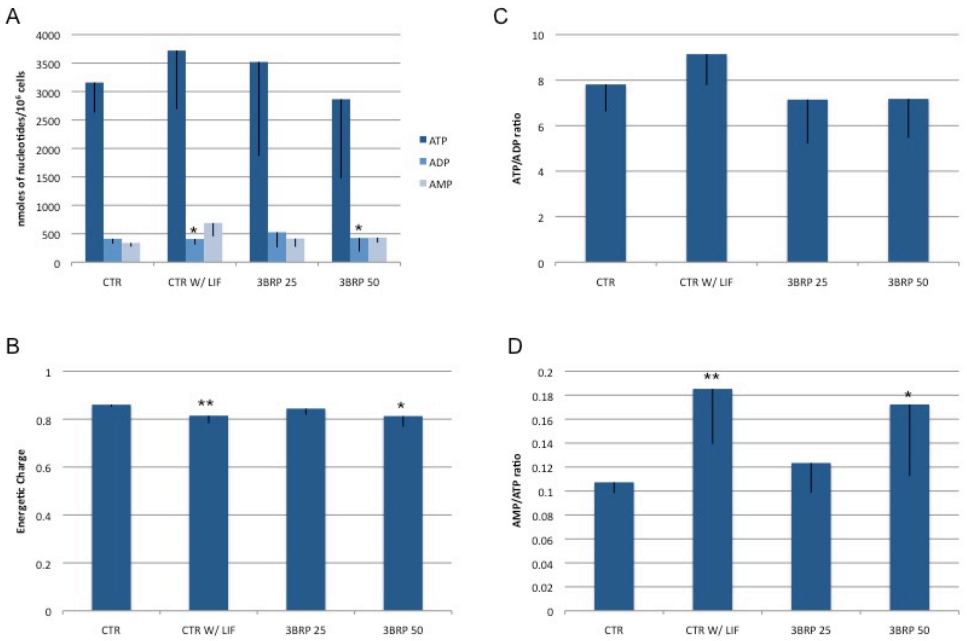

Figure 4.6. Effect of 3BRP on the energy status of mESC. A)- Nucleotide levels determined by HPLC analysis, N=10. **B)-** Determination of the energetic charge if the cells, N=10. **C)-** ATP/ADP ratio, N=10. **D)-** AMP/ADP ratio, N=10. Results are expressed as means with Standard deviation of mean.

4.2.5 3BRP effects on the metabolic status of mESCs:

The MTT assay was used to indirectly infer the metabolic activity of the cells, given that the assay measures cellular NADPH and NADH dehydrogenase activity. As we can see in figure 4.7A, our results demonstrate that 3BRP negatively affects mESC ($P<0.05$) and, again, that differentiated cells are more active when compared to our control condition ($P<0.01$). We did not observe any statistically

significant difference between the experimental conditions concerning pyruvate (Figure 4.7B) and lactate (Figure 4.7C) secretion.

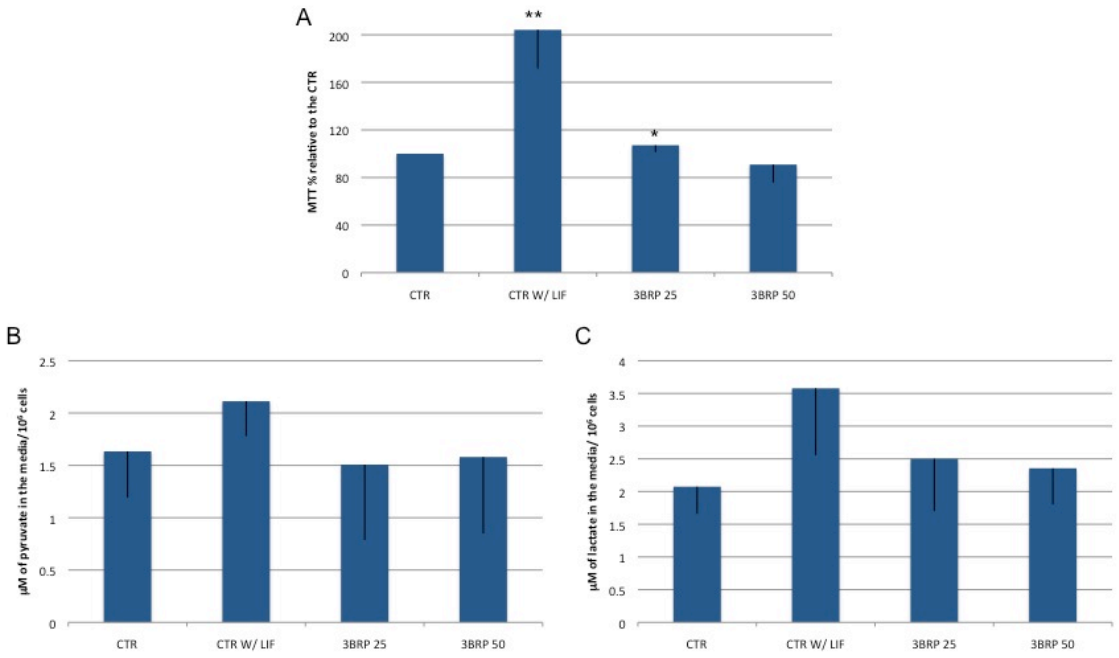

Figure 4.7. 3BRP effects on the metabolic status of E14 mESC. A)- Results for the MTT assay are presented as percentage of formazan crystals normalized to the control. N=10 **B)-** Lactate levels determined by the Lactate Kit from bioVision. N=5 **C).** Determination of Pyruvate levels determined by a kit from Bioassays, N=5. Results are expressed as means with Standard deviation of means.

4.2.6 Effect of 3BRP on Hexokinase I and Hexokinase II:

Given that 3BRP is known for its inhibition on Hexokinase II we next examined protein and mRNA levels for Hexokinase I and Hexokinase II. Western Blot analysis revealed that interestingly although we are inhibiting Hexokinase II and to some extent Hexokinase I we do not observe a compensatory mechanism.

When we look to protein levels for Hexokinase II we observe that comparative to control we have a significant decrease for the control without LIF and 50μM 3BRP ($P<0.05$) (Figure 4.8A). In contrast, for 25μM 3BRP we observe a tendency for an increase, which could reflect an adaptation effect of the cells in the presence of 3BRP at this concentration given that for the higher concentration we do not observe this effect. There is a significant decrease in mRNA levels when compared to the control cells for CTR W/ LIF and for 3BRP 25μM ($P<0.05$) (Figure 4.8B). Regarding Hexokinase I at the protein level the observed differences were statistically significant for CTR W/LIF ($P<0.01$) and 3BRP 25μM ($P<0.05$).

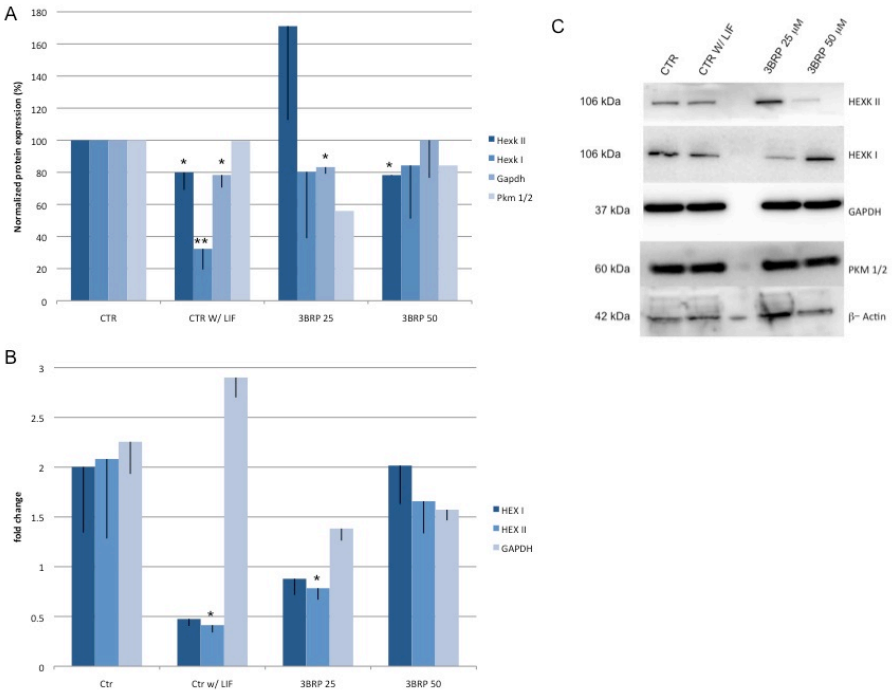

Figure 4.8. 3BRP effect on glycolytic enzymes. A)- Protein levels for Hexokinases II and I, Gapdh and PKM1/2 were determined by western Blot. Results were normalized to β-Actin protein levels and they are represented as percentage relative to the control, N=4 **B)-** RT-PCR analysis for Hexokinases I and II and Gapdh. Results are presented as fold changes and normalized to the reference house keeping gene β-Actin, N=3. Results are expressed as means with Standard deviation of means.

Because hexokinases are involved in the first step in glycolysis it was important to understand if glycolysis was being affected downstream of our target. We focused on both Gapdh and PKM1/2, the first because besides its role in glycolysis it can also function as a metabolic switch, and PKM because it catalyzes the last step of glycolysis, controlling the production of pyruvate. Regarding Gapdh, it is interesting to observe that for differentiating cells, the significant decrease in protein content for 25μM 3BRP and cells grown without LIF ($P<0.05$), although we observed a tendency for an upregulation in mRNA levels for the last, which is contrary to the observed trend of 3BRP. To note for protein levels the decrease observed in 25μM 3BRP is statistically significant.

4.2.7 Possible signaling pathways involved in 3BRP-mediated effects on mESCs:

Given that 3BRP is affecting metabolism and that we are inhibiting Hexokinase II, we analyzed proteins involved in metabolic signaling pathways, trying to shed some light into possible mechanisms that can be involved in 3BRP-induced alterations. Specifically, we analyzed the protein levels for Pdh, Hif-1α, c-Myc and p53 (Figure 4.9A). The first target was thought to be important given that the PDH complex determines if the cell will have a higher production of lactate or more acetyl-CoA for the TCA cycle, favoring a more oxidative metabolism instead of a more glycolytic one, the other targets were analyzed given their emergent role in re-modulation of cellular metabolism [164], and they also have key roles in metabolic shifting in cancer, as mentioned in the general introduction.

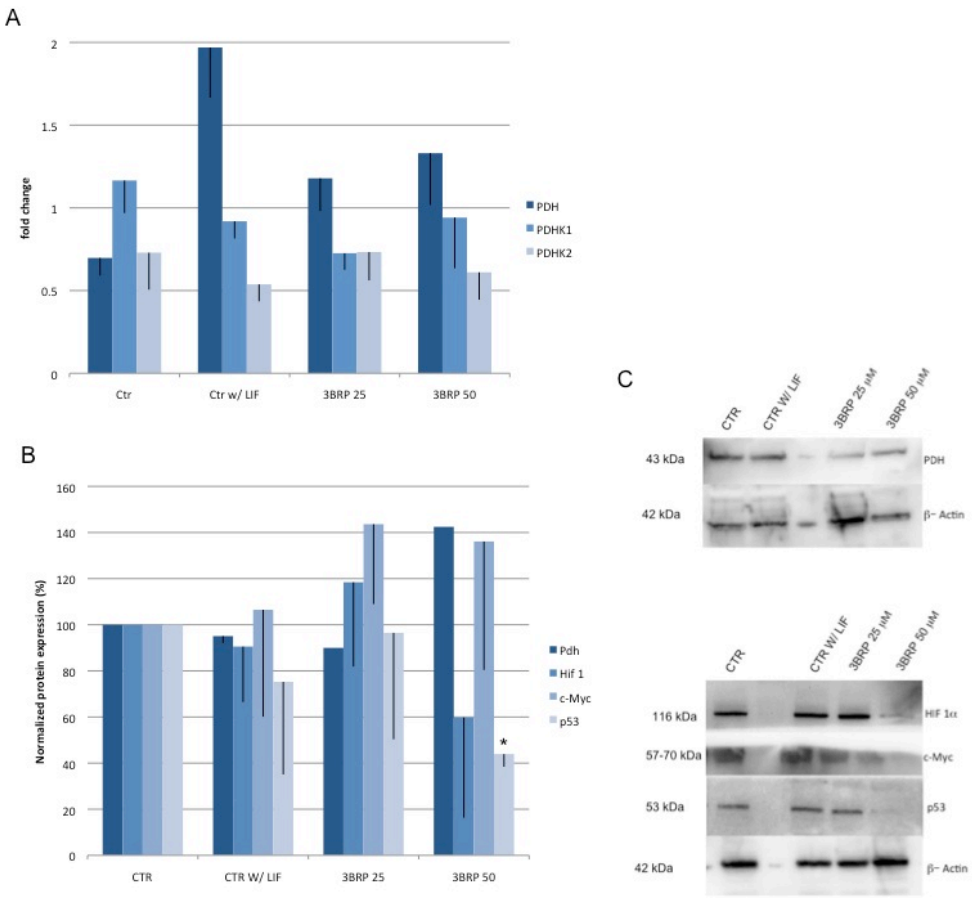

Figure 4.9. Possible signaling pathways involved in 3BRP-mediated effects on mESC. A)- RT-PCR analysis for PDH, PDHK1 and PDHK2 genes. Results are presented as fold changes and normalized to the reference house keeping gene β-Actin, N=2. **B)-** Protein levels for Pdh, Hif-1α, c-Myc and p53 were determined by western Blot. Results were normalized to β-Actin protein levels and they are represented as percentage relative to the control, N=3. Results are expressed as means with Standard deviation of means. **C)-** Western-Blot membranes after revelation with ECL.

No changes were seen at the RNA level (figure 4.9A). When protein expression levels are considered there is a tendency for a decrease in Pdh protein levels in cells grown in the absence of LIF as well as in the presence of 25µM 3BRP, for the highest concentration of 3BRP the effect seems to be the opposite. Interestingly for Hif-1α, although there are no significant differences, it seems to decrease in cells grown without LIF and in cells exposed to 50µM 3BRP but not for the 25µM 3BRP. A reduction in

p53 was observed for all experimental conditions, but only for 50μM BRP this effect was statistically significant ($P<0.05$). On the contrary we observe a trend in c-Myc levels to increase for all the experimental conditions with 3BRP possibly having a different additive effect on the differentiation stimulus, given that the increase in c-Myc in the presence of 3BRP is more prominent when compared to cells grown with LIF (figure 4.9B).

4.3 Discussion:

Due to the metabolic characteristics already noted in cancer cells, new therapeutic approaches have been arising focusing on inhibiting glycolysis in order to fight cancer. In that regard 3BRP has become a promising compound in this field because it inhibits glycolytic enzymes such as Hk2, and some good results, regarding decrease in tumor size and cell death, haven been obtained with this approach [182].

Taking into consideration the parallelism between ESC and cancer cells and our previous results (chapter3), we thus hypothesized that Hk2 could have a key role in maintaining pluripotency in ESC. In order to address this issue we treated cells with 3BRP and monitored changes in mESC pluripotency. To our knowledge this is the first paper describing such an experimental approach.

Titrations were performed in order to determine the lowest concentration of 3BRP needed to affect ESC, and we chose as a positive control cells grown without LIF (i.e. differentiating cells, cells losing their pluripotency). The concentrations chosen are within the range used in research for cancer research (0-80 μM) [182]. Our first approach was to analyze 3BRP effects on colony morphology, cell number and viability given that it this compound may cause mitochondria-mediated cell death [270]. Our results clearly demonstrate that 3BRP has a negative impact, although not as negative as growing ESCs without LIF in a media that is designed to promote pluripotency. Overall, in the presence of 3BRP colonies are smaller and borders start to lose definition. These observations are paralleled by differences in total cell number, with no detrimental effects on viability, suggesting that 3BRP affects the proliferation rate at the highest concentration used. The effects of 3BRP on cell viability are well described, as this compound will cause both apoptosis and necrosis by depleting ATP due to a profound alteration in mitochondrial function [271,272]. The reason why we did not observe such an effect is probably because the cells that do attach are viable and the concentrations used are not as aggressive

as those employed with cancer cells, given that our purpose was not to induce cell death but rather to clarify if inhibition of glycolysis has a role in pluripotency.

It is noteworthy that for differentiating cells the low total cell number is probably due to the fact that cells undergoing loss of pluripotency do not adapt to the culture medium. The 25 µM 3BRP concentration probably represents an adaptive state of the cells to both 3BRP as well as to the medium.

Regarding the pluripotent state of ESCs in our experimental conditions we saw that inhibition of Hexokinase II leads to a loss of pluripotency as analyzed by the mRNA levels for OCT4 as well as reducing AP+ positive colonies. It should be noted that the results for cells grown without LIF are similar to the ones obtained with cells exposed to 50µM of 3BRP, showing that the highest 3BRP concentration is more detrimental for pluripotency.

The main common characteristic that a pluripotent stem cell shares with certain cancer cells is that they both proliferate extensively, although they do it with different objective, given that a stem cell proliferates with the ultimate purpose of differentiation into a specific cell type. At any rate, both cell types need a certain metabolic prolife capable of providing the bioenergetic and synthetic blocks for cell growth and proliferation.

As discussed previously, 3BRP affects mitochondrial function in cancer cells, so we investigated mitochondrial-related changes in ESCs in the presence of this compound. Overall we conclude that mitochondria become more active, reflected by the significant increase in MMP and with a trend towards increase in ROS production. For the higher concentration of 3BRP this alteration was such that energy charge decreased, which could mean that mitochondrial function is becoming impaired. This outcome is characteristic of 3BRP given that for cells grown without LIF results were slightly different, and cells growing under these conditions had higher concentrations of ATP, and although the energy charge is negatively affected with differentiation it seems cells have enough ATP for proliferation, as

demonstrated by the ATP/ADP ratio. To note however, that the AMP/ATP ratio points significantly to an increase in AMP pool which impairs cellular processes that are high energy demanding.

We next wondered if our results were linear, For example: if Hexokinase II was being inhibited by 3BRP then pyruvate levels should decrease. However, there were no significant changes, as was the case with lactate. MTT results also suggest a slower metabolic state of cells exposed to 3BRP. Also given that MTT measures desidrogenase activity we can infer our cells will have a lower capability to balance oxidative stress.

We also quantified protein and mRNA levels for Hexokinase I and II, as well as other glycolytic enzymes further down the pathway. Although results were not linear they suggest a decrease in Hexokinase protein and mRNA levels upon differentiation, and that 3BRP induces alteration in protein levels for PKM1/2 and GAPDH. For the last case they are significant. Also the differences observed between the two concentrations of 3BRP could reflect a fine-tuning in cellular function. However, more experiments are needed, before definitive conclusions can be drawn.

Overall our results suggest that glycolysis is indeed very important for pluripotency, and that by inhibiting Hexokinase II we are promoting a shift in metabolism. Following this rationale we thought to determine the protein levels for Hif-1α, p53, c-MYC, PDH and PDHK1 and 2. These targets were chosen given the well-known crosstalk between them, and also due to the fact that they control the expression of some glycolytic enzymes. The end product of glycolysis is pyruvate and this substrate either will be converted to lactate or to acetyl-CoA. This reaction will ultimately depend on PDH complex activity. Namely, if PDH is phosphorylated than it is inactive, and pyruvate will be converted to lactate; conversely, if PDH is in its active form (non-phosphorylated) then acetyl-CoA will be produced to enter the TCA cycle. A family of PDH kinases (PDHK1-4) controls this inactive/active state of PDH and their activity that will control the final outcome of pyruvate produced during glycolysis. So if blocking

Hexokinase II was causing a shift in metabolism than it should be expected that PDH levels, as well as PDHK levels, would change.

Although, again further experiments are needed there a few tendencies regarding p53 protein at the highest concentration of 3BRP, suggesting that some of the mechanisms postulated for other cells are indeed active in ESC.

Overall we can conclude that inhibition of glycolysis has a detrimental effect in pluripotency and that 3BRP seems to be causing impairment on mitochondrial function that could be affecting cellular function. It is also interesting to observe that a lower concentration of 3BRP seems to be less harmful because although it affects pluripotency the shift in metabolism is not as clear, which could reflect an intermediary adaptation step to culture conditions. More importantly we believe that in order to have effects on ESCs differentiation alterations in the PDH cycle and HIF-1α should occur. This will be discussed more extensively in the following chapter.

The role of Pyruvate Dehydrogenase in pluripotency: Can we affect pluripotency metabolically?

Chapter 5

Abstract

Under normoxic conditions glycolysis is defined as the conversion of glucose to pyruvate that can be further metabolized in the mitochondria via the activity of pyruvate dehydrogenase (PDH), which converts pyruvate to acetyl-CoA. The PDH complex is localized in the mitochondrial matrix, and catalyzes the irreversible decarboxylation of pyruvate to acetyl-CoA and NADH. PDH E1-α subunit, functions as an on/off switch regulated by phosphorylation/dephosphorylation. One of the four-pyruvate dehydrogenase kinase isoforms (PDHK1-4) will phosphorylate this subunit causing inactivation of PDH. Our previous results with hESC, suggest that PDHK may be a key regulator in the metabolic profile of pluripotent cells given that PDHK is upregulated in pluripotent stem cells. Given that an inactive PDH would be beneficial for ESC, we wondered if metabolic modulation, by inhibition of PDHK, could impact metabolism and pluripotency, raising the hypothesis that PDH complex could be a good target to modulate both aspects. PDHK activity is inhibited by its substrate pyruvate, but also by the therapeutic compound dichloroacetate (DCA). In order to assess the importance of the PDH cycle in pluripotency on mESC, we incubated cells with DCA and observed that in its presence ESC start to differentiate. Alterations in mitochondrial function and proliferation potential were also determined. The PDH cycle was also assess by monitoring protein levels for PDH (both phosphorylated and non-phosphorylated) and PDHK1. Interestingly, we were also able to describe a possible pathway that involves Hif-1alpha, c-Myc and p53 during the loss of pluripotency. It is important to mention that the obtained results with DCA were comparable to ones obtained for cells grown without LIF (our positive control for differentiation). This way, we proved that PDHK functions as a possible gatekeeper for metabolism in ESC and would be a good target to modulate metabolism and differentiation. Also our research points to the fact that indeed an inactive PDH favors pluripotency and that ESC have similar strategies as cancer cells to maintain the glycolytic profile by making use of some of the signaling pathways found in the latter cells.

5.1 Introduction:

The results described in chapter 3 suggest that PDHK may be a key regulator in the metabolic profile of pluripotent cells. PDHK is upregulated in pluripotent stem cells and phosphorylates the key metabolic enzyme PDH, inactivating it. As a result pyruvate obtained from glycolysis cannot be transformed into acetyl-CoA, and is instead converted to lactate. This reduces mitochondrial activity due to lack of electron donors (NADH, $FADH_2$) formed in large amounts during the TCA/Krebs cycle from acetyl-CoA and maintains the glycolytic profile of proliferating cells. Intriguingly, PDHK has already been suggested as a specific target in cancer cells, with inhibitors of the enzyme (such as Dichloroacetate - DCA) being considered for therapeutic purposes [179,180]. Therefore, the metabolic switch that controls coupling of glycolysis to OXPHOS could constitute a common link between cancer proliferation and stem cell pluripotency, as noted earlier.

Indeed, DCA is known for inhibiting all PDHK isoforms and it as been used in clinical trials for several types of tumours (lung, endometrial and breast cancer) and other clinical conditions such as type II diabetes [273], congestive heart failure and congenital mitochondrial diseases [274] due to side effect of lowering lactate levels by inhibition of PDHK and consequently activating the PDH complex. DCA is a small molecule of 150 Da that penetrates easily into the cell and activates PDH in a dose dependent manner. It has been described that DCA would lead to an increase in ROS production due to the shift in metabolism, accompanied by a decrease in mitochondrial membrane potential [179,180].

The emergent role of PDHK in regulating the PDH status in cancer in parallel with our previous results raised the hypothesis that modulation of PDH cycle could have an impact on pluripotency. Therefore, we wanted to test if PDHK could indeed be crucial for pluripotency, and if some of the metabolic regulatory pathways, found in cancer cells are also present in ESCs. In order to address this

question we used DCA to decrease PDHK activity and infer if pluripotency of ESCs was indeed compromised, and determined possible alterations in metabolism. Also, recent reports linking PDHK status to HIF-1α levels led us to look into some key players in metabolic pathways such as HIF-1α, p53, c-Myc and PKM in order to clarify if they have a role in ESC metabolism/pluripotency status, once more highlighting the possible similarities between cancer cells and ESC. Overall we present a possible target for metabolic modulation with consequences for pluripotency and shed some light into some possible metabolic regulators in ESC.

5.2 Results:

5.2.1 DCA effects on colony morphology, total cell number and viability:

There are no data on the effect of DCA on stem cell pluripotency, namely on possible effects on morphology, viability and cell number. Our experimental conditions were maintained according to the experimental design and at the different collection points morphology was analyzed by phase-contrast microscopy. Figure 5.1A show that control cells are arranged in tightly packed round colonies with well-defined borders. There are some differentiating cells in culture but that is a common feature, as it is very difficult to have a 100% pluripotent culture. On the other hand, and as described previously, cells growing without LIF have colonies that are not well-defined, and we can observe elongated cells with a low nucleus/cytoplasm ratio which is characteristic of differentiated cells. When cells were grown with DCA we can observe an intermediate phenotype between the control condition with cells grown without LIF, although cells exposed to 5mM DCA show high differentiation levels. Another important effect to point out regards total number of cells; there is a significant decrease in the number of cells present in the culture at the end of the experiment for DCA ($P<0.05$ for DCA 3mM and $P<0.01$ for DCA 5mM) and this is comparable to the effect of cells grown without LIF ($P<0.05$) (Figure 5.1B). Because we observed such a significant effect on the total cell number, we next assessed cellular viability. Interestingly, although the cell number is decreased we observe no differences in terms of the percentage of live cells. Only cells growing without LIF presented a significant decrease in cell viability ($P<0.05$). Overall we can infer that although we have an effect on total number of cells, the ones present in the culture as colonies, they are all alive.

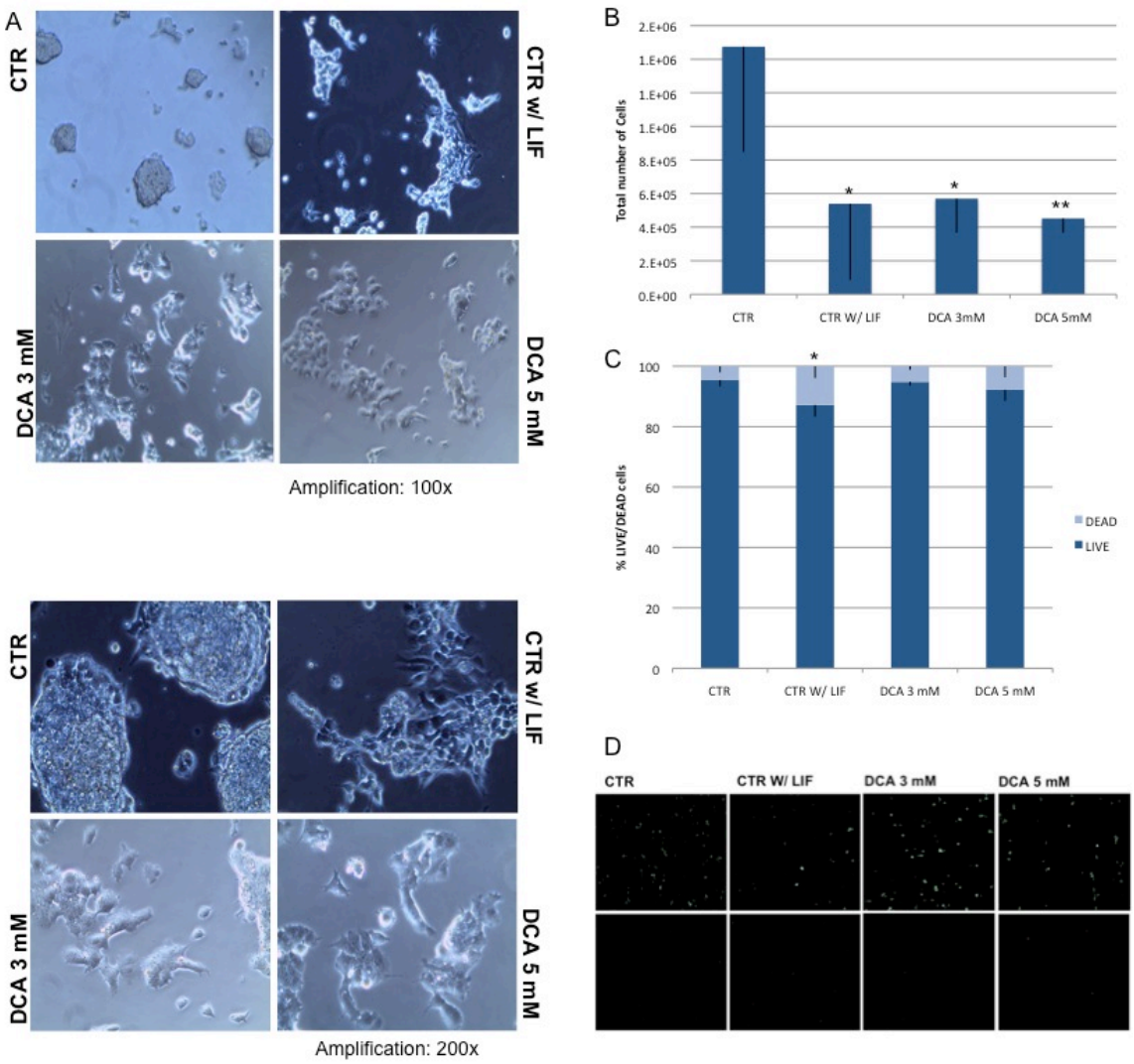

Figure 5.1. DCA effects on colony morphology, total cell number and viability. A)- Phase microscopy photographs of the colonies in all conditions, in the upper panel we can observe cells in culture at 100x amplification and at the lower panel photographs for all experimental conditions at 200x amplification. **B)-** Total number of cells. Cells were counted when collected for experiments, N=20. **C)-** Percentage of viable cells *versus* dead ones. Cells stained green were counted as live while IP positive cells were counted as dead, 100 cells per condition were counted. N=10. **D)-** Fluorescent photographs of the cells in order to confirm that the vast majority is alive. Results are presented as means from all experiments with standard deviation of mean.

5.2.2 mESCs proliferation profile in the different experimental conditions:

To sort out if the differences in terms of cell number could be due to an alteration in proliferation, we stained cells for PCNA and analyzed 20000 cells per condition by flow cytometry. PCNA is highly expressed in rapid proliferating cells and this assay has been used to infer the proliferating rate of tumor cells, for example [217]. Results in Figure 5.2 show that there is a notorious and significant increase in PCNA levels in cells without LIF ($P<0.01$) and cells incubated with 5 mM DCA ($P<0.05$), suggesting that they are both more proliferative.

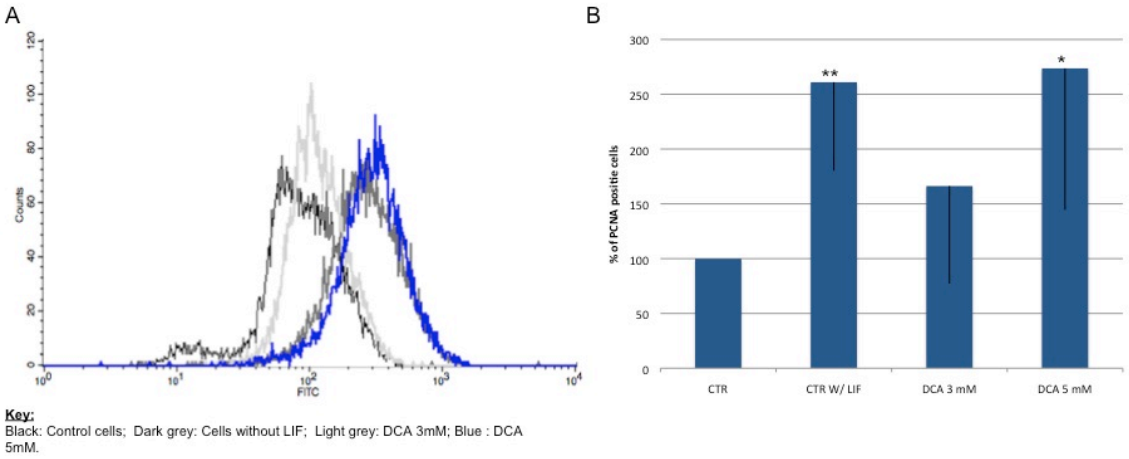

Figure 5.2. mESCs proliferation under the influence of DCA. A)- Schematic representation of the shift during the flow cytometry analysis of each population. **B)-** Quantification of the proliferation rates accessed by PCNA levels in the cells. Results are presented as percentage relative to the control and represent the average of 20000 cells for each condition. N=4, results are presented as means from all experiments with standard deviation of mean.

5.2.3 Pluripotent status of E14 mESCs: is DCA affecting pluripotency?

DCA is described as a chemical compound capable of inhibiting the four isoenzymes of PDHK and it has been used in cancer research due to its collateral effect of promoting oxidative phosphorylation, cell death and cell cycle arrest [241]. We wondered if DCA could be affecting pluripotency of mouse embryonic stem cells and in attempt to answer to this question we perform a battery of assays, including as alkaline phosphatase staining, high resolution ELISA and RT-PCR.

The alkaline phosphatase assay was performed using a kit from Millipore which resulted in red stained alkaline phosphatase positive colonies (AP+) and colonies with no color (alkaline phosphatase negative colonies- AP-). Both types of colonies were counted and data normalized. Results are represented in Figure 5.3A, and cells without LIF (negative control) have a significant higher number of AP- colonies when compared to the other experimental conditions ($P<0.01$). When cells were exposed to 5mM DCA the obtained results are similar to our negative control ($P<0.05$).

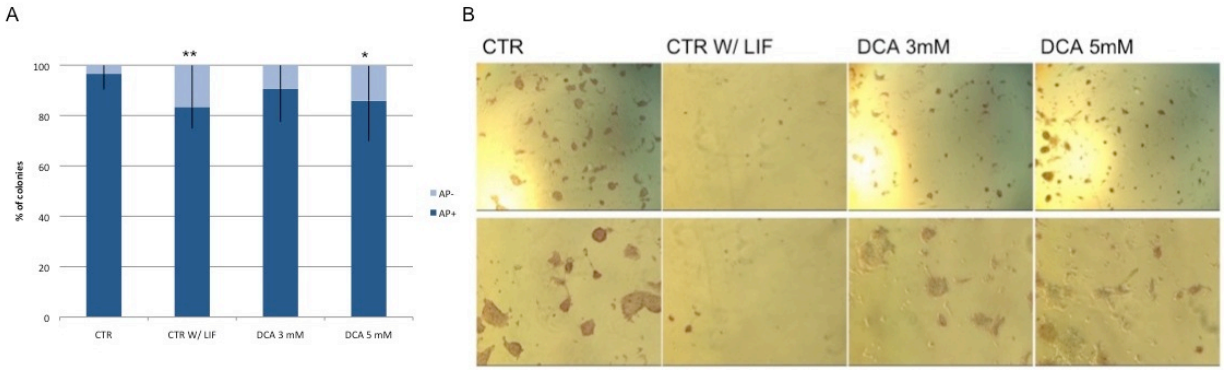

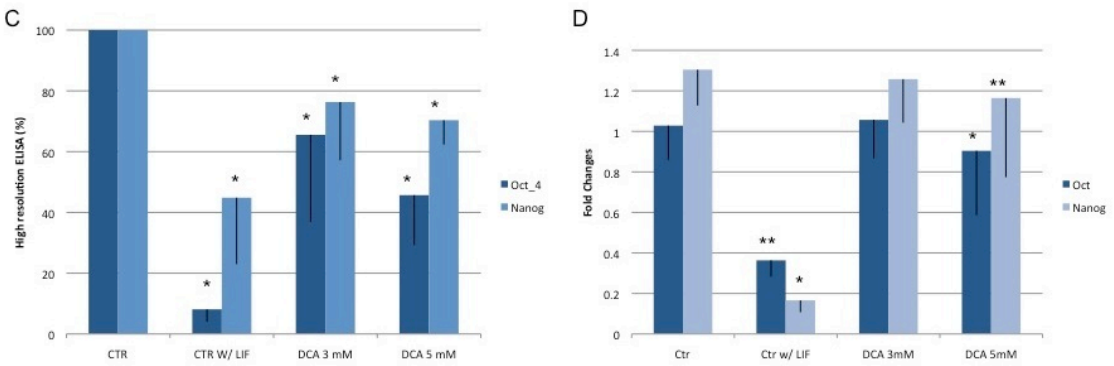

Figure 5.3. Effects of DCA on pluripotency. A)- Alkaline phosphatase assay. Colonies stained red were counted as positive (AP+) pluripotent colonies whereas colonies with no stained were counted as negative for pluripotency (AP-). N=10 **B).** Photographs of AP staining for all experimental conditions. Differences between experimental conditions are clear. **C)-** High resolution Elisa quantification for Oct4, and Nanog, results are presented as percentage relative to the CTR and were normalized for β-actin and for protein content by SRB assay. N=5 **D)**- RT-PCR analysis for the Oct4 and Nanog, results are represented as fold changes. N=3, results are presented as means from all experiments with standard deviation of mean.

When we analyze protein levels for Oct4 and Nanog, two of the major players in pluripotency, by high resolution ELISA (Figure 5.3C) a significant decrease in both Oct4 and Nanog levels for cells without LIF and in cells subjected to DCA is observed ($P<0.05$). The decrease in Oct4 is more pronounced when compared to Nanog levels and once more the results obtained for 5mM DCA are similar to the ones obtained for the experimental negative control. Interestingly, Nanog seemed to be less sensitive than Oct4 to a differentiation stimulus. More importantly mRNA results obtained by RT-PCR confirmed the protein results. We can observe that mRNA levels for Oct4 and Nanog significantly dropped in the CTRW/ LIF (Oct4, $P<0.01$ and Nanog $P<0.05$) and in the presence of 5mM DCA (Oct4, $P<0.05$ and Nanog, $P<0.01$) (Figure 5.3D). There were no statistical differences for DCA 3mM were the decrease in the mRNA was not so notorious, mirroring the protein data.

5.2.4 Mitochondrial Function and metabolic status:

If DCA is inhibiting PDHK, we would expect more active mitochondria in the cell. In order to assess mitochondrial function we analyzed mitochondrial membrane potential (MMP) using the TMRM dye (Figure 5.4C).

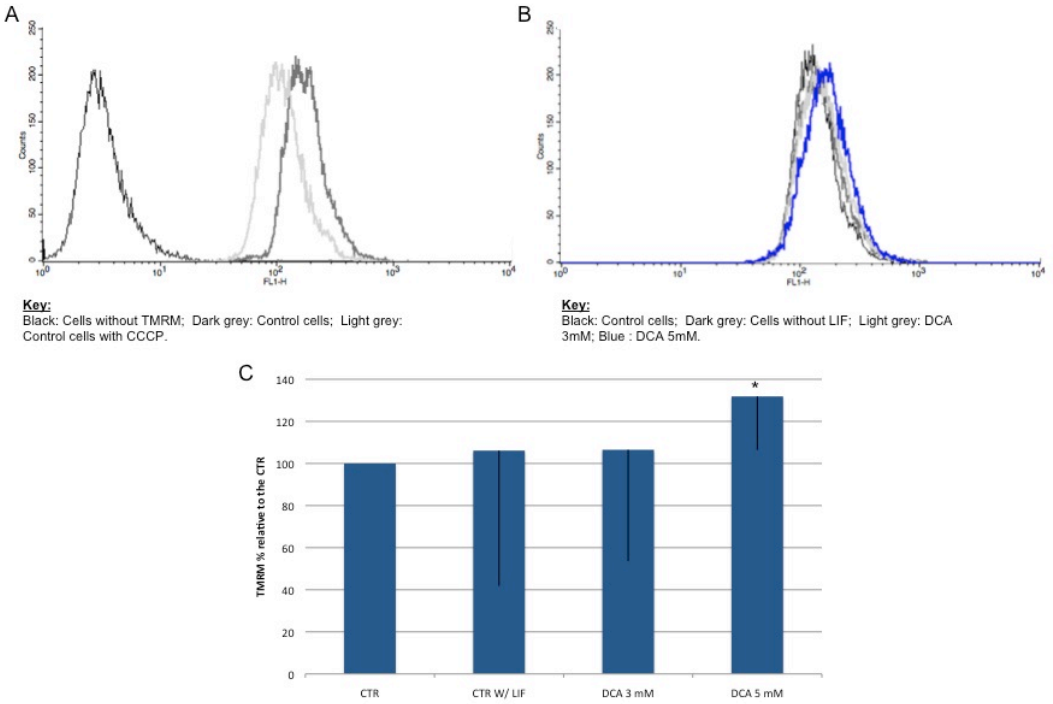

Figure 5.4. Assessment of the mitochondrial membrane potential by flow cytometry with the TMRM dye. A)- Schematic representation of the populations used for defining population gates. Cells without TMRM as negative CTR, CTR cells with dye and CTR cells with CCCP, an uncoupler, to determine the lowest MMP potential possible in these cells. **B)-** Schematic representation of the experimental conditions populations obtained by flow cytometry. **C)-** Quantification of the MMP potential using TMRM dye, results are expressed as percentage relative to the CTR, 20000 cells were evaluated for each population. N=5, results are presented as means from all experiments with standard deviation of mean.

Our results demonstrate that with increasing concentrations of DCA mitochondria become more hyperpolarized which leads to a higher MMP, statistically significant for DCA 5mM ($p<0.05$). Interestingly, there was no increase in MMP for cells grown without LIF, similarly to what was described in chapter 4. Regarding MitoSOX Red analyzes the proper gates were defined. As discussed previously we obtained three different populations: a negative one (M1/pop-) consisting of cells that are producing very low amounts of ROS, a positive population of cells producing normal quantities of ROS (M2/pop+) and a third population (M3/pop ++) that represents cells that are producing higher amounts of ROS. Only for DCA 5mM a significant decrease in the number of cells producing low amounts of ROS was detected (M1/pop-) ($P<0.05$) (Figure 5.5C).

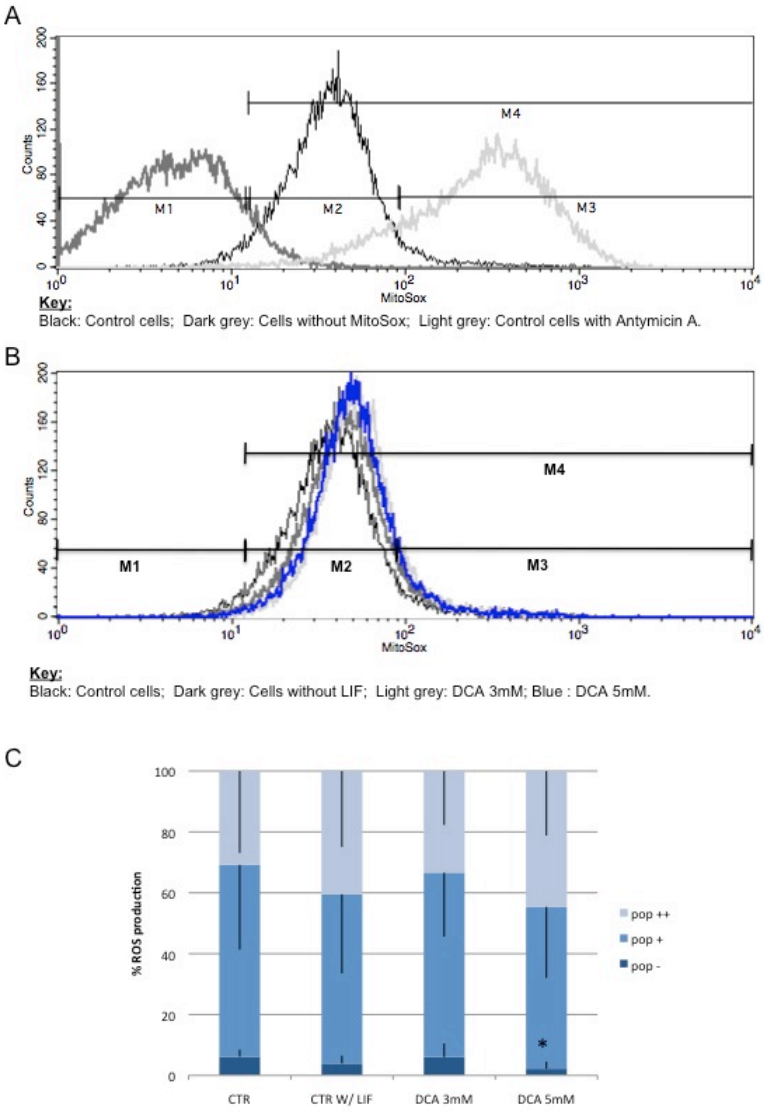

Figure 5.5. Flow cytometry analysis ROS production quantified by MitoSOX Red dye. A)- Schematic representation of the populations used for defining population gates. Cells without MitoSOX as negative CTR, CTR cells with dye and CTR cells with Antimycin A, an inductor of ROS production, as a positive CTR, to determine the highest levels of ROS production in these cells. **B)-** Schematic representation of the experimental conditions populations obtained by flow cytometry. **C)-** Quantification of ROS production, results are expressed as percentage relative to the CTR, 20000 cells were evaluated for each population. N=4, results are expressed as means with Standard deviation of means.

Next, we asked if the increase in MMP could be reflected in ATP levels within the cells, and therefore we analyzed nucleotide concentration for our experimental conditions by HPLC. In order to infer the oxidative state of the cells MTT assay was also performed and lactate levels were determined in order to in infer about a possible metabolic shift.

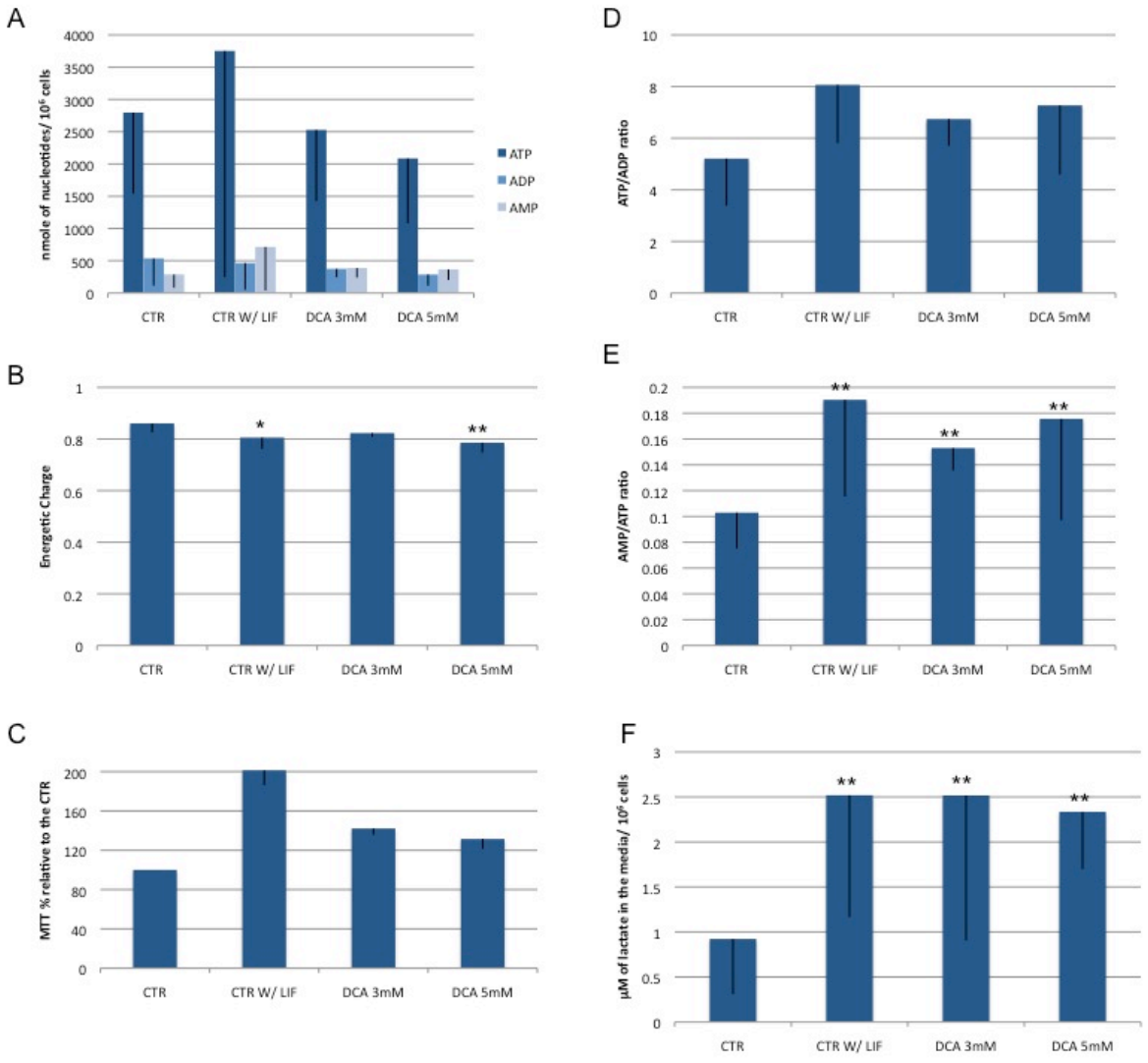

Figure 5.6. Effect of DCA on the energy status of mESC. A)- Nucleotide levels determined by HPLC analysis, N=10. **B)-** Determination of the energetic charge if the cells, N=10. **C)-** Results for the MTT assay are presented as percentage of formazan crystals normalized to the control. N=10 **D)-** ATP/ADP ratio, N=10. **E)-** AMP/ADP ratio, N=10. **F)-** Lactate levels determined by the Lactate Kit from bioVision. N=5. Results are expressed as means with Standard deviation of mean.

Although ATP levels did not significantly change (figure 5.6A), the energetic charge (Figure 5.6B) was decreased for the negative control ($P<0.05$) as well as for cells incubated with 5mM DCA ($P<0.01$). MTT is routinely used as a proliferation test, however given that this assay measures the activity of cellular NADPH if we normalize the obtain results to the number of cells we can infer cellular oxidative status. No significant differences were observed for the experimental conditions, although there is a trend for increased metabolic activity (figure 5.6C). When we look to the ATP/ADP ratio (figure 5.6D) there are no significant differences, however when we look to AMP/ATP ratio we can observe a significant increase for all conditions ($P<0.01$) which could be a reflection for the decreased content of ATP, although this change was not significant (Figure 5.6E). Interestingly, when we measured lactate levels in the media contrary to what would be expected we observed that differentiating cells and cells grown with DCA had a significant increase in the secretion of lactate to the media ($P<0.01$) (Figure 5.6F). All together these results point out to a more active mitochondria but not necessarily with an increase in oxidative metabolism.

5.2.5 Effect of DCA on the PDH cycle:

If DCA is inhibiting PDHK we wondered if the cell would try to adapt by altering the protein levels for PDHK and if the PDH cycle was being affected or not. To evaluate the PDH cycle we determined both the phosphorylated as well as the non-phosphorylated form of PDH besides PDHK1 levels, by western blot.

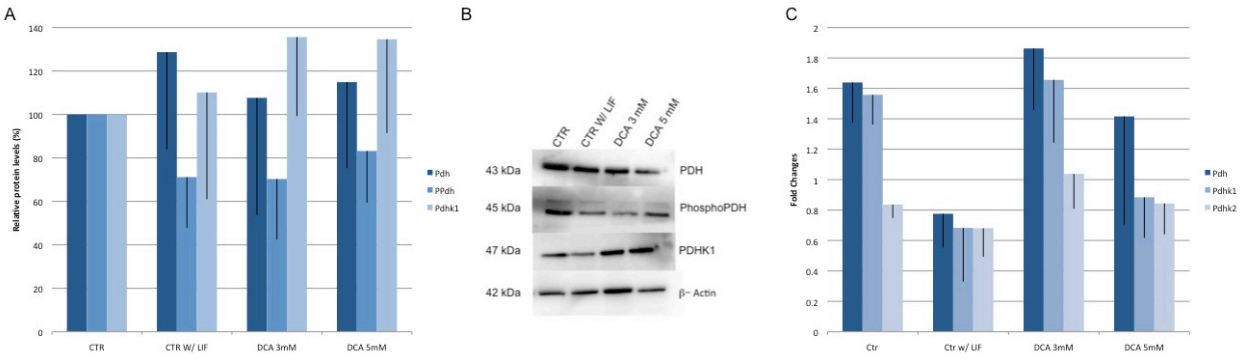

Figure 5.7. Effect of DCA on PDH function and regulation. A)- Western Blot analysis for PDH, PPDH and PDHK1. Results were normalized to β-Actin protein levels and they are represented as percentage relative to the control, N=3 **B)-** Western Blot images. **D)-** RT-PCR analysis for PDH, PDHK1 and PDHK2 genes. Results are presented as fold changes and normalized to the reference house keeping gene β-Actin. N=2. Results are expressed as means with Standard deviation of mean.

If DCA was inhibiting PDHK then we should expect more PDH in its active form (non-phosphorylated) and less phosphorylated PDH (inactive form). Although we didn't observe any significant alteration regarding both protein and mRNA levels (Figure 5.7A and C) a trend compatible with a more active PDH for cells grown without LIF and in the presence of DCA is visible.

5.2.6 Analysis of some key elements in metabolic shifts:

Given that DCA was affecting pluripotency and the results are suggesting a shift in PDH regulation we assessed the protein levels for some keys players in metabolic pathways.

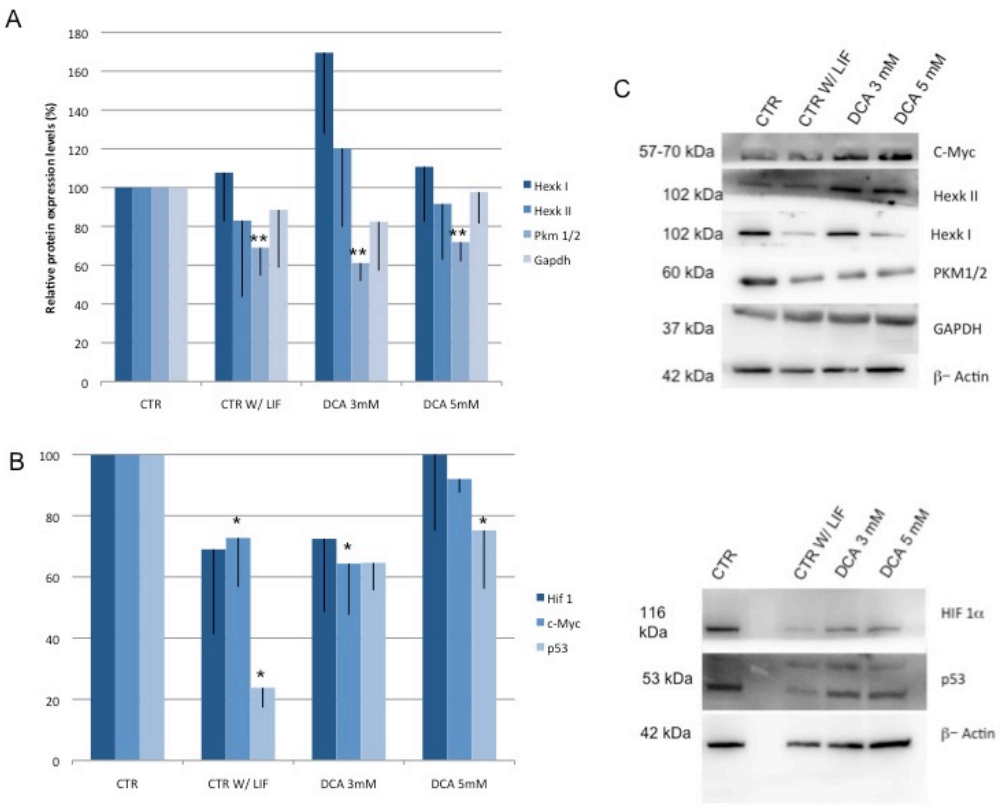

Figure 5.8. Western Blot analysis of some key elements in metabolic shifts A)- Western Blot analysis for Hexokinases I and II, PKM1/2 and Gapdh. Results were normalized to β-Actin protein levels and they are represented as percentage relative to the control, N=3. **B)-** Western Blot analysis for HIF1 alfa, c-Myc and p53. Results were normalized to β-Actin protein levels and they are represented as percentage relative to the control, N=3. **C)-** Western Blot images. Results are expressed as means with Standard deviation of mean.

We looked at Hexokinase I and II levels because if cells in the presence of DCA are becoming more oxidative it could be possible that they lose some of the common characteristics with cancer cells such as high levels of Hexokinase II. No significant differences were observed for Hexokinases and Gapdh. However regarding PKM1/2 we could observe a significant decrease for all experimental conditions ($P<0.01$) (figure 5.8A).

Given that most of these enzymes are downstream targets for signaling pathways controlled by Hif-1α, c-Myc and p53 we inferred the protein levels for these key players as well (figure 5.8B). The first thing to notice was the appearance of HIF1-α in pluripotent cells grown in normoxia and what seems to be a decrease in protein levels with differentiation. In general we can conclude that with differentiation and in the presence of DCA protein levels for c-Myc and p53 significantly decreases ($P<0.05$). To note that for CTR W/ LIF we observe a decrease in both proteins while for DCA the results are not so cohesive given that c-Myc only decreases in DCA 3mM and p53 only for DCA 5mM. More experiments would be needed to fully clarify these aspects.

5.3 Discussion:

In this chapter we present results demonstrating the effect of modulating pluripotency by inhibiting PDHK. We can consider this kinase as a gatekeeper in metabolism given that its activity will determine the active or inactive state of PDH, resulting therefore in more or less acetyl-CoA levels for the TCA cycle consequently determining the availability of substrates for mitochondrial OXPHOS [179,275]. If we consider the normal glycolytic metabolism of ESC [276,277] we know that an inactive (phosphorylated) form of PDH is preferred because it will promote the Warburg effect therefore accomplishing this way a more rapid glucose turnover accompanied with more quiescent mitochondria. The available literature concerning inhibition of PDHK with DCA is for different types of medical conditions but non-existent for ESC (for review [274]). Therefore it was imperative to start our study with a characterization of our cultured cells in the presence of DCA. In order to have a proper positive control (given that our main hypothesis was to access if PDHK had a role in pluripotency), we grew cells without LIF, thus promoting differentiation.

It is important to note that PDHK inhibition affected pluripotency and that was translated into differences in morphology within the colonies as well as cell morphology. Meaning that although colonies where still growing in a dome shape the well-defined borders were no longer visible and the nucleus/cytoplasm ratio was altered. Another important aspect was the total cell number, it is important to keep in mind that our culture conditions promotes pluripotency, allowing a positive selection for pluripotent cells that will attach and grow more easily than differentiated ones. Probably in the presence of DCA cells could have died or if they started to differentiate more rapidly that could have interfered with their ability to attach and grow. However the cells that do attach are more proliferative when compared to control cells (which was shown by PCNA) and are able to divide and form colonies.

The obtained results for AP staining and Oct4 as well as Nanog protein/mRNA levels clearly demonstrate a clear deleterious effect of DCA on pluripotency. Although the results for assessing PDH status were not significant we could speculate that an inactive PDH and a functional PDHK could be beneficial for the cells. It is also important to note that although AP staining is commonly applied to assess pluripotency and constitutes an easy, fast protocol, this is not the best marker, given that the differences where not as significant as the ones found for the two key regulators of the pluripotency network and were only significant for the experimental conditions that would promote a higher degree of differentiation.

It is described that DCA leads to a decrease in mitochondrial membrane potential (MMP), however that was not the case for ESC. Given that to date this is the first paper were DCA was added to ESC we can not ruled out that mitochondria in ESC will respond differently when compared to cancer cells or cardiac, pancreatic and liver cells. Another important factor to take into consideration is that maybe the loss of pluripotency could confound DCA effect on mitochondria. Despite this different outcome we do observe a small increase in ROS production, which is described as a side effect of inhibiting PDHK. Interestingly, 3mM DCA doesn't seem to have an effect in ROS production when compared to 5mM DCA.

Inhibition of PDHK leads to a more oxidative metabolism that in cancer cells will result in an increase in apoptosis via the intrinsic mitochondrial pathway due to high ROS levels, causing mitochondrial depolarization and a decrease in ATP production. Given that in our culture system only the "capable" cells will attach and divide we believe that rather than an extreme effect of DCA we are observing the effects of a shift in metabolism that will not lead to cell death and possibly this could be the reason why some of our results are not according to the literature. Although it was not significant, ATP levels is another parameter that did not vary according to what is described. This could be an effect of the compound given that for cells grown without LIF we did observe an increase in ATP levels, which

is in accordance with what we know happens during differentiation of stem cells. However, the change in the energetic charge was significant. Overall we can conclude that DCA is increasing mitochondrial activity but at the same time impairing cell energy charge which could imply that DCA may have an effect on mitochondrial complex V (ATP-synthase) in ESC.

There are four different isoforms of the PDHK (1-4) described in mammalian cells and they present different affinities for DCA and to different concentrations of mitochondrial effectors. High acetyl-CoA/ CoA and NADH/NAD+ ratios will activate PDHK, leading to an inhibitory phosphorylation of PDH [278]. On the other hand pyruvate will inhibit PDHK activity resulting in lower levels of phosporylated PDH and consequently more substrates will be available for the TCA cycle [279].

We choose PDHK1 given that it has already been described that Hif-1α and c-Myc upregulate this kinase in order to achieve a functional inhibition of the mitochondria promoting the Warburg effect in cancer cells [179,181,280]. Also, our previous results, described in chapter 3, point out a possible role for PDHK1, and mRNA results for our control cells demonstrate that PDHK1 exists in higher amounts in ESCs. The available literature regarding DCA has a wide range of used concentrations, in our study we performed titrations with the ultimate goal to obtain the lowest effective concentration that would inhibit all the four PDHKs and would promote an active PDH in order to observe a shift in metabolism. Although we did observe a tendency towards our goal but to our surprise we did not observe significant changes.

Is has been described that Hif-1α is upregulated in cancer cells as is c-Myc, activating signaling pathways that will lead to an increase of PHDK, PKM1/2 and HEXOKINASE II genes in order to promote a high rate of glycolysis so that ATP demand is met [281]. To date, and to our knowledge there is no paper demonstrating the same type of regulation in ESCs in order to maintain the glycolytic metabolism. Although it has been described that in order to have endogenous induction of pluripotency genes in iPSC

first a shift to glycolysis must occur and that high expression of some enzymes as Hexokinase are beneficial for pluripotency [80,187,265]. Our results seem to point out a similar strategy for ESC as in the case for cancer cells, given that we observed detectable levels of Hif-1α in our cells (grown in normoxia). Also, in a pluripotent state they present high levels for hexokinases, gapdh, pkm1/2 and c-Myc clearly demonstrating that these could be key players in metabolism modulation by maintaining high levels of key enzymes in glycolysis in ESC, which would be important to maintain pluripotency.

Although it was not statistically different, and more experiments are needed, it is important to highlight that in cells grown without LIF we observed a tendency for a decrease in Hif-1α and c-Myc levels with an alteration in mitochondrial function and a decrease in enzymes known to be important in sustaining the glycolytic profile. Similar effects were obtain for these cells and the ones grown with DCA, were a decrease in Hexokinase levels was observed which could limit the first step of glycolysis thereby compromising a strategy known to be effective in maintaining high glycolysis rates. Also, we observed a decrease in Gapdh, an enzyme commonly used as a loading control for several experiments. It is known that this enzyme will control the availability of substrates for the penthose phosphate pathway (PPP) that is extremely important to maintain the production of pentoses and to maintain proper levels of NAPDH in the cells, and both characteristics are important for rapid dividing cells [190]. To note that PPP is also controlled by c-Myc, the levels of which were significantly diminished. This way it is tempting to consider that maybe throughout loss of pluripotency PPP becomes impaired.

Regarding the p53 results, they can be interpreted following two different points of view. If we consider that p53 functions as a protector against cellular stress that controls cellular proliferation by inhibiting it if a cell is compromised, than it should be expected that p53 levels would drop in differentiating cells as well as in cells grown in the presence of DCA [56,266,267]. However given that p53 will repress Hif-1α and its expression is induced by ROS it could also be expected that p53 levels

would increase in our experimental conditions. However this was not the case [177,178]. We can only speculate that maintenance of proliferation rates and therefore cell survival could overcome the other effects of p53.

Finally, another important result was the significant decrease in PKM1/2 levels. This enzyme has been implicated as a possible target for cancer therapeutics for metabolic modulation by controlling the amount of pyruvate that is produced. Also because PKM1/2 interacts with Hif-1α, β-catenin and Oct4 [194,282], this enzyme could also be involved in the maintenance of the pluripotency status of the cell reinforcing PKM as a good target.

It is important to consider that our results points towards similar pathways involved in controlling metabolism as observed for cancer cells and that PDH could indeed be a good target for metabolic modulation given its downstream effects.

Overall we can conclude that, by adding DCA to our cells we are promoting loss of pluripotency and a shift in metabolism, meaning that inhibition of PDHK1 in these cells bypasses LIF action, and this effect is very similar to one obtain for cells that are differentiating. We observe an intricate network for controlling metabolism that needs to be altered in order for differentiation to take place. It is tempting to propose that if PHDK is inhibited, or that is a signal that promotes differentiation, cells will change their metabolism in order to have a more active PDH. This besides leading to more active mitochondria, by interfering with PDHK levels, will lead to lower levels of Hif-1α, c-Myc, p53 and PKM1/2 resulting in alteration of some key enzymes in metabolism, and disrupting the glycolytic profile that they need to maintain pluripotency.

General Conclusion and Future Perspectives

Chapter 6

The main goal of this thesis was to determine if metabolism and mitochondrial function had a role in ESCs pluripotency. Throughout this thesis we discussed results that shed some light on our hypothesis and overall the goals were accomplished. In this section the main conclusions will be summarized stressing out some of the most important findings in this thesis and how they integrate with the literature.

Before going to through the results presented in this thesis it is important to note that hESC sand mESCs are indeed different, as mentioned in chapter 1, which could also justify some discrepancies between results regarding MMP and lactate [14]. These differences can be due to species-specific characteristics or to the fact that both ESCs represent different developmental status, an issue raised since the isolation and characterization of EpiSCs [43]. However, and most interestingly our results clearly demonstrate that loss of pluripotency implies higher levels of ATP present in these cells, which become clear with the ATP levels obtained for differentiated cell lines and for mESCs grown without LIF.

The available knowledge about the metabolic status in ESCs and iPSCs was unclear at the time this research work begun. This was the main reason why the first goal was to assess and characterize metabolism and mitochondrial function in parallel for hPSCs and their differentiated counterparts. It is interesting to consider that the results present in chapter 3 were pointing out to a more glycolytic profile with silent mitochondria with low O_2 consumption and an inactive PDH for PSCs while the contrary was observed for the differentiated counterparts [276]. An interesting result was the intermediate position of iPSCs, suggesting that this type of PSCs were not completely reprogrammed. At the time other papers were published demonstrating similar results [76,148]. It is very tempting to consider that the variability observed in these cells could be related with the metabolic profile observed in the “parental” cells before reprogramming, stressing out once again the importance of metabolism in

ESCs. The results obtained allowed for the identification of some strategies common with cancer cells in terms of maintaining a glycolytic profile. At the time, these results were novel and more importantly they become corroborated by recent reports where the glycolytic profile was proven to be of outmost importance to achieve pluripotency in iPSCs [187] and that modulation of metabolism could have an effect in the differentiation pattern [190]. Interestingly, the array results demonstrated that hPSCs have higher transcription for TCA cycle genes as well as for genes coding enzymes for the PPP in particular enzymes of the non-oxidative branch of this pathway, which could reflect an adaptation for nucleotide synthesis as well as metabolic intermediates used in lipid synthesis. Once more this is also observed for some cancer cells [184]. These results in parallel with the fact that hPSCs present high levels of Hk2 linked to the mitochondria, high levels of PDHK1 along with an inactive PDH lead to the possibility that these could be essential for pluripotency in ESCs and a good target to metabolic modulation, which led to chapters four and five.

The results presented in these last two chapters allowed us to conclude that an inactive PDHK1 and consequently a more active PDH seems more detrimental for pluripotency than inhibition of Hk2. This last observation could be partially explained by the fact that both Hif-1α and c-Myc interact with PDHK1 [251,283] and considering that 3BRP effect in Hk2 is more upstream, and cells could overcome this effect. Also, this could be a possible explanation for the fact that with 3BRP there is an increase for c-Myc levels while for DCA there is a decrease. Another important fact to take into consideration refers to the concentrations used for both compounds. Although the used concentrations are within the range used for cancer research, it should be noted that while the main goal in this case is to cause cell death we titrated the compound in order to find the concentration that had an effect in pluripotency. An interesting point to consider, recalling the results for total number of cells, is the possibility that in our culture conditions the cells that attach and form colonies are more resistant to the compounds in terms of cell death when compared to the ones that die during plating. It would be interesting to apply the

same methodology to different cancer cell lines in order to assess if this could be a mechanism of selection for cancer stem cells.

Overall we can conclude that for both compounds the highest concentration was always more detrimental for pluripotency with notable negative consequences in terms of mitochondrial function. When we consider loss of pluripotency our negative control was essential to differentiate between the effects of the compounds comparative to the effects of inhibited enzymes. Following the example of cancer cells we looked for possible similarities for pathways involved in controlling the glycolytic phenotype essential for pluripotency. Surprisingly, we found that differentiation is accompanied with a decrease in protein levels for PKM1/2 and Hif-1α, which as not been described yet for ESCs although for cancer cells it has been already described that a decrease in these proteins has a detrimental effect in cancer cells [164,194,284]. Although we cannot conclude that a shift in metabolism occurred, due to the lack of statistical significance, our results could point to a possible beginning in such a shift. Probably if we kept cells in culture for longer periods of time and taking into account the decrease in protein levels for these key players in metabolism regulation, a metabolic shift could be clear.

It would be very interesting as future work to better clarify the role of PDHK inhibition using another methodology, such as RNA interference. This technique would allow to better understand the role of each PDHK given that we could silence specifically each PDHK. Another interesting line of research that was not approach in this thesis contemplates differentiation patterns. If indeed a shift in metabolism is being initiated with comitant loss of pluripotency it would be important to infer if a specific pattern towards a lineage or cell type occurs. This could be evaluated recurring to the embryoid body formation this assay is rottenly used as an assay for assessing pluripotency to test if the cells are able to generate multilineage structures.

In figure 6.1 the main conclusions of this thesis regarding PDHK inactivation are present, given that indeed it seems to be the target with more noticeable consequences when inhibited.

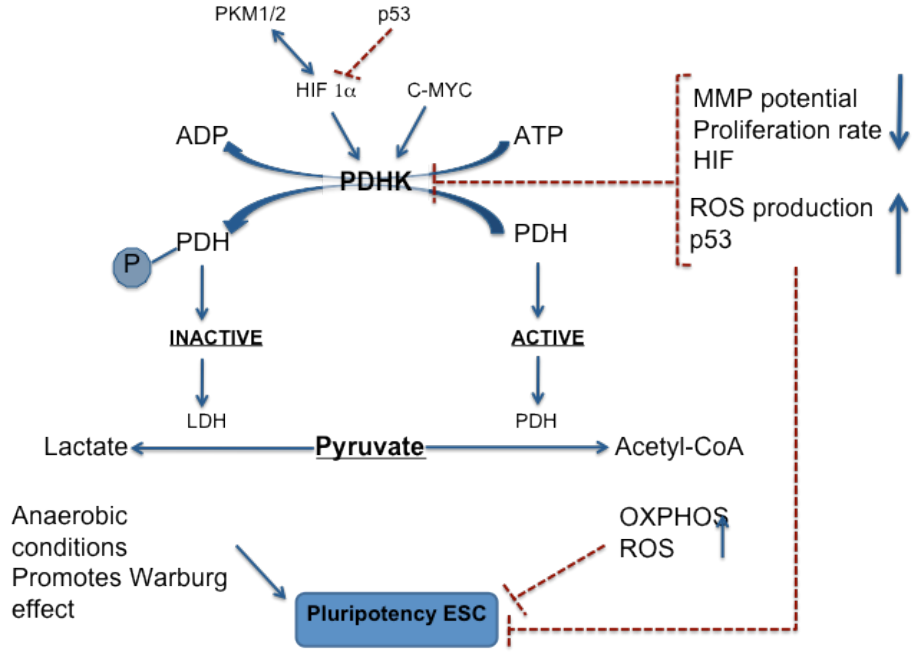

Figure 1.6 – Main conclusions from PDHK inhibition. Overall when PDHK is inhibited MMP will decrease as well as proliferation rates and Hif-1α protein levels. In contrast, ROS production will increase as well as p53 protein levels. All together this will impair pluripotency as well as a more oxidative metabolism. By disrupting Hif-1α protein levels PKM1/2 will also be affected and protein levels will also decrease in ESC. This way it is reasonable to conclude that indeed a Phospho-PDH (inactive form) is beneficial for pluripotency because promotes the Warburg effect which in turn promotes pluripotency.

Bibliography

Chapter 7

References:

2. Evans MJ, Kaufman MH (1981) Establishment in culture of pluripotential cells from mouse embryos. Nature 292: 154-156.

3. Martin GR (1981) Isolation of a pluripotent cell line from early mouse embryos cultured in medium conditioned by teratocarcinoma stem cells. Proc Natl Acad Sci U S A 78: 7634-7638.

4. Nichols J, Smith A (2012) Pluripotency in the embryo and in culture. Cold Spring Harb Perspect Biol 4: a008128.

5. Kleinsmith LJ, Pierce GB, Jr. (1964) Multipotentiality of Single Embryonal Carcinoma Cells. Cancer Res 24: 1544-1551.

6. Knowles BB, Aden DP, Solter D (1978) Monoclonal antibody detecting a stage-specific embryonic antigen (SSEA-1) on preimplantation mouse embryos and teratocarcinoma cells. Curr Top Microbiol Immunol 81: 51-53.

7. Solter D, Knowles BB (1978) Monoclonal antibody defining a stage-specific mouse embryonic antigen (SSEA-1). Proc Natl Acad Sci U S A 75: 5565-5569.

8. Thomson JA, Itskovitz-Eldor J, Shapiro SS, Waknitz MA, Swiergiel JJ, et al. (1998) Embryonic stem cell lines derived from human blastocysts. Science 282: 1145-1147.

9. Yamanaka S (2008) Induction of pluripotent stem cells from mouse fibroblasts by four transcription factors. Cell Prolif 41 Suppl 1: 51-56.

10. Fuchs E, Chen T (2013) A matter of life and death: self-renewal in stem cells. EMBO Rep 14: 39-48.

11. Pera MF, Reubinoff B, Trounson A (2000) Human embryonic stem cells. J Cell Sci 113 (Pt 1): 5-10.

12. Hochedlinger K, Plath K (2009) Epigenetic reprogramming and induced pluripotency. Development 136: 509-523.

13. Smith KP, Luong MX, Stein GS (2009) Pluripotency: toward a gold standard for human ES and iPS cells. J Cell Physiol 220: 21-29.

14. Ramalho-Santos J, Varum S, Amaral S, Mota PC, Sousa AP, et al. (2009) Mitochondrial functionality in reproduction: from gonads and gametes to embryos and embryonic stem cells. Hum Reprod Update 15: 553-572.

15. Alvarez CV, Garcia-Lavandeira M, Garcia-Rendueles ME, Diaz-Rodriguez E, Garcia-Rendueles AR, et al. (2012) Defining stem cell types: understanding the therapeutic potential of ESCs, ASCs, and iPS cells. J Mol Endocrinol 49: R89-111.

16. Knoblich JA (2001) Asymmetric cell division during animal development. Nat Rev Mol Cell Biol 2: 11-20.

17. Rogers I, Casper RF (2003) Stem cells: you can't tell a cell by its cover. Hum Reprod Update 9: 25-33.

18. Graf T, Stadtfeld M (2008) Heterogeneity of embryonic and adult stem cells. Cell Stem Cell 3: 480-483.

19. Klimanskaya I, Chung Y, Becker S, Lu SJ, Lanza R (2007) Derivation of human embryonic stem cells from single blastomeres. Nat Protoc 2: 1963-1972.

20. Cartwright P, McLean C, Sheppard A, Rivett D, Jones K, et al. (2005) LIF/STAT3 controls ES cell self-renewal and pluripotency by a Myc-dependent mechanism. Development 132: 885-896.

21. Okita K, Ichisaka T, Yamanaka S (2007) Generation of germline-competent induced pluripotent stem cells. Nature 448: 313-317.

22. O'Connor MD, Kardel MD, Eaves CJ (2011) Functional assays for human embryonic stem cell pluripotency. Methods Mol Biol 690: 67-80.

23. Nagano K, Yoshida Y, Isobe T (2008) Cell surface biomarkers of embryonic stem cells. Proteomics 8: 4025-4035.

24. Pan G, Thomson JA (2007) Nanog and transcriptional networks in embryonic stem cell pluripotency. Cell Res 17: 42-49.

25. Avilion AA, Nicolis SK, Pevny LH, Perez L, Vivian N, et al. (2003) Multipotent cell lineages in early mouse development depend on SOX2 function. Genes Dev 17: 126-140.

26. Chambers I, Colby D, Robertson M, Nichols J, Lee S, et al. (2003) Functional expression cloning of Nanog, a pluripotency sustaining factor in embryonic stem cells. Cell 113: 643-655.

27. Liedtke S, Stephan M, Kogler G (2008) Oct4 expression revisited: potential pitfalls for data misinterpretation in stem cell research. Biol Chem 389: 845-850.

28. Nichols J, Zevnik B, Anastassiadis K, Niwa H, Klewe-Nebenius D, et al. (1998) Formation of pluripotent stem cells in the mammalian embryo depends on the POU transcription factor Oct4. Cell 95: 379-391.

29. Aksoy I, Jauch R, Chen J, Dyla M, Divakar U, et al. (2013) Oct4 switches partnering from Sox2 to Sox17 to reinterpret the enhancer code and specify endoderm. EMBO J 32: 938-953.

30. Boyer LA, Lee TI, Cole MF, Johnstone SE, Levine SS, et al. (2005) Core transcriptional regulatory circuitry in human embryonic stem cells. Cell 122: 947-956.

31. Kopp JL, Ormsbee BD, Desler M, Rizzino A (2008) Small increases in the level of Sox2 trigger the differentiation of mouse embryonic stem cells. Stem Cells 26: 903-911.

32. Masui S, Nakatake Y, Toyooka Y, Shimosato D, Yagi R, et al. (2007) Pluripotency governed by Sox2 via regulation of Oct3/4 expression in mouse embryonic stem cells. Nat Cell Biol 9: 625-635.

33. Fong H, Hohenstein KA, Donovan PJ (2008) Regulation of self-renewal and pluripotency by Sox2 in human embryonic stem cells. Stem Cells 26: 1931-1938.

34. Chambers I, Silva J, Colby D, Nichols J, Nijmeijer B, et al. (2007) Nanog safeguards pluripotency and mediates germline development. Nature 450: 1230-1234.

35. Mitsui K, Tokuzawa Y, Itoh H, Segawa K, Murakami M, et al. (2003) The homeoprotein Nanog is required for maintenance of pluripotency in mouse epiblast and ES cells. Cell 113: 631-642.

36. Theunissen TW, Silva JC (2011) Switching on pluripotency: a perspective on the biological requirement of Nanog. Philos Trans R Soc Lond B Biol Sci 366: 2222-2229.

37. Welling M, Geijsen N (2013) Uncovering the true identity of naive pluripotent stem cells. Trends Cell Biol.

38. Evans M (2011) Discovering pluripotency: 30 years of mouse embryonic stem cells. Nat Rev Mol Cell Biol 12: 680-686.

39. Brons IG, Smithers LE, Trotter MW, Rugg-Gunn P, Sun B, et al. (2007) Derivation of pluripotent epiblast stem cells from mammalian embryos. Nature 448: 191-195.

40. Dietrich JE, Hiiragi T (2007) Stochastic patterning in the mouse pre-implantation embryo. Development 134: 4219-4231.

41. Plusa B, Piliszek A, Frankenberg S, Artus J, Hadjantonakis AK (2008) Distinct sequential cell behaviours direct primitive endoderm formation in the mouse blastocyst. Development 135: 3081-3091.

42. Nichols J, Silva J, Roode M, Smith A (2009) Suppression of Erk signalling promotes ground state pluripotency in the mouse embryo. Development 136: 3215-3222.

43. De Los Angeles A, Loh YH, Tesar PJ, Daley GQ (2012) Accessing naive human pluripotency. Curr Opin Genet Dev 22: 272-282.

44. Buecker C, Geijsen N (2010) Different flavors of pluripotency, molecular mechanisms, and practical implications. Cell Stem Cell 7: 559-564.

45. Nichols J, Smith A (2009) Naive and primed pluripotent states. Cell Stem Cell 4: 487-492.

46. Ryu BY, Orwig KE, Kubota H, Avarbock MR, Brinster RL (2004) Phenotypic and functional characteristics of spermatogonial stem cells in rats. Dev Biol 274: 158-170.

47. Nagano M, Brinster CJ, Orwig KE, Ryu BY, Avarbock MR, et al. (2001) Transgenic mice produced by retroviral transduction of male germ-line stem cells. Proc Natl Acad Sci U S A 98: 13090-13095.

48. De Felici M, Scaldaferri ML, Lobascio M, Iona S, Nazzicone V, et al. (2004) Experimental approaches to the study of primordial germ cell lineage and proliferation. Hum Reprod Update 10: 197-206.

49. Fagoonee S, Pellicano R, Silengo L, Altruda F (2011) Potential applications of germline cell-derived pluripotent stem cells in organ regeneration. Organogenesis 7: 116-122.

50. Amit M, Carpenter MK, Inokuma MS, Chiu CP, Harris CP, et al. (2000) Clonally derived human embryonic stem cell lines maintain pluripotency and proliferative potential for prolonged periods of culture. Dev Biol 227: 271-278.

51. Edel MJ, Menchon C, Vaquero JM, Izpisua Belmonte JC (2011) A protocol to assess cell cycle and apoptosis in human and mouse pluripotent cells. Cell Commun Signal 9: 8.

52. Mandal S, Lindgren AG, Srivastava AS, Clark AT, Banerjee U (2011) Mitochondrial function controls proliferation and early differentiation potential of embryonic stem cells. Stem Cells 29: 486-495.

53. White J, Dalton S (2005) Cell cycle control of embryonic stem cells. Stem Cell Rev 1: 131-138.

54. Savatier P, Lapillonne H, Jirmanova L, Vitelli L, Samarut J (2002) Analysis of the cell cycle in mouse embryonic stem cells. Methods Mol Biol 185: 27-33.

55. McLenachan S, Menchon C, Raya A, Consiglio A, Edel MJ (2012) Cyclin A1 is essential for setting the pluripotent state and reducing tumorigenicity of induced pluripotent stem cells. Stem Cells Dev 21: 2891-2899.

56. Kawamura T, Suzuki J, Wang YV, Menendez S, Morera LB, et al. (2009) Linking the p53 tumour suppressor pathway to somatic cell reprogramming. Nature 460: 1140-1144.

57. Hong H, Takahashi K, Ichisaka T, Aoi T, Kanagawa O, et al. (2009) Suppression of induced pluripotent stem cell generation by the p53-p21 pathway. Nature 460: 1132-1135.

58. Marion RM, Strati K, Li H, Murga M, Blanco R, et al. (2009) A p53-mediated DNA damage response limits reprogramming to ensure iPS cell genomic integrity. Nature 460: 1149-1153.

59. Meshorer E, Misteli T (2006) Chromatin in pluripotent embryonic stem cells and differentiation. Nat Rev Mol Cell Biol 7: 540-546.

60. Serrano L, Vazquez BN, Tischfield J (2013) Chromatin structure, pluripotency and differentiation. Exp Biol Med (Maywood) 238: 259-270.

61. Lengner CJ, Gimelbrant AA, Erwin JA, Cheng AW, Guenther MG, et al. (2010) Derivation of pre-X inactivation human embryonic stem cells under physiological oxygen concentrations. Cell 141: 872-883.

62. Matsuda T, Nakamura T, Nakao K, Arai T, Katsuki M, et al. (1999) STAT3 activation is sufficient to maintain an undifferentiated state of mouse embryonic stem cells. EMBO J 18: 4261-4269.

63. Xu RH, Chen X, Li DS, Li R, Addicks GC, et al. (2002) BMP4 initiates human embryonic stem cell differentiation to trophoblast. Nat Biotechnol 20: 1261-1264.

64. Eiselleova L, Peterkova I, Neradil J, Slaninova I, Hampl A, et al. (2008) Comparative study of mouse and human feeder cells for human embryonic stem cells. Int J Dev Biol 52: 353-363.

65. Briggs R, King TJ (1952) Transplantation of Living Nuclei From Blastula Cells into Enucleated Frogs' Eggs. Proc Natl Acad Sci U S A 38: 455-463.

66. Wilmut I, Schnieke AE, McWhir J, Kind AJ, Campbell KH (1997) Viable offspring derived from fetal and adult mammalian cells. Nature 385: 810-813.

67. Cowan CA, Atienza J, Melton DA, Eggan K (2005) Nuclear reprogramming of somatic cells after fusion with human embryonic stem cells. Science 309: 1369-1373.

68. Takahashi K, Yamanaka S (2006) Induction of pluripotent stem cells from mouse embryonic and adult fibroblast cultures by defined factors. Cell 126: 663-676.

69. Takahashi K, Tanabe K, Ohnuki M, Narita M, Ichisaka T, et al. (2007) Induction of pluripotent stem cells from adult human fibroblasts by defined factors. Cell 131: 861-872.

70. Yamanaka S, Blau HM (2010) Nuclear reprogramming to a pluripotent state by three approaches. Nature 465: 704-712.

71. Samavarchi-Tehrani P, Golipour A, David L, Sung HK, Beyer TA, et al. (2010) Functional genomics reveals a BMP-driven mesenchymal-to-epithelial transition in the initiation of somatic cell reprogramming. Cell Stem Cell 7: 64-77.

72. Hansson J, Rafiee MR, Reiland S, Polo JM, Gehring J, et al. (2012) Highly coordinated proteome dynamics during reprogramming of somatic cells to pluripotency. Cell Rep 2: 1579-1592.

73. Zhang J, Nuebel E, Daley GQ, Koehler CM, Teitell MA (2012) Metabolic regulation in pluripotent stem cells during reprogramming and self-renewal. Cell Stem Cell 11: 589-595.

74. Takasaki Y, Deng JS, Tan EM (1981) A nuclear antigen associated with cell proliferation and blast transformation. J Exp Med 154: 1899-1909.

75. Maherali N, Sridharan R, Xie W, Utikal J, Eminli S, et al. (2007) Directly reprogrammed fibroblasts show global epigenetic remodeling and widespread tissue contribution. Cell Stem Cell 1: 55-70.

76. Prigione A, Fauler B, Lurz R, Lehrach H, Adjaye J (2010) The senescence-related mitochondrial/oxidative stress pathway is repressed in human induced pluripotent stem cells. Stem Cells 28: 721-733.

77. Li R, Liang J, Ni S, Zhou T, Qing X, et al. (2010) A mesenchymal-to-epithelial transition initiates and is required for the nuclear reprogramming of mouse fibroblasts. Cell Stem Cell 7: 51-63.

78. Polo JM, Anderssen E, Walsh RM, Schwarz BA, Nefzger CM, et al. (2012) A molecular roadmap of reprogramming somatic cells into iPS cells. Cell 151: 1617-1632.

79. Sancho-Martinez I, Izpisua Belmonte JC (2013) Stem cells: Surf the waves of reprogramming. Nature 493: 310-311.

80. Folmes CD, Nelson TJ, Dzeja PP, Terzic A (2012) Energy metabolism plasticity enables stemness programs. Ann N Y Acad Sci 1254: 82-89.

81. Buganim Y, Faddah DA, Jaenisch R (2013) Mechanisms and models of somatic cell reprogramming. Nat Rev Genet 14: 427-439.

82. Alfatah Mansour A, Hanna JH (2013) Oct4 shuffles Sox partners to direct cell fate. EMBO J 32: 917-919.

83. Rosner MH, Vigano MA, Ozato K, Timmons PM, Poirier F, et al. (1990) A POU-domain transcription factor in early stem cells and germ cells of the mammalian embryo. Nature 345: 686-692.

84. Scholer HR, Dressler GR, Balling R, Rohdewohld H, Gruss P (1990) Oct-4: a germline-specific transcription factor mapping to the mouse t-complex. EMBO J 9: 2185-2195.

85. Palmieri SL, Peter W, Hess H, Scholer HR (1994) Oct-4 transcription factor is differentially expressed in the mouse embryo during establishment of the first two extraembryonic cell lineages involved in implantation. Dev Biol 166: 259-267.

86. Kehler J, Tolkunova E, Koschorz B, Pesce M, Gentile L, et al. (2004) Oct4 is required for primordial germ cell survival. EMBO Rep 5: 1078-1083.

87. Wamelink MM, Struys EA, Huck JH, Roos B, van der Knaap MS, et al. (2005) Quantification of sugar phosphate intermediates of the pentose phosphate pathway by LC-MS/MS: application to two new inherited defects of metabolism. J Chromatogr B Analyt Technol Biomed Life Sci 823: 18-25.

88. Sato N, Meijer L, Skaltsounis L, Greengard P, Brivanlou AH (2004) Maintenance of pluripotency in human and mouse embryonic stem cells through activation of Wnt signaling by a pharmacological GSK-3-specific inhibitor. Nat Med 10: 55-63.

89. Ogawa K, Nishinakamura R, Iwamatsu Y, Shimosato D, Niwa H (2006) Synergistic action of Wnt and LIF in maintaining pluripotency of mouse ES cells. Biochem Biophys Res Commun 343: 159-166.

90. Vallier L, Alexander M, Pedersen RA (2005) Activin/Nodal and FGF pathways cooperate to maintain pluripotency of human embryonic stem cells. J Cell Sci 118: 4495-4509.

91. Boiani M, Scholer HR (2005) Regulatory networks in embryo-derived pluripotent stem cells. Nat Rev Mol Cell Biol 6: 872-884.

92. Ohtsuka S, Dalton S (2008) Molecular and biological properties of pluripotent embryonic stem cells. Gene Ther 15: 74-81.

93. Xu RH, Peck RM, Li DS, Feng X, Ludwig T, et al. (2005) Basic FGF and suppression of BMP signaling sustain undifferentiated proliferation of human ES cells. Nat Methods 2: 185-190.

94. Dvorak P, Hampl A (2005) Basic fibroblast growth factor and its receptors in human embryonic stem cells. Folia Histochem Cytobiol 43: 203-208.

95. Massague J (2000) How cells read TGF-beta signals. Nat Rev Mol Cell Biol 1: 169-178.

96. Xu RH, Sampsell-Barron TL, Gu F, Root S, Peck RM, et al. (2008) NANOG is a direct target of TGFbeta/activin-mediated SMAD signaling in human ESCs. Cell Stem Cell 3: 196-206.

97. Ernst J, Kheradpour P, Mikkelsen TS, Shoresh N, Ward LD, et al. (2011) Mapping and analysis of chromatin state dynamics in nine human cell types. Nature 473: 43-49.

98. van den Berg DL, Snoek T, Mullin NP, Yates A, Bezstarosti K, et al. (2010) An Oct4-centered protein interaction network in embryonic stem cells. Cell Stem Cell 6: 369-381.

99. Kim J, Chu J, Shen X, Wang J, Orkin SH (2008) An extended transcriptional network for pluripotency of embryonic stem cells. Cell 132: 1049-1061.

100. Chen X, Xu H, Yuan P, Fang F, Huss M, et al. (2008) Integration of external signaling pathways with the core transcriptional network in embryonic stem cells. Cell 133: 1106-1117.

101. Feng B, Jiang J, Kraus P, Ng JH, Heng JC, et al. (2009) Reprogramming of fibroblasts into induced pluripotent stem cells with orphan nuclear receptor Esrrb. Nat Cell Biol 11: 197-203.

102. Jiang J, Chan YS, Loh YH, Cai J, Tong GQ, et al. (2008) A core Klf circuitry regulates self-renewal of embryonic stem cells. Nat Cell Biol 10: 353-360.

103. Tanimura N, Saito M, Ebisuya M, Nishida E, Ishikawa F (2012) Stemness-related factor Sall4 interacts with transcription factors Oct-3/4 and Sox2 and occupies Oct-Sox elements in mouse embryonic stem cells. J Biol Chem 288: 5027-5038.

104. Zhang J, Tam WL, Tong GQ, Wu Q, Chan HY, et al. (2006) Sall4 modulates embryonic stem cell pluripotency and early embryonic development by the transcriptional regulation of Pou5f1. Nat Cell Biol 8: 1114-1123.

105. Ng HH, Surani MA (2011) The transcriptional and signalling networks of pluripotency. Nat Cell Biol 13: 490-496.

106. Wang J, Rao S, Chu J, Shen X, Levasseur DN, et al. (2006) A protein interaction network for pluripotency of embryonic stem cells. Nature 444: 364-368.

107. Kim J, Woo AJ, Chu J, Snow JW, Fujiwara Y, et al. (2010) A Myc network accounts for similarities between embryonic stem and cancer cell transcription programs. Cell 143: 313-324.

108. Nakamura K, Hirano K, Wu SM (2013) iPS cell modeling of cardiometabolic diseases. J Cardiovasc Transl Res 6: 46-53.

109. Bellin M, Marchetto MC, Gage FH, Mummery CL (2012) Induced pluripotent stem cells: the new patient? Nat Rev Mol Cell Biol 13: 713-726.

110. Desagher S, Martinou JC (2000) Mitochondria as the central control point of apoptosis. Trends Cell Biol 10: 369-377.

111. Brookes PS (2005) Mitochondrial H(+) leak and ROS generation: an odd couple. Free Radic Biol Med 38: 12-23.

112. Youle RJ, van der Bliek AM (2012) Mitochondrial fission, fusion, and stress. Science 337: 1062-1065.

113. Alexander C, Votruba M, Pesch UE, Thiselton DL, Mayer S, et al. (2000) OPA1, encoding a dynamin-related GTPase, is mutated in autosomal dominant optic atrophy linked to chromosome 3q28. Nat Genet 26: 211-215.

114. Yaffe MP (2003) The cutting edge of mitochondrial fusion. Nat Cell Biol 5: 497-499.

115. Fariss MW, Chan CB, Patel M, Van Houten B, Orrenius S (2005) Role of mitochondria in toxic oxidative stress. Mol Interv 5: 94-111.

116. Saed GM, Fletcher NM, Jiang ZL, Abu-Soud HM, Diamond MP (2011) Dichloroacetate induces apoptosis of epithelial ovarian cancer cells through a mechanism involving modulation of oxidative stress. Reprod Sci 18: 1253-1261.

117. Zick M, Rabl R, Reichert AS (2009) Cristae formation-linking ultrastructure and function of mitochondria. Biochim Biophys Acta 1793: 5-19.

118. Chance B, Williams GR (1956) The respiratory chain and oxidative phosphorylation. Adv Enzymol Relat Subj Biochem 17: 65-134.

119. Jezek P, Hlavata L (2005) Mitochondria in homeostasis of reactive oxygen species in cell, tissues, and organism. Int J Biochem Cell Biol 37: 2478-2503.

120. Barritt JA, Cohen J, Brenner CA (2000) Mitochondrial DNA point mutation in human oocytes is associated with maternal age. Reprod Biomed Online 1: 96-100.

121. St John JC, Facucho-Oliveira J, Jiang Y, Kelly R, Salah R (2010) Mitochondrial DNA transmission, replication and inheritance: a journey from the gamete through the embryo and into offspring and embryonic stem cells. Hum Reprod Update 16: 488-509.

122. Boneh A (2006) Regulation of mitochondrial oxidative phosphorylation by second messenger-mediated signal transduction mechanisms. Cell Mol Life Sci 63: 1236-1248.

123. Collins TJ, Berridge MJ, Lipp P, Bootman MD (2002) Mitochondria are morphologically and functionally heterogeneous within cells. EMBO J 21: 1616-1627.

124. Mazat JP, Ransac S, Heiske M, Devin A, Rigoulet M (2013) Mitochondrial energetic metabolism-some general principles. IUBMB Life 65: 171-179.

125. Scheffler IE (2001) Mitochondria make a come back. Adv Drug Deliv Rev 49: 3-26.

126. Boyer PD (1993) The binding change mechanism for ATP synthase--some probabilities and possibilities. Biochim Biophys Acta 1140: 215-250.

127. Balaban RS, Nemoto S, Finkel T (2005) Mitochondria, oxidants, and aging. Cell 120: 483-495.

128. Murphy MP (2009) How mitochondria produce reactive oxygen species. Biochem J 417: 1-13.

129. Kowaltowski AJ, de Souza-Pinto NC, Castilho RF, Vercesi AE (2009) Mitochondria and reactive oxygen species. Free Radic Biol Med 47: 333-343.

130. Yesodi V, Yaron Y, Lessing JB, Amit A, Ben-Yosef D (2002) The mitochondrial DNA mutation (deltamtDNA5286) in human oocytes: correlation with age and IVF outcome. J Assist Reprod Genet 19: 60-66.

131. Cho YM, Kwon S, Pak YK, Seol HW, Choi YM, et al. (2006) Dynamic changes in mitochondrial biogenesis and antioxidant enzymes during the spontaneous differentiation of human embryonic stem cells. Biochem Biophys Res Commun 348: 1472-1478.

132. Finkel T, Holbrook NJ (2000) Oxidants, oxidative stress and the biology of ageing. Nature 408: 239-247.

133. Berridge MV, Herst PM, Tan AS (2010) Metabolic flexibility and cell hierarchy in metastatic cancer. Mitochondrion 10: 584-588.

134. Costello LC, Franklin RB (2005) 'Why do tumour cells glycolyse?': from glycolysis through citrate to lipogenesis. Mol Cell Biochem 280: 1-8.

135. Oh SK, Kim HS, Ahn HJ, Seol HW, Kim YY, et al. (2005) Derivation and characterization of new human embryonic stem cell lines: SNUhES1, SNUhES2, and SNUhES3. Stem Cells 23: 211-219.

136. St John JC, Ramalho-Santos J, Gray HL, Petrosko P, Rawe VY, et al. (2005) The expression of mitochondrial DNA transcription factors during early cardiomyocyte in vitro differentiation from human embryonic stem cells. Cloning Stem Cells 7: 141-153.

137. Varum S, Momcilovic O, Castro C, Ben-Yehudah A, Ramalho-Santos J, et al. (2009) Enhancement of human embryonic stem cell pluripotency through inhibition of the mitochondrial respiratory chain. Stem Cell Res 3: 142-156.

138. Schieke SM, Ma M, Cao L, McCoy JP, Jr., Liu C, et al. (2008) Mitochondrial metabolism modulates differentiation and teratoma formation capacity in mouse embryonic stem cells. J Biol Chem 283: 28506-28512.

139. Kondoh H, Lleonart ME, Nakashima Y, Yokode M, Tanaka M, et al. (2007) A high glycolytic flux supports the proliferative potential of murine embryonic stem cells. Antioxid Redox Signal 9: 293-299.

140. Chung S, Dzeja PP, Faustino RS, Perez-Terzic C, Behfar A, et al. (2007) Mitochondrial oxidative metabolism is required for the cardiac differentiation of stem cells. Nat Clin Pract Cardiovasc Med 4 Suppl 1: S60-67.

141. Saretzki G, Walter T, Atkinson S, Passos JF, Bareth B, et al. (2008) Downregulation of multiple stress defense mechanisms during differentiation of human embryonic stem cells. Stem Cells 26: 455-464.

142. Piccoli C, Ria R, Scrima R, Cela O, D'Aprile A, et al. (2005) Characterization of mitochondrial and extra-mitochondrial oxygen consuming reactions in human hematopoietic stem cells. Novel evidence of the occurrence of NAD(P)H oxidase activity. J Biol Chem 280: 26467-26476.

143. Crespo FL, Sobrado VR, Gomez L, Cervera AM, McCreath KJ (2010) Mitochondrial reactive oxygen species mediate cardiomyocyte formation from embryonic stem cells in high glucose. Stem Cells 28: 1132-1142.

144. Carriere A, Carmona MC, Fernandez Y, Rigoulet M, Wenger RH, et al. (2004) Mitochondrial reactive oxygen species control the transcription factor CHOP-10/GADD153 and adipocyte differentiation: a mechanism for hypoxia-dependent effect. J Biol Chem 279: 40462-40469.

145. Luoma P, Melberg A, Rinne JO, Kaukonen JA, Nupponen NN, et al. (2004) Parkinsonism, premature menopause, and mitochondrial DNA polymerase gamma mutations: clinical and molecular genetic study. Lancet 364: 875-882.

146. Facucho-Oliveira JM, Alderson J, Spikings EC, Egginton S, St John JC (2007) Mitochondrial DNA replication during differentiation of murine embryonic stem cells. J Cell Sci 120: 4025-4034.

147. Facucho-Oliveira JM, St John JC (2009) The relationship between pluripotency and mitochondrial DNA proliferation during early embryo development and embryonic stem cell differentiation. Stem Cell Rev 5: 140-158.

148. Armstrong L, Tilgner K, Saretzki G, Atkinson SP, Stojkovic M, et al. (2009) Human induced pluripotent stem cell lines show stress defense mechanisms and mitochondrial regulation similar to those of human embryonic stem cells. Stem Cells 28: 661-673.

149. Yoshida Y, Takahashi K, Okita K, Ichisaka T, Yamanaka S (2009) Hypoxia enhances the generation of induced pluripotent stem cells. Cell Stem Cell 5: 237-241.

150. Esteban MA, Wang T, Qin B, Yang J, Qin D, et al. (2010) Vitamin C enhances the generation of mouse and human induced pluripotent stem cells. Cell Stem Cell 6: 71-79.

151. Blaschke K, Ebata KT, Karimi MM, Zepeda-Martinez JA, Goyal P, et al. (2013) Vitamin C induces Tet-dependent DNA demethylation and a blastocyst-like state in ES cells. Nature 500: 222-226.

152. Prigione A, Hossini AM, Lichtner B, Serin A, Fauler B, et al. (2011) Mitochondrial-associated cell death mechanisms are reset to an embryonic-like state in aged donor-derived iPS cells harboring chromosomal aberrations. PLoS One 6: e27352.

153. Hanahan D, Weinberg RA (2000) The hallmarks of cancer. Cell 100: 57-70.

154. Luo J, Solimini NL, Elledge SJ (2009) Principles of cancer therapy: oncogene and non-oncogene addiction. Cell 136: 823-837.

155. Reya T, Morrison SJ, Clarke MF, Weissman IL (2001) Stem cells, cancer, and cancer stem cells. Nature 414: 105-111.

156. Warburg O (1956) On the origin of cancer cells. Science 123: 309-314.

157. Hsu PP, Sabatini DM (2008) Cancer cell metabolism: Warburg and beyond. Cell 134: 703-707.

158. Pedersen PL (2007) The cancer cell's "power plants" as promising therapeutic targets: an overview. J Bioenerg Biomembr 39: 1-12.

159. Hamanaka RB, Chandel NS (2011) Cell biology. Warburg effect and redox balance. Science 334: 1219-1220.

160. Dang CV, Semenza GL (1999) Oncogenic alterations of metabolism. Trends Biochem Sci 24: 68-72.

161. Ho HY, Cheng ML, Lu FJ, Chou YH, Stern A, et al. (2000) Enhanced oxidative stress and accelerated cellular senescence in glucose-6-phosphate dehydrogenase (G6PD)-deficient human fibroblasts. Free Radic Biol Med 29: 156-169.

162. Nakashima RA, Mangan PS, Colombini M, Pedersen PL (1986) Hexokinase receptor complex in hepatoma mitochondria: evidence from N,N'-dicyclohexylcarbodiimide-labeling studies for the involvement of the pore-forming protein VDAC. Biochemistry 25: 1015-1021.

163. Pedersen PL (2007) Warburg, me and Hexokinase 2: Multiple discoveries of key molecular events underlying one of cancers' most common phenotypes, the "Warburg Effect", i.e., elevated glycolysis in the presence of oxygen. J Bioenerg Biomembr 39: 211-222.

164. Bayley JP, Devilee P (2012) The Warburg effect in 2012. Curr Opin Oncol 24: 62-67.

165. Robey RB, Hay N (2005) Mitochondrial hexokinases: guardians of the mitochondria. Cell Cycle 4: 654-658.

166. Mathupala SP, Ko YH, Pedersen PL (2009) Hexokinase-2 bound to mitochondria: cancer's stygian link to the "Warburg Effect" and a pivotal target for effective therapy. Semin Cancer Biol 19: 17-24.

167. Son J, Lyssiotis CA, Ying H, Wang X, Hua S, et al. (2013) Glutamine supports pancreatic cancer growth through a KRAS-regulated metabolic pathway. Nature 496: 101-105.

168. Hitchler MJ, Domann FE (2007) An epigenetic perspective on the free radical theory of development. Free Radic Biol Med 43: 1023-1036.

169. Sonveaux P, Vegran F, Schroeder T, Wergin MC, Verrax J, et al. (2008) Targeting lactate-fueled respiration selectively kills hypoxic tumor cells in mice. J Clin Invest 118: 3930-3942.

170. Semenza GL (2010) Defining the role of hypoxia-inducible factor 1 in cancer biology and therapeutics. Oncogene 29: 625-634.

171. Pistollato F, Chen HL, Rood BR, Zhang HZ, D'Avella D, et al. (2009) Hypoxia and HIF1alpha repress the differentiative effects of BMPs in high-grade glioma. Stem Cells 27: 7-17.

172. Laurenti E, Wilson A, Trumpp A (2009) Myc's other life: stem cells and beyond. Curr Opin Cell Biol 21: 844-854.

173. Kim JW, Tchernyshyov I, Semenza GL, Dang CV (2006) HIF-1-mediated expression of pyruvate dehydrogenase kinase: a metabolic switch required for cellular adaptation to hypoxia. Cell Metab 3: 177-185.

174. Semenza GL, Jiang BH, Leung SW, Passantino R, Concordet JP, et al. (1996) Hypoxia response elements in the aldolase A, enolase 1, and lactate dehydrogenase A gene promoters contain essential binding sites for hypoxia-inducible factor 1. J Biol Chem 271: 32529-32537.

175. Hochachka PW, Buck LT, Doll CJ, Land SC (1996) Unifying theory of hypoxia tolerance: molecular/metabolic defense and rescue mechanisms for surviving oxygen lack. Proc Natl Acad Sci U S A 93: 9493-9498.

176. Papandreou I, Cairns RA, Fontana L, Lim AL, Denko NC (2006) HIF-1 mediates adaptation to hypoxia by actively downregulating mitochondrial oxygen consumption. Cell Metab 3: 187-197.

177. Vousden KH, Prives C (2009) Blinded by the Light: The Growing Complexity of p53. Cell 137: 413-431.

178. Ma W, Sung HJ, Park JY, Matoba S, Hwang PM (2007) A pivotal role for p53: balancing aerobic respiration and glycolysis. J Bioenerg Biomembr 39: 243-246.

179. Niewisch MR, Kuci Z, Wolburg H, Sautter M, Krampen L, et al. (2012) Influence of dichloroacetate (DCA) on lactate production and oxygen consumption in neuroblastoma cells: is DCA a suitable drug for neuroblastoma therapy? Cell Physiol Biochem 29: 373-380.

180. Sun RC, Board PG, Blackburn AC (2011) Targeting metabolism with arsenic trioxide and dichloroacetate in breast cancer cells. Mol Cancer 10: 142.

181. Sutendra G, Dromparis P, Kinnaird A, Stenson TH, Haromy A, et al. (2013) Mitochondrial activation by inhibition of PDKII suppresses HIF1a signaling and angiogenesis in cancer. Oncogene 32: 1638-1650.

182. Macchioni L, Davidescu M, Sciaccaluga M, Marchetti C, Migliorati G, et al. (2011) Mitochondrial dysfunction and effect of antiglycolytic bromopyruvic acid in GL15 glioblastoma cells. J Bioenerg Biomembr 43: 507-518.

183. Thurlimann B, Hess D, Koberle D, Senn I, Ballabeni P, et al. (2004) Anastrozole ('Arimidex') versus tamoxifen as first-line therapy in postmenopausal women with advanced breast cancer: results of the double-blind cross-over SAKK trial 21/95--a sub-study of the TARGET (Tamoxifen or 'Arimidex' Randomized Group Efficacy and Tolerability) trial. Breast Cancer Res Treat 85: 247-254.

184. Yamaguchi R, Perkins G (2012) Challenges in targeting cancer metabolism for cancer therapy. EMBO Rep 13: 1034-1035.

185. Madani SY, Naderi N, Dissanayake O, Tan A, Seifalian AM (2011) A new era of cancer treatment: carbon nanotubes as drug delivery tools. Int J Nanomedicine 6: 2963-2979.

186. Hamanaka RB, Chandel NS (2012) Targeting glucose metabolism for cancer therapy. J Exp Med 209: 211-215.

187. Folmes CD, Nelson TJ, Martinez-Fernandez A, Arrell DK, Lindor JZ, et al. (2011) Somatic oxidative bioenergetics transitions into pluripotency-dependent glycolysis to facilitate nuclear reprogramming. Cell Metab 14: 264-271.

188. Kondoh H, Lleonart ME, Bernard D, Gil J (2007) Protection from oxidative stress by enhanced glycolysis; a possible mechanism of cellular immortalization. Histol Histopathol 22: 85-90.

189. Ezashi T, Das P, Roberts RM (2005) Low O2 tensions and the prevention of differentiation of hES cells. Proc Natl Acad Sci U S A 102: 4783-4788.

190. Manganelli G, Fico A, Masullo U, Pizzolongo F, Cimmino A, et al. (2012) Modulation of the pentose phosphate pathway induces endodermal differentiation in embryonic stem cells. PLoS One 7: e29321.

191. Wegrzyn J, Potla R, Chwae YJ, Sepuri NB, Zhang Q, et al. (2009) Function of mitochondrial Stat3 in cellular respiration. Science 323: 793-797.

192. Kang J, Shakya A, Tantin D (2009) Stem cells, stress, metabolism and cancer: a drama in two Octs. Trends Biochem Sci 34: 491-499.

193. Jaenisch R, Young R (2008) Stem cells, the molecular circuitry of pluripotency and nuclear reprogramming. Cell 132: 567-582.

194. Luo W, Semenza GL (2011) Pyruvate kinase M2 regulates glucose metabolism by functioning as a coactivator for hypoxia-inducible factor 1 in cancer cells. Oncotarget 2: 551-556.

195. Luo W, Hu H, Chang R, Zhong J, Knabel M, et al. (2011) Pyruvate kinase M2 is a PHD3-stimulated coactivator for hypoxia-inducible factor 1. Cell 145: 732-744.

196. Brookes E, de Santiago I, Hebenstreit D, Morris KJ, Carroll T, et al. (2012) Polycomb associates genome-wide with a specific RNA polymerase II variant, and regulates metabolic genes in ESCs. Cell Stem Cell 10: 157-170.

197. Mohyeldin A, Garzon-Muvdi T, Quinones-Hinojosa A (2010) Oxygen in stem cell biology: a critical component of the stem cell niche. Cell Stem Cell 7: 150-161.

198. Forristal CE, Wright KL, Hanley NA, Oreffo RO, Houghton FD (2010) Hypoxia inducible factors regulate pluripotency and proliferation in human embryonic stem cells cultured at reduced oxygen tensions. Reproduction 139: 85-97.

199. Folmes CD, Dzeja PP, Nelson TJ, Terzic A (2012) Metabolic plasticity in stem cell homeostasis and differentiation. Cell Stem Cell 11: 596-606.

200. Zhang J, Khvorostov I, Hong JS, Oktay Y, Vergnes L, et al. (2011) UCP2 regulates energy metabolism and differentiation potential of human pluripotent stem cells. EMBO J 30: 4860-4873.

201. Elorza A, Hyde B, Mikkola HK, Collins S, Shirihai OS (2008) UCP2 modulates cell proliferation through the MAPK/ERK pathway during erythropoiesis and has no effect on heme biosynthesis. J Biol Chem 283: 30461-30470.

202. Panopoulos AD, Yanes O, Ruiz S, Kida YS, Diep D, et al. (2012) The metabolome of induced pluripotent stem cells reveals metabolic changes occurring in somatic cell reprogramming. Cell Res 22: 168-177.

203. Kim K, Doi A, Wen B, Ng K, Zhao R, et al. (2010) Epigenetic memory in induced pluripotent stem cells. Nature 467: 285-290.

204. Zhu S, Li W, Zhou H, Wei W, Ambasudhan R, et al. (2010) Reprogramming of human primary somatic cells by OCT4 and chemical compounds. Cell Stem Cell 7: 651-655.

205. Wieckowski MR, Giorgi C, Lebiedzinska M, Duszynski J, Pinton P (2009) Isolation of mitochondria-associated membranes and mitochondria from animal tissues and cells. Nat Protoc 4: 1582-1590.

206. Qian W, Van Houten B (2010) Alterations in bioenergetics due to changes in mitochondrial DNA copy number. Methods 51: 452-457.

207. Wakayama T, Rodriguez I, Perry AC, Yanagimachi R, Mombaerts P (1999) Mice cloned from embryonic stem cells. Proc Natl Acad Sci U S A 96: 14984-14989.

208. Ohtsuka M, Ishii K, Kikuti YY, Warita T, Suzuki D, et al. (2006) Construction of mouse 129/Ola BAC library for targeting experiments using E14 embryonic stem cells. Genes Genet Syst 81: 143-146.

209. Berridge MV, Herst PM, Tan AS (2005) Tetrazolium dyes as tools in cell biology: new insights into their cellular reduction. Biotechnol Annu Rev 11: 127-152.

210. Parnas D, Linial M (1998) Highly sensitive ELISA-based assay for quantifying protein levels in neuronal cultures. Brain Res Brain Res Protoc 2: 333-338.

211. Branco AF, Pereira SL, Moreira AC, Holy J, Sardao VA, et al. (2011) Isoproterenol cytotoxicity is dependent on the differentiation state of the cardiomyoblast H9c2 cell line. Cardiovasc Toxicol 11: 191-203.

212. Perry SW, Norman JP, Barbieri J, Brown EB, Gelbard HA (2011) Mitochondrial membrane potential probes and the proton gradient: a practical usage guide. Biotechniques 50: 98-115.

213. Floryk D, Houstek J (1999) Tetramethyl rhodamine methyl ester (TMRM) is suitable for cytofluorometric measurements of mitochondrial membrane potential in cells treated with digitonin. Biosci Rep 19: 27-34.

214. Mukhopadhyay P, Rajesh M, Hasko G, Hawkins BJ, Madesh M, et al. (2007) Simultaneous detection of apoptosis and mitochondrial superoxide production in live cells by flow cytometry and confocal microscopy. Nat Protoc 2: 2295-2301.

215. Lee S, Van Remmen H, Csete M (2009) Sod2 overexpression preserves myoblast mitochondrial mass and function, but not muscle mass with aging. Aging Cell 8: 296-310.

216. Dingley S, Chapman KA, Falk MJ (2012) Fluorescence-activated cell sorting analysis of mitochondrial content, membrane potential, and matrix oxidant burden in human lymphoblastoid cell lines. Methods Mol Biol 837: 231-239.

217. Mahler M, Miyachi K, Peebles C, Fritzler MJ (2012) The clinical significance of autoantibodies to the proliferating cell nuclear antigen (PCNA). Autoimmun Rev 11: 771-775.

218. Nair RP, Krishnan LK (2013) Identification of p63+ keratinocyte progenitor cells in circulation and their matrix-directed differentiation to epithelial cells. Stem Cell Res Ther 4: 38.

219. Amaral S, Mota PC, Lacerda B, Alves M, Pereira Mde L, et al. (2009) Testicular mitochondrial alterations in untreated streptozotocin-induced diabetic rats. Mitochondrion 9: 41-50.

220. Stocchi V, Cucchiarini L, Magnani M, Chiarantini L, Palma P, et al. (1985) Simultaneous extraction and reverse-phase high-performance liquid chromatographic determination of adenine and pyridine nucleotides in human red blood cells. Anal Biochem 146: 118-124.

221. Hansen JL, Freier EF (1978) Direct assays of lactate, pyruvate, beta-hydroxybutyrate, and acetoacetate with a centrifugal analyzer. Clin Chem 24: 475-479.

222. Yu J, Vodyanik MA, Smuga-Otto K, Antosiewicz-Bourget J, Frane JL, et al. (2007) Induced pluripotent stem cell lines derived from human somatic cells. Science 318: 1917-1920.

223. Chin MH, Mason MJ, Xie W, Volinia S, Singer M, et al. (2009) Induced pluripotent stem cells and embryonic stem cells are distinguished by gene expression signatures. Cell Stem Cell 5: 111-123.

224. Doi A, Park IH, Wen B, Murakami P, Aryee MJ, et al. (2009) Differential methylation of tissue- and cancer-specific CpG island shores distinguishes human induced pluripotent stem cells, embryonic stem cells and fibroblasts. Nat Genet 41: 1350-1353.

225. Hawkins RD, Hon GC, Lee LK, Ngo Q, Lister R, et al. (2010) Distinct epigenomic landscapes of pluripotent and lineage-committed human cells. Cell Stem Cell 6: 479-491.

226. Deng J, Shoemaker R, Xie B, Gore A, LeProust EM, et al. (2009) Targeted bisulfite sequencing reveals changes in DNA methylation associated with nuclear reprogramming. Nat Biotechnol 27: 353-360.

227. Lister R, Pelizzola M, Kida YS, Hawkins RD, Nery JR, et al. (2011) Hotspots of aberrant epigenomic reprogramming in human induced pluripotent stem cells. Nature 471: 68-73.

228. Bock C, Kiskinis E, Verstappen G, Gu H, Boulting G, et al. (2011) Reference Maps of human ES and iPS cell variation enable high-throughput characterization of pluripotent cell lines. Cell 144: 439-452.

229. Hussein SM, Batada NN, Vuoristo S, Ching RW, Autio R, et al. (2011) Copy number variation and selection during reprogramming to pluripotency. Nature 471: 58-62.

230. Fischer B, Bavister BD (1993) Oxygen tension in the oviduct and uterus of rhesus monkeys, hamsters and rabbits. J Reprod Fertil 99: 673-679.

231. Gore A, Li Z, Fung HL, Young JE, Agarwal S, et al. (2011) Somatic coding mutations in human induced pluripotent stem cells. Nature 471: 63-67.

232. Zhao T, Zhang ZN, Rong Z, Xu Y (2011) Immunogenicity of induced pluripotent stem cells. Nature.

233. Leese HJ, Barton AM (1984) Pyruvate and glucose uptake by mouse ova and preimplantation embryos. J Reprod Fertil 72: 9-13.

234. Semenza GL (2007) Life with oxygen. Science 318: 62-64.

235. Bustamante E, Pedersen PL (1977) High aerobic glycolysis of rat hepatoma cells in culture: role of mitochondrial hexokinase. Proc Natl Acad Sci U S A 74: 3735-3739.

236. Bustamante E, Morris HP, Pedersen PL (1981) Energy metabolism of tumor cells. Requirement for a form of hexokinase with a propensity for mitochondrial binding. J Biol Chem 256: 8699-8704.

237. Holness MJ, Sugden MC (2003) Regulation of pyruvate dehydrogenase complex activity by reversible phosphorylation. Biochem Soc Trans 31: 1143-1151.

238. Roche TE, Hiromasa Y (2007) Pyruvate dehydrogenase kinase regulatory mechanisms and inhibition in treating diabetes, heart ischemia, and cancer. Cell Mol Life Sci 64: 830-849.

239. Ferreira LM (2010) Cancer metabolism: the Warburg effect today. Exp Mol Pathol 89: 372-380.

240. Yeung TM, Gandhi SC, Bodmer WF (2011) Hypoxia and lineage specification of cell line-derived colorectal cancer stem cells. Proc Natl Acad Sci U S A 108: 4382-4387.

241. Madhok BM, Yeluri S, Perry SL, Hughes TA, Jayne DG (2010) Dichloroacetate induces apoptosis and cell-cycle arrest in colorectal cancer cells. Br J Cancer 102: 1746-1752.

242. Loiseau D, Morvan D, Chevrollier A, Demidem A, Douay O, et al. (2009) Mitochondrial bioenergetic background confers a survival advantage to HepG2 cells in response to chemotherapy. Mol Carcinog 48: 733-741.

243. Jose C, Bellance N, Rossignol R (2010) Choosing between glycolysis and oxidative phosphorylation: A tumor's dilemma? Biochim Biophys Acta.

244. Huttemann M, Jaradat S, Grossman LI (2003) Cytochrome c oxidase of mammals contains a testes-specific isoform of subunit VIb--the counterpart to testes-specific cytochrome c? Mol Reprod Dev 66: 8-16.

245. Lambert AJ, Brand MD (2004) Inhibitors of the quinone-binding site allow rapid superoxide production from mitochondrial NADH:ubiquinone oxidoreductase (complex I). J Biol Chem 279: 39414-39420.

246. Kletzien RF, Harris PK, Foellmi LA (1994) Glucose-6-phosphate dehydrogenase: a "housekeeping" enzyme subject to tissue-specific regulation by hormones, nutrients, and oxidant stress. FASEB J 8: 174-181.

247. Tian WN, Braunstein LD, Pang J, Stuhlmeier KM, Xi QC, et al. (1998) Importance of glucose-6-phosphate dehydrogenase activity for cell growth. J Biol Chem 273: 10609-10617.

248. Boros LG, Torday JS, Lim S, Bassilian S, Cascante M, et al. (2000) Transforming growth factor beta2 promotes glucose carbon incorporation into nucleic acid ribose through the nonoxidative pentose cycle in lung epithelial carcinoma cells. Cancer Res 60: 1183-1185.

249. Cascante M, Centelles JJ, Veech RL, Lee WN, Boros LG (2000) Role of thiamin (vitamin B-1) and transketolase in tumor cell proliferation. Nutr Cancer 36: 150-154.

250. Kim JW, Zeller KI, Wang Y, Jegga AG, Aronow BJ, et al. (2004) Evaluation of myc E-box phylogenetic footprints in glycolytic genes by chromatin immunoprecipitation assays. Mol Cell Biol 24: 5923-5936.

251. Gordan JD, Thompson CB, Simon MC (2007) HIF and c-Myc: sibling rivals for control of cancer cell metabolism and proliferation. Cancer Cell 12: 108-113.

252. Li F, Wang Y, Zeller KI, Potter JJ, Wonsey DR, et al. (2005) Myc stimulates nuclearly encoded mitochondrial genes and mitochondrial biogenesis. Mol Cell Biol 25: 6225-6234.

253. Wu KJ, Polack A, Dalla-Favera R (1999) Coordinated regulation of iron-controlling genes, H-ferritin and IRP2, by c-MYC. Science 283: 676-679.

254. Adams FH, Yanagisawa M, Kuzela D, Martinek H (1971) The disappearance of fetal lung fluid following birth. J Pediatr 78: 837-843.

255. Cinelli P, Casanova EA, Uhlig S, Lochmatter P, Matsuda T, et al. (2008) Expression profiling in transgenic FVB/N embryonic stem cells overexpressing STAT3. BMC Dev Biol 8: 57.

256. Heikkinen S, Pietila M, Halmekyto M, Suppola S, Pirinen E, et al. (1999) Hexokinase II-deficient mice. Prenatal death of homozygotes without disturbances in glucose tolerance in heterozygotes. J Biol Chem 274: 22517-22523.

257. Arora KK, Pedersen PL (1988) Functional significance of mitochondrial bound hexokinase in tumor cell metabolism. Evidence for preferential phosphorylation of glucose by intramitochondrially generated ATP. J Biol Chem 263: 17422-17428.

258. Golshani-Hebroni SG, Bessman SP (1997) Hexokinase binding to mitochondria: a basis for proliferative energy metabolism. J Bioenerg Biomembr 29: 331-338.

259. Majewski N, Nogueira V, Robey RB, Hay N (2004) Akt inhibits apoptosis downstream of BID cleavage via a glucose-dependent mechanism involving mitochondrial hexokinases. Mol Cell Biol 24: 730-740.

260. Coussens M, Davy P, Brown L, Foster C, Andrews WH, et al. (2010) RNAi screen for telomerase reverse transcriptase transcriptional regulators identifies HIF1alpha as critical for telomerase function in murine embryonic stem cells. Proc Natl Acad Sci U S A 107: 13842-13847.

261. Suhr ST, Chang EA, Tjong J, Alcasid N, Perkins GA, et al. (2010) Mitochondrial rejuvenation after induced pluripotency. PLoS One 5: e14095.

262. Wolf A, Agnihotri S, Micallef J, Mukherjee J, Sabha N, et al. (2011) Hexokinase 2 is a key mediator of aerobic glycolysis and promotes tumor growth in human glioblastoma multiforme. J Exp Med 208: 313-326.

263. Ko YH, Smith BL, Wang Y, Pomper MG, Rini DA, et al. (2004) Advanced cancers: eradication in all cases using 3-bromopyruvate therapy to deplete ATP. Biochem Biophys Res Commun 324: 269-275.

264. Jogi A, Ora I, Nilsson H, Lindeheim A, Makino Y, et al. (2002) Hypoxia alters gene expression in human neuroblastoma cells toward an immature and neural crest-like phenotype. Proc Natl Acad Sci U S A 99: 7021-7026.

265. Folmes CD, Martinez-Fernandez A, Faustino RS, Yamada S, Perez-Terzic C, et al. (2013) Nuclear reprogramming with c-Myc potentiates glycolytic capacity of derived induced pluripotent stem cells. J Cardiovasc Transl Res 6: 10-21.

266. Cicalese A, Bonizzi G, Pasi CE, Faretta M, Ronzoni S, et al. (2009) The tumor suppressor p53 regulates polarity of self-renewing divisions in mammary stem cells. Cell 138: 1083-1095.

267. Bensaad K, Tsuruta A, Selak MA, Vidal MN, Nakano K, et al. (2006) TIGAR, a p53-inducible regulator of glycolysis and apoptosis. Cell 126: 107-120.

268. Ko YH, Verhoeven HA, Lee MJ, Corbin DJ, Vogl TJ, et al. (2012) A translational study "case report" on the small molecule "energy blocker" 3-bromopyruvate (3BP) as a potent anticancer agent: from bench side to bedside. J Bioenerg Biomembr 44: 163-170.

269. O'Connor MD, Kardel MD, Iosfina I, Youssef D, Lu M, et al. (2008) Alkaline phosphatase-positive colony formation is a sensitive, specific, and quantitative indicator of undifferentiated human embryonic stem cells. Stem Cells 26: 1109-1116.

270. Qin JZ, Xin H, Nickoloff BJ (2010) 3-Bromopyruvate induces necrotic cell death in sensitive melanoma cell lines. Biochem Biophys Res Commun 396: 495-500.

271. Kim JS, Ahn KJ, Kim JA, Kim HM, Lee JD, et al. (2008) Role of reactive oxygen species-mediated mitochondrial dysregulation in 3-bromopyruvate induced cell death in hepatoma cells : ROS-mediated cell death by 3-BrPA. J Bioenerg Biomembr 40: 607-618.

272. Xu RH, Pelicano H, Zhou Y, Carew JS, Feng L, et al. (2005) Inhibition of glycolysis in cancer cells: a novel strategy to overcome drug resistance associated with mitochondrial respiratory defect and hypoxia. Cancer Res 65: 613-621.

273. Mayers RM, Leighton B, Kilgour E (2005) PDH kinase inhibitors: a novel therapy for Type II diabetes? Biochem Soc Trans 33: 367-370.

274. Michelakis ED, Webster L, Mackey JR (2008) Dichloroacetate (DCA) as a potential metabolic-targeting therapy for cancer. Br J Cancer 99: 989-994.

275. Babu E, Ramachandran S, CoothanKandaswamy V, Elangovan S, Prasad PD, et al. (2011) Role of SLC5A8, a plasma membrane transporter and a tumor suppressor, in the antitumor activity of dichloroacetate. Oncogene 30: 4026-4037.

276. Varum S, Rodrigues AS, Moura MB, Momcilovic O, Easley CAt, et al. (2011) Energy metabolism in human pluripotent stem cells and their differentiated counterparts. PLoS One 6: e20914.

277. Zhou W, Choi M, Margineantu D, Margaretha L, Hesson J, et al. (2012) HIF1alpha induced switch from bivalent to exclusively glycolytic metabolism during ESC-to-EpiSC/hESC transition. EMBO J 31: 2103-2116.

278. Rardin MJ, Wiley SE, Naviaux RK, Murphy AN, Dixon JE (2009) Monitoring phosphorylation of the pyruvate dehydrogenase complex. Anal Biochem 389: 157-164.

279. Roche TE, Baker JC, Yan X, Hiromasa Y, Gong X, et al. (2001) Distinct regulatory properties of pyruvate dehydrogenase kinase and phosphatase isoforms. Prog Nucleic Acid Res Mol Biol 70: 33-75.

280. Venigalla RK, McGuire VA, Clarke R, Patterson-Kane JC, Najafov A, et al. (2013) PDK1 regulates VDJ recombination, cell-cycle exit and survival during B-cell development. EMBO J 32: 1008-1022.

281. Pistollato F, Abbadi S, Rampazzo E, Viola G, Della Puppa A, et al. (2010) Hypoxia and succinate antagonize 2-deoxyglucose effects on glioblastoma. Biochem Pharmacol 80: 1517-1527.

282. Anastasiou D, Poulogiannis G, Asara JM, Boxer MB, Jiang JK, et al. (2011) Inhibition of pyruvate kinase M2 by reactive oxygen species contributes to cellular antioxidant responses. Science 334: 1278-1283.

283. Hitosugi T, Fan J, Chung TW, Lythgoe K, Wang X, et al. (2011) Tyrosine phosphorylation of mitochondrial pyruvate dehydrogenase kinase 1 is important for cancer metabolism. Mol Cell 44: 864-877.

284. DeBerardinis RJ, Lum JJ, Hatzivassiliou G, Thompson CB (2008) The biology of cancer: metabolic reprogramming fuels cell growth and proliferation. Cell Metab 7: 11-20.